WHITEPAPER

Nonlinear Finite Element Analysis of Elastomers

MSC Software

MSC Software Corporation, the worldwide leader in rubber analysis, would like to share some of our experiences and expertise in analyzing elastomers with you.

This White Paper introduces you to the nonlinear finite element analysis (FEA) of rubber-like polymers generally grouped under the name “elastomers”. You may have a nonlinear rubber problem—and not even know it...

The Paper is primarily intended for two types of readers:

ENGINEERING MANAGERS who are involved in manufacturing of elastomeric components, but do not currently possess nonlinear FEA tools, or who may have an educational/ professional background other than mechanical engineering.

DESIGN ENGINEERS who are perhaps familiar with linear, or even nonlinear, FEA concepts but would like to know more about analyzing elastomers.

It is assumed that the reader is familiar with basic principles in strength of materials theory.

The contents of this White Paper are intentionally organized for the convenience of these two kinds of readers.

For an “Engineering Manager”, topics of interest include, an Executive Summary to obtain an overview of the subject, the Case Studies to see some real-world rubber FEA applications, and any other industry specific topics.

The “Design Engineer”, on the other hand, can exami ne the significant features on analysis of elastomers (which constitute the bulk of the Paper). The Appendices describe the physics and mechanical properties of rubber, proper modeling of incompressibility in rubber FEA, and most importantly, testing methods for determination of material properties. Simulation issues and useful hints are found throughout the text and in the Case Studies.

Rubber FEA is an extensive subject, which involves rubber chemistry, manufacturing processes, material characterization, finite element theory, and the latest advances in computational mechanics. A selected list of Suggestions for Further Reading is included. These references cite some of the most recent research on FEA of elastomers and demonstrate practical applications. They are categorized by subject for readers convenience.

On the Cover

The cover shows a deformed configuration of a washing machine seal with fringe plots of deformation magnitude. You can observe the wrinkling the seal undergoes due to excessive deformation.

INDEX

APPENDICES

CASE STUDIES

1. EXECUTIVE SUMMARY

This white paper discusses the salient features regarding the mechanics and finite element analysis (FEA) of elastomers. Although, the main focus of the paper is on elastomers (or rubber-like materials) and foams, many of these concepts are also applicable to the FEA of glass, plastics, and biomaterials. Therefore, this White Paper should be of value not only to the rubber and tire industries, but also to those involved in the following:

- Glass, plastics, ceramic, and solid propellant industries
- Biomechanics and the medical/dental professions—implantable surgery devices, prosthesis, orthopedics, orthodontics, dental implants, artificial limbs, artificial organs, wheelchairs and beds, monitoring equipment
- Highway safety and flight safety—seat belt design, impact analysis, seat and padding design, passenger protection
- Packaging industry
- Sports and consumer industries—helmet design, shoe design, athletic protection gear, sports equipment safety.

Elastomers are used extensively in many industries because of their wide availability and low cost. They are also used because of their excellent damping and energy absorption characteristics, flexibility, resiliency, long service life, ability to seal against moisture, heat, and pressure, non-toxic properties, moldability, and variable stiffness.

Rubber is a very unique material. During processing and shaping, it behaves mostly like a highly viscous fluid. After its polymer chains have been crosslinked by vulcanization (or by curing), rubber can undergo large reversible elastic deformations. Unless damage occurs, it will return to its original shape after removal of the load.

Proper analysis of rubber components requires special material modeling and nonlinear finite element analysis tools that are quite different than those used for metallic parts. The unique properties of rubber are such that:

1. It can undergo large deformations under load, sustaining strains of up to 500 percent in engineering applications.
2. Its load-extension behavior is markedly nonlinear.
3. Because it is viscoelastic, it exhibits significant damping properties. Its behavior is time- and temperature-dependent, making it similar to glass and plastics in this respect.
4. It is nearly incompressible. This means its volume does not change appreciably with stress. It cannot be compressed significantly under hydrostatic load.

For certain foam rubber materials, the assumption of near incompressibility is relaxed, since large volume change can be achieved by the application of relatively moderate stresses.

The nonlinear FEA program, Marc possesses specially-formulated elements, material and friction models, and automated contact analysis procedures to model elastomers. Capabilities and uniqueness of Marc in analyzing large, industry-scale problems are highlighted throughout this white paper.

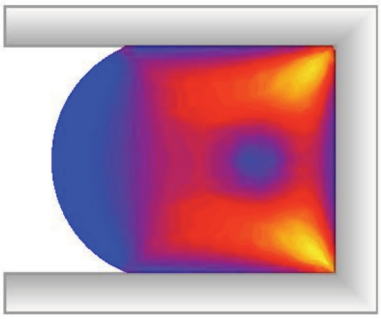

O-ring

Car Tire

Rubber Boot

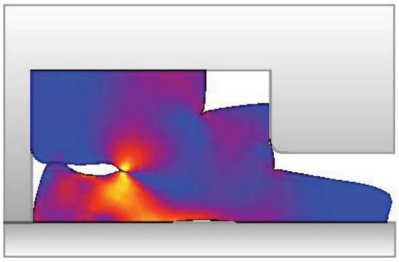

Shock Mount

Car Door Seal

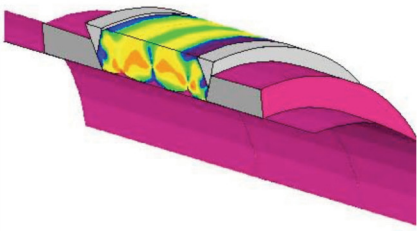

Oil Packer

Efficient and realistic analysis for design of elastomeric products relies on several important concepts outlined below:

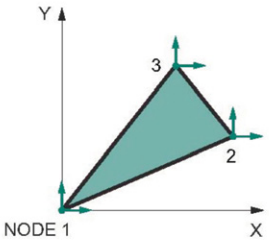

1956: Triangular Element

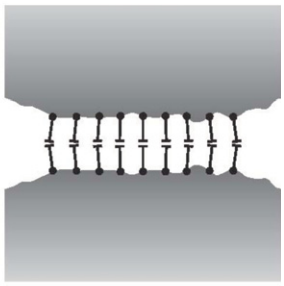
1970s: Gap Elements

1. Nonlinear material behavior—compressible or incompressible material models, time and temperature effects, presence of anisotropy due to fillers or fibers, hysteresis due to cyclic loading and manifestation of instabilities.
2. Determination of Material Parameters from Test Data—perhaps the single most troublesome step for most engineers in analyzing elastomers, that is, how to "curve fit" test data and derive parameters necessary to characterize a material.
3. Failure—causes and analysis of failure resulting due to material damage and degradation, cracking, and debonding.
4. Dynamics—shock and vibration isolation concerns, damping, harmonic analysis of viscoelastic materials, time versus frequency domain viscoelastic analysis, and implicit versus explicit direct time integration methods.
5. Modern automated contact analysis techniques—friction effects, and the use of "contact bodies" to handle boundary conditions at an interface. Automated solution strategies—issues related to model preparation, nonlinear analysis, parallelization, and ease-of-use of the simulation software.
6. Automated Remeshing - for effective solution of problems involving distorted meshes which can lead to premature termination of analysis.

MSC Software Corporation offers a well-balanced combination of sophisticated analysis code integrated seamlessly with easy-to-use Graphical User Interface (GUI) Mentat and Patran, for the simulation of elastomeric products. This makes Marc uniquely suitable for the simulation of complex physics of rubber, foam, glass, plastics, and biomaterials. The following sections briefly explains the 'insides' of a nonlinear FEA code (and its differences from a linear FEA program) along with the accompanying GUI capabilities.

The Finite Element Method

The finite element method is a computer-aided engineering technique for obtaining approximate numerical solutions to boundary value problems which predict the response of physical systems subjected to external loads. It is based on the principle of virtual work. One approximation method is the so-called weighted residuals method, the most popular example of which is the Galerkin method (see any of the finite element texts listed in the Suggestions for Further Reading section at the back). A structure is idealized as many small, discrete pieces called finite elements, which are connected at nodes. In finite element analysis, thousands of simultaneous equations are typically solved using computers. In structural analysis, the unknowns are the nodal degrees of freedom, like displacements, rotations, or the hydrostatic pressure.

History of Nonlinear and Rubber FEA

A National Research Council report on computational mechanics research needs in the 1990s [Oden, 1991] emphasized the "materials" field as a national critical technology for the United States, and that areas such as damage, crack initiation and propagation, nonlinear analysis, and coupled field problems still require extensive research.

Before embarking on the issues related to the material behavior, it is interesting to review how the finite element method has matured in the past sixty years—paying special attention to recent improvements in nonlinear FEA techniques for handling rubber contact problems:

1943 Applied mathematician Courant used triangular elements to solve a torsion problem.

1947 Prager and Synge used triangular elements to solve a 2-D elasticity problem using the "hypercircle method".

1954-55 Argyris published work on energy methods in structural analysis (creating the "Force Method" of FEA).

1956 Classical paper on the "Displacement (Stiffness) Method" of FEA by Turner, Clough, Martin, and Topp (using triangles).

1960 Clough first coined the term "Finite Element Method."

1965 Herrmann developed first "mixed method" solution for incompressible and nearly incompressible isotropic materials.

1968 Taylor, Pister, and Herrmann extended Herrmann's work to orthotropic materials. S.W. Key extended it to anisotropy [1969].

1971 First release of the Marc program by Marc Analysis Research Corporation, MARC. It was the world's first commercial, nonlinear general-purpose FEA code.

1970s-today Most FEA codes claiming ability to analyze contact problems use "gap" or "interface" elements. (The user needs to know a priori where to specify these interface elements—not an easy task!)

1974 MARC introduced Mooney-Rivlin model and special Herrmann elements to analyze incompressible behavior.

1979 Special viscoelastic models for harmonic analysis to model damping behavior introduced by MARC. Generalized Maxwell model added shortly thereafter.

1985
- Oden and Martins published comprehensive treatise on modeling and computational issues for dynamic friction phenomena.
- MARC pioneered use of rigid or deformable contact bodies in an automated solution procedure to solve 2-D variable contact problems—typically found in metal forming and rubber applications. Also, first introduction of large-strain viscoelastic capabilities for rubber materials by MARC.

1988 • Oden and Kikuchi published monograph on contact problems in elasticity—treating this class of problems

• MARC extended automated contact FEA capability to 3-D problems.

1990 Martins, Oden, and Simoes published exhaustive study on static and kinetic friction (concentrating on metal contact).

1991 MARC introduced Ogden rubber model and rubber damage model.

1994 MARC introduced Rubber Foam model.

MARC introduced Adaptive Meshing Capability.

1995 MARC and Axel Products, Inc. to create "Experimental Elastomer Analysis" course

1997 MARC introduced Narayanswamy model for Glass Relaxation behavior.

1998 MARC introduced fully parallel software based on domain decomposition.

1999 MARC was acquired by MSC Software

2000 Marc introduced the following:

• Boyce-Arruda and Gent rubber models

• Special lower-order triangular and tetrahedral elements to handle incompressible materials

• Global adaptive remeshing for rubber and metallic materials.

• Coupled structural-acoustic model for harmonic analysis.

2003 Marc introduced the following:

• Steady state tire rolling

• Cavity pressure calculation

• Insert option for tire chords

• Global adaptive meshing in 3-D

• The J-integral (Lorenzi option) now supports large strains, both in the total and the updated Lagrange formulation. This makes it possible to calculate the J-integral for rubber applications.

• Strain energy is correctly output for rubber models in total Lagrangian analysis.

2005 Marc introduced the following:

• Global adaptive meshing allows general boundary conditions in 3-D

• New unified rubber model with improved volumetric behavior

• Coupling with CFD using MPCCI

• Global adaptive remeshing enhanced in two-dimensional analyses such that distributed loads and nodal boundary conditions are reapplied to the model after remeshing occurs.

2005 (cont.) • A framework, based on the updated Lagrangian formulation, has been set up for hyperelastic material models. Within the framework, users can easily define their own generalized strain energy function models through a UELASTOMER user subroutine.

• A new friction model, bilinear, is introduced which is more accurate than the model using the velocity-based smoothing function, arc tangent, and less expensive and more general than the stick-slip model.

2007 Marc introduced the following:

• Virtual Crack Closure Technique with remeshing to see crack growth during the loading.

• Cohesive zone method (CZM) for delamination

• Connector elements for assembly modeling

• Steady state tire rolling

• Puck and Hashin failure criteria

• Crack propagation in 2-D using global adaptive remeshing

• Simplified nonlinear elastic material models

• Solid shell element which can be used with elastomeric materials

• Nonlinear cyclic symmetry

• Rubber example using volumetric strain energy function

2008 Marc introduced the following:

• Simple material mixture model

• Moment carrying glued contact

• Hilbert-Hughes-Taylor Dynamic procedure

• Interface elements added automatically on crack opening with adaptive meshing

2010 Marc introduced the following:

• Incorporated generalized 5th order Mooney-Rivlin hyperelastic model

• Parallel solver technology to utilize multi-core processors

• Segment to segment contact

2011 A new directional friction model is introduced. It is beneficial to solve problems which have two friction behaviors due to either material surface behavior or geometric features

2013 Bergström-Boyce model to help analyze the time-dependent large strain viscoelastic behavior of hyper-eleastic materials. This model may also be combined with damage models to represent the permanent set of the elastomers

Marlow model to give the ability to directly enter the experimental stress-strain data representing incompressible materials

2013 (Cont.)

Frequency dependent damping and stiffness for harmonic (frequency response) analysis. Support for damping as a function of the amount of static pre-deformation/pre-stress is also included

General crack propagation in 3D solids

Insertion of cracks in solid mesh with the help of NURBS surface

Five new methods added to remove interference between contact bodies (applicable to both Node-to-Segment and Segment-to-Segment contact)

Three new models have been added to represent the behavior of anisotropic incompressibility of hyperelastic materials (Qiu and Pence, Brow and Smith, Gasser et al.)

The benefits of performing nonlinear FEA of elastomeric products are essentially the same as those for linear FEA. FEA should be an integral part of the design process, preferably from the CAD. The advantages of this enhanced design process include: improved performance and quality of the finished product; faster time to market; optimal use of materials; weight savings; verification of structural integrity before prototyping; and overall reduction of development and production costs. Furthermore, a good predictive capability can help to reduce the scrap rate in manufacturing stage; that is, "green" stage to the finally "molded" state, thereby ensuring a competitive edge.

2. MATERIAL BEHAVIOR

This section discusses the issues central to the description of material modeling of elastomers. Any material behavior must be determined experimentally, and the wide variety of rubber compounds make this experimental determination even more important. A brief overview of the concepts of nonlinearity and the stress-strain descriptions suitable for nonlinear analysis is presented first. The features of time-independent and dependent material behavior, anisotropy, hysteresis, and other polymeric materials are detailed next. In the final note, other polymeric materials which share common material characteristics with elastomers are reviewed. The most important concept to recognize about rubber is that its deformation is not directly proportional to the applied load, in other words, it exhibits a 'nonlinear' behavior.

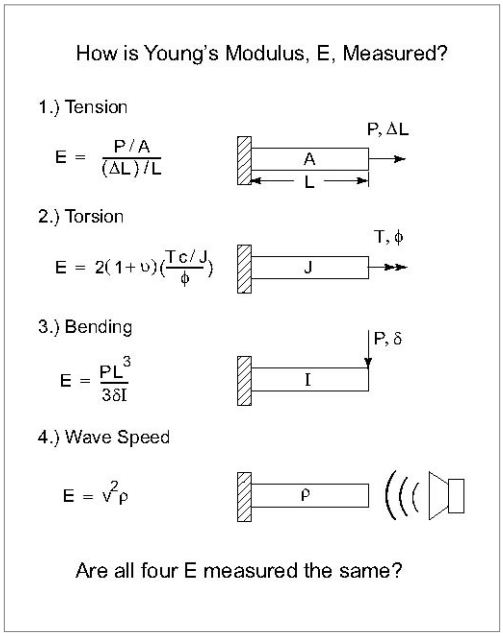

Linear Elastic Behavior (Hooke's Law)

"As the extension, so the force" [Hooke 1660] suggested a simple linear relation exists between force (stress) and deflection (strain). For a steel spring under small strain, this means that the force is the product of the stiffness and the deflection or, the deflection can be obtained by dividing the force by the spring stiffness. This relation is valid as long as the spring remains linear elastic, and the deflections are such that they do not cause the spring to yield or break. Apply twice the load, obtain twice the deflection. For a linear spring, the typical force-displacement (or stress-strain) plot is thus a straight line, where the stiffness represents the slope. While we may think Hooke's Law is simple, let's examine how to measure Young's modulus. What test should we use: tension, torsion, bending, wave speed? Performing these four tests shall yield four different values of Young's modulus for the same material, since the material knows nothing about Hooke's Law or these simple formulas. We must be careful in what we seek, how it is measured, and how what we measure is used in analysis. Changing the material from steel to rubber, the force-displacement curve is no longer linear; stress is never proportional to strain.

Hyperelastic (Neo-Hookean Law)

It is very instructive to view the stress-strain behavior for rubber. Here a tensile test is preformed on a synthetic rubber called EPDM (Ethylene Propylene Diene Monomer) cycled to 10%, 20%, 50% and 100% strain with each cycle repeated twice. The stress-strain behavior of rubber is very different from Hooke's Law in four basic areas. First, as the rubber is deformed into a larger strain territory for the first time, it is very stiff, but upon recycling in this same strain territory, the rubber softens dramatically. This phenomenon is often referred to as the Mullins' effect. In most applications this one time very stiff event is usually discarded where it is assumed in these applications repetitive behavior will dominate. Nonlinear elasticity has several stress and strain measures (Appendix B), however, it is most common to measure elastomeric experimental data using engineering stress and engineering strain measures, whereby the engineering stress is the current force is divided by the original area, and the engineering strain is the change in length divided by the original length. All test data presented and discussed herein will use engineering stress and engineering strain measures.

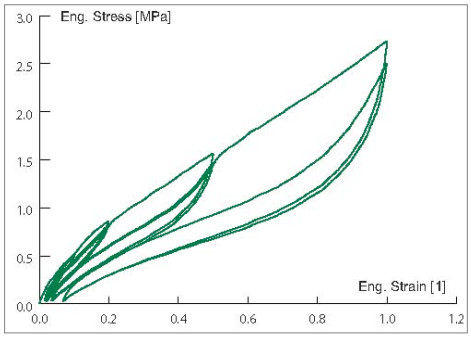

Secondly, there is always a viscoelastic effect present in rubber leading to a stable hysteresis loop when cycled over the same strain range. Hyperelastic models seek to find a simple equilibrium curve, not a hysteresis loop because viscoelastic effects may be

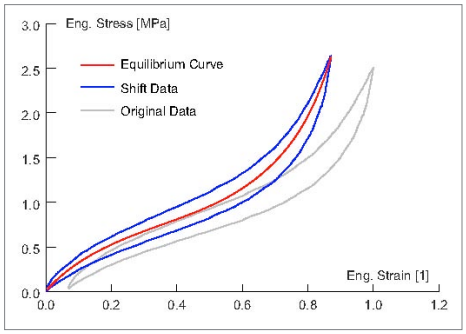

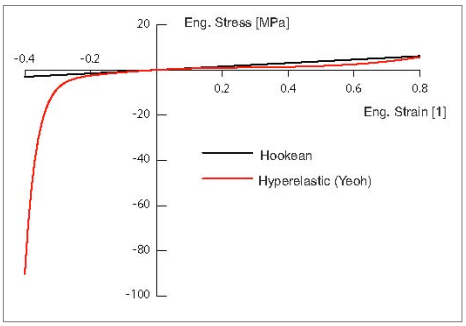

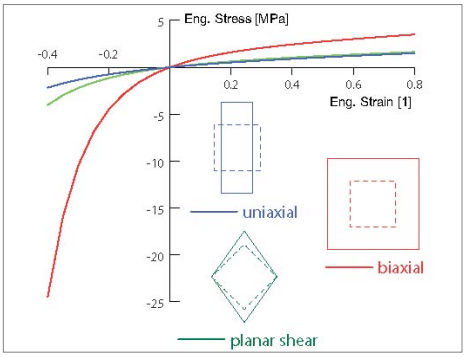

included as we shall see later. Also discarded with the "one time" stiffness event is the shifting of the data to go through the origin, a requirement for hyperelastic materials; this will cause an apparent change in gage length and original cross sectional area. This shift ignores irreversible damage in the material when first stretched.

The third area of difference between hyperelastic laws and Hooke's law, is the enormous difference between tension and compression of hyperelastic materials. Hooke's law always assumes that stress is proportional to strain, whereas this is never observed for elastomeric materials, hence Hooke's law is inadequate for rubber. The incompressibility of rubber with its ratio of bulk to shear modulus over 1,000 times larger than steel, causes the larger stress magnitudes in compression as compared to tension for the same strain magnitude.

The final difference between hyperelastic laws (there are many) and Hooke's law is the sensitivity of the hyperelastic constants to deformation states. As Treloar [1975] points out, any comprehensive treatment of rubber behavior should address these different strain states. For example, uniaxial, biaxial and planar shear are show here with their corresponding stress-strain responses. As the hyperelastic laws become more sophisticated with more constants to be determined experimentally, data from these three modes becomes more important to prevent spurious analytical behavior not observed experimentally. If you only have one mode, say tension, stick to the Neo-Hookean (one constant Mooney), Gent or Arruda-Boyce hyperelastic material models to be safe.

2.1 TIME-INDEPENDENT NONLINEAR ELASTICITY

This section discusses aspects of nonlinear elasticity: namely, strain energy density functions and incompressibility constraint. The strain energy density is usually represented as a product of two functions, one that depends on strain (or stretch ratio), another that depends on time. This section is referring to only that function of the product that depends on strain.

Stretch Ratio

Strain is the intensity of deformation. If we pull a slender rubber rod along its length, the stretch ratio, λ, (or stretch) is defined as the ratio of the deformed gauge length L divided by the initial gauge length L_0, namely, $\lambda = L / L_0 = (L_0 + L - L_0) / L_0 = 1 + (L - L_0) / L_0 = 1 - e$, where e is the engineering strain. Generally, if we apply an in-plane, biaxial load to a piece of rubber, we can define three principal stretch ratios in the three respective principal directions. In large deformation analysis of nonlinear materials (such as elastomers), the stretch ratios are a convenient measure of deformation and are used to define strain invariants, I_j for $j = 1,3$, which are used in many strain energy functions.

Strain Energy Density Functions

Elastomeric material models are characterized by different forms of their strain energy (density) functions. Such a material is also called hyperelastic. Implicit in the use of these functions (usually denoted by W) is the assumption that the material is isotropic and elastic. If we take the derivative of W with respect to strain, we obtain the stress, the intensity of force. The commonly available strain energy functions have been represented either in terms of the strain invariants which are functions of the stretch ratios or directly in terms of the stretch ratios themselves. The three strain invariants can be expressed as:

$$I_1 = \lambda_1^2 + \lambda_2^2 + \lambda_3^2$$
$$I_2 = \lambda_1^2\lambda_2^2 + \lambda_2^2\lambda_3^2 + \lambda_3^2\lambda_1^2$$
$$I_3 = \lambda_1^2\lambda_2^2\lambda_3^2$$

In case of perfectly incompressible material, $I_3 - 1$. In Marc, the strain energy function is composed of a deviatoric (shear) and dilitational (volumetric) component as: $W_{total} = W + W_{dilitation}$, where the dilitational part, W, is of most concern for elastomers, whereas the dilitation component is of most concern for foams. We shall discuss the deviatoric component first.

From statistical mechanics and thermodynamics principals, the simplest model of rubber elasticity is the Neo-Hookean model represented by a strain energy density of: $W = c_{10}(I_1 - 3)$.

This model exhibits a single modulus $(2C_{10} = G)$, and gives a good correlation with the experimental data up to 40% strain in uniaxial tension and up to 90% strains in simple shear. Let's now suppose our uniaxial rod above is stretched so $\lambda_1 = \lambda$ where λ is an arbitrary stretch along the rods length. Furthermore if our rod is incompressible, then $\lambda_2 = \lambda_3 = 1/\sqrt{\lambda}$ so that $\lambda_1^2\lambda_2^2\lambda_3^2 = 1$. Assuming a Neo-Hookean material, the rod would have a strain energy density function of:

$$W = C_{10}(I_1 - 3) = C_{10}(\lambda_1^2 + \lambda_2^2 + \lambda_3^2 - 3) = C_{10}\left(\lambda^2 \frac{2}{\lambda} - 3\right)$$

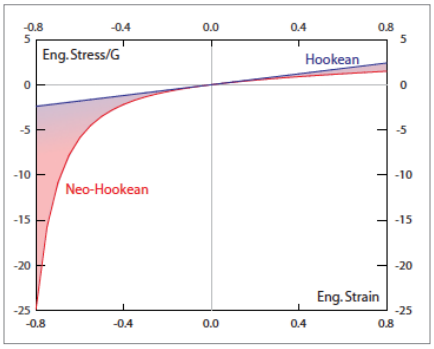

and the stress becomes:

$$\sigma = \frac{\partial W}{\partial \lambda} = 2C_{10}\left(\lambda^2 + \frac{2}{\lambda} - 3\right)$$

Plotting stress versus strain for our Neo-Hookean rod along side a Hookean rod (whose Poisson's ratio is 0.5, so Young's modulus becomes), has the linear Hookean behavior tangent at the origin to the Neo-Hookean curve. Notice how much compression differs from tension for Neo-Hookean behavior.

The earliest phenomenological theory of nonlinear elasticity was proposed by Mooney as: $W = C_{10}(I_1 - 3) + C_{01}(I_2 - 3)$.

Although, it shows a good agreement with tensile test data up to 100% strains, it has been found inadequate in describing the compression mode of deformation. Moreover, the Mooney-Rivlin model fails to account for the hardening of the material at large strains.

Tschoegl's investigations [Tschoegl, 1971] underscored the fact that the retention of higher order terms in the generalized Mooney-Rivlin polynomial function of strain energy led to a better agreement with test data for both unfilled as well as filled rubbers. The models along these lines incorporated in Marc are:

Three term Mooney-Rivlin:

$$W = C_{10}(I_1 - 3) + C_{01}(I_2 - 3) + C_{11}(I_1 - 3)(I_2 - 3)$$

Signiorini:

$$W = C_{10}(I_1 - 3) + C_{01}(I_2 - 3) + C_{20}(I_1 - 3)^2$$

Third Order Invariant:

$$W = C_{10}(I_1 - 3) + C_{01}(I_2 - 3) + C_{11}(I_1 - 3) + C_{20}(I_1 - 3)^2$$

Third Order Deformation (or James-Green-Simpson):

$$W = C_{10}(I_1 - 3) + C_{01}(I_2 - 3) + C_{11}(I_1 - 3) + C_{20}(I_1 - 3)^2 + C_{30}(I_1 - 3)^2$$

This family of polynomial strain energy functions has been generalized to a complete 5th order, namely:

$$W = \sum_{i=1}^{5}\sum_{j=1}^{5} C_{ij}(I_1 - 3)^i (I_2 - 3)^j$$

All the models listed above account for non-constant shear modulus. However, caution needs to be exercised on inclusion of higher order terms to fit the data, since this may result in unstable energy functions yielding nonphysical results outside the range of the experimental data. Please see Appendix B for issues regarding material stability.

The Yeoh model differs from the above higher order models in that it depends on the first strain invariant only:

$$W = C_{10}(I_1 - 3) + C^{20}(I_1 - 3)^2 + C_{30}(I_1 - 3)^3$$

This model is more versatile than the others since it has been demonstrated to fit various modes of deformation using the data obtained from a uniaxial tension test only for certain rubber compounds. This leads to reduced requirements on material testing. However, caution needs to be exercised when applying this model for deformations involving low strains [Yeoh, 1995]. The Arruda-Boyce model claims to ameliorate this defect and is unique since the standard tensile test data provides sufficient accuracy for multiple modes of deformation at all strain levels.

In the Arruda-Boyce and Gent strain energy models, the underlying molecular structure of elastomer is represented to simulate the non-Gaussian behavior of individual chains in the network thus representing the physics of network deformation, as such they are called micro-mechanical models.

The Arruda-Boyce model is described as:

$$W = nk\Theta\left[\frac{1}{2}(I_1 - 3) + \frac{1}{20N}(I_1^2 - 9) + \frac{11}{1050N^2}(I_1^3 - 27) + \frac{19}{7000N^3}(I_1^4 - 81) + \frac{519}{673750N^4}(I_1^5 - 243)\right]$$

where n is the chain density, k is the Boltzmann constant, Θ is the temperature and N is the number of statistical links of length 1 in the chain between chemical crosslinks.

The constitutive relation from Gent can be represented as:

$$W = \frac{-EI_m}{6}\log\left[\frac{I_m - 1_1^*}{I_m}\right]$$

where E is the small-strain tensile modulus, $I_1^* = I_1 - 3$ and I_m is the maximum value of I_1^* that the molecular network can attain.

Ogden proposed the energy function as separable functions of principal stretches, which is implemented in Marc in its generalized form as:

$$W = \sum_{n-1}^{N} \frac{\mu_n}{\alpha_n} J^{\frac{-\alpha_n}{3}} (\lambda_1^{\alpha_n} + \lambda_2^{\alpha_n} + \lambda_3^{\alpha_n} - 3)$$

where J, is the Jacobian measuring dilatancy, defined as the determinant of deformation gradient F (Appendix B). The Neo-Hookean, Mooney-Rivlin, and Varga material models can be recovered as special cases from the Ogden model. The model gives a good correlation with test data in simple tension up to 700%. The model accommodates non-constant shear modulus and slightly compressible material behavior. Also, for $\alpha < 2$ or > 2, the material softens or stiffens respectively with increasing strain. The Ogden model has become quite popular; it has been successfully applied to the analysis of O-rings, seals and other industrial products. Other strain energy functions include *Klesner-Segel, Hart-Smith, Gent-Thomas*, and *Valanis-Landel* for modeling the nonlinear elastic response.

While the above classical representations of the strain energy function indicate no volumetric changes occur, three different models have been incorporated facilitating different levels of compressibility. The simplest is to introduce a constant bulk modulus such that, $W_{dilitation} = 4.5(J-1)^2$. The second form is to introduce a fifth order volumetric strain energy function:

$$W_{dilitation} = \sum_{n=1}^{5} D_n (J-1)2^n$$

Finally, for materials going through large volumetric deformations, several models have been suggested; for example, Blatz-Ko's, Penn's, and Storaker's. Marc has adopted the foam model for compressible materials with the following representation:

$$W_{total} = \sum_{n=1}^{N} \frac{\mu_n}{\alpha_n}\left(\lambda_1^{a_n} + \lambda_2^{a_n} + \lambda_3^{a_n} - 3\right) + \sum_{n=1}^{N} \frac{\mu_n}{\beta_n}\left(I - J^{\beta_n}\right)$$

where α_n, μ_n, and β_n are material constants, and the second term represents volumetric change. This model [Hill-1978, Storakers-1986] with $n = 2$ provides good correspondence with data in uniaxial and equibiaxial tension. The Blatz-Ko model [Blatz and Ko, 1968] proposed for polymers and compressible foam-like materials is a subcase of above model with $n = 2$.

Editor's Comment: Many hyperelastic models have been proposed since Ronald Rivlin began with the Neo-Hookean model in 1948, some of these models proclaim needing only one test, usually tension. If that model only has one modulus, that one test claim is most likely correct. However, should that hyperelastic model require several moduli, politely ignore the claim and test other deformation modes. What single test can simultaneously determine both Young's modulus and the shear modulus for a Hookean material? - None. Be skeptical of such claims particularly for the phenomenological hyperelastic models.

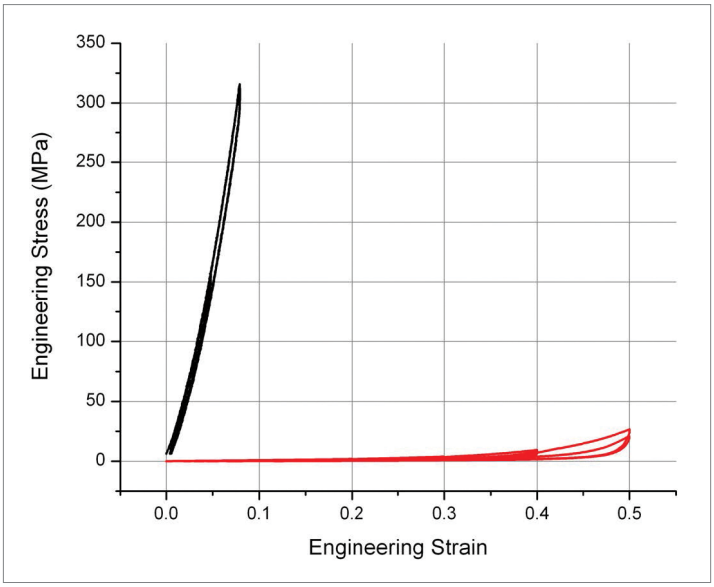

Incompressible Behavior

Exact (or total) incompressibility literally means the material exhibits zero volumetric change (*isochoric*) under hydrostatic pressure. The pressure in the material is not related to the strain in the material; it is an indeterminate quantity as far as the stress-strain relationship is concerned. Poisson's ratio is exactly one-half, while the bulk modulus is infinite. Mathematically, the incompressibility of the material can be represented by: $I_3 = 1$, $\lambda_1\lambda_2\lambda_3 = 1$, and $\det F = 1$, where F is the deformation gradient (Appendix B).

Incompressibility was first considered in FEA by [Herrmann, 1965]. Analytical difficulties arise when it is combined with nonlinearities such as large displacements, large strains, and contact. "Near incompressibility" means that Poisson's ratio is not exactly one-half; for example, 0.49+. Perfect incompressibility is an idealization to make modeling more amenable for obtaining closed form solutions. In the real world, natural as well as filled rubbers are slightly compressible, thereby, facilitating development of algorithms with greater numerical stability. Special formulation for lower-order triangular and tetrahedral elements satisfying the LBB condition (Appendix B) or simply the Babuska-Brezzi stability condition effectively handles analysis of incompressible materials [Liu, Choudhry, Wertheimer, 1997]. These elements exist in Marc and show a very close correlation of results when compared to their quadrilateral or hexahedral counterparts.

In addition to rubber problems, the engineer may also encounter aspects of incompressibility in metal plasticity and fluid mechanics (Stokes flow) problems. Appendix B provides more details about the FEA of incompressible materials, and gives an overview of analytical approaches.

WHITEPAPER

MSC Software: Case Study - A

O-Ring Under Compression

Most people had probably never heard of an "O-ring"—until the failure of an O-ring was blamed for the *Challenger* disaster in January, 1986. In the subsequent televised failure investigation, we witnessed (the late) Professor Richard Feynman of California Institute of Technology dipping a small O-ring into a glass of ice water to dramatize its change in properties with temperature.

This study demonstrates only one of the complexities involved in analyzing 2-D rubber contact, where an axisymmetric model of an O-ring seal is first compressed by three rigid surfaces, then loaded uniformly with a distributed pressure. The O-ring has an inner radius of 10 cm and an outer radius of 13.5 cm, and is bounded by three contact surfaces. During the first 20 increments, the top surface moves down in the radial direction of a total distance of 0.2 cm, compressing the O-ring. During the subsequent 50 increments, a total pressure load of 2 MPa is applied in the Z-direction, compressing the O-ring against the opposite contact surface. The deformed shapes, equivalent Cauchy stress contours and the final contact force distribution are shown below. The *Ogden* material parameters are assigned values of:

$\mu_1 = 0.63$ MPa, $\mu_2 = 0.0012$ MPa, $\mu_3 = 0.01$ MPa, $a_1 = 1.3$, $a_2 = 5.0$, and $a_3 = 2.0$ (see Section 2).

At the end of increment 70, the originally circular cross-section of the O-ring has filled the rectangular region on the right while remaining circular on the left (where the pressure loading is applied).

This type of elastomeric analysis may encounter instability problems because of the large compressive stresses; the solution algorithm in the FEA code must be able to pinpoint such difficulties during the analysis and follow alternative paths. Otherwise, the FEA code may give incorrect results!

The O-ring is also analyzed using a 2-term *Mooney-Rivlin* model. It is found that the CPU and memory usage are about the same per iteration as for the 3-term Ogden model.

Notes: For this type of rubber contact analysis, the nonlinear FEA code must be able to handle "deformable-to-rigid" contact, the incompressibility of the material, friction, mesh distortions (especially at the two corners), and potential instability problems as the analysis progresses. The important point to note about this example is that the applied pressure is many times larger than the shear stiffness ($\sim 10\mu_1$). Although the analysis is 2-D, the solution of this rubber problem is not trivial.

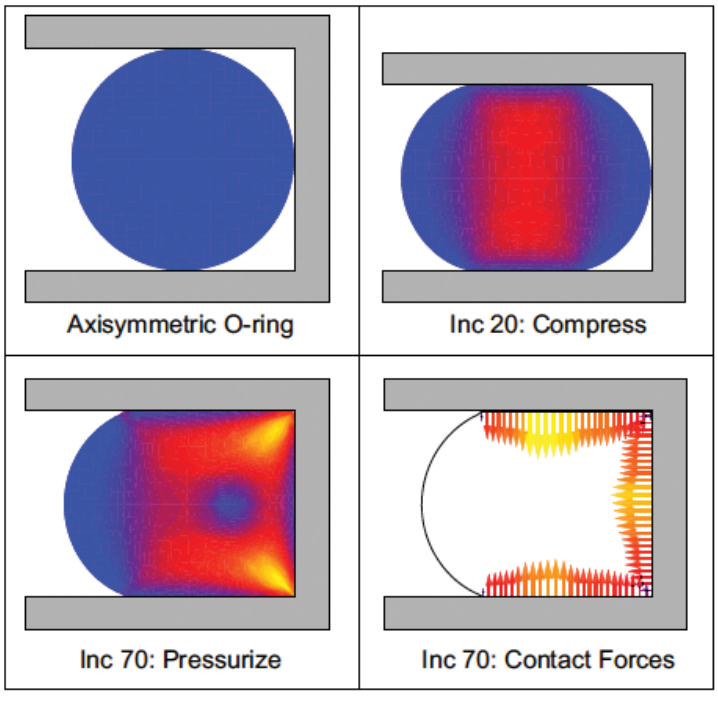

2.2. VISCOELASTICITY

This section introduces the concept of viscoelasticity and mentions some important mechanisms through which temperature and fillers influence rubber behavior. Rubber exhibits a rate-dependent behavior and can be modeled as a viscoelastic material, with its properties depending on both temperature and time. When unloaded, it eventually returns to the original, undeformed state. When subjected to a constant stress, it creeps. When given a prescribed strain, the stress decreases with time; this phenomenon is called stress relaxation. Hysteresis refers to the different stress-strain relationship during unloading (as compared to the loading process) in such materials when the material is subjected to cyclic loading (see Section 2.4). Collectively, these features of hysteresis, creep, and relaxation—all dependent upon temperature—are often called features of "viscoelasticity" [See the texts by Fung-1965, Christensen-1982, and Ferry-1970.]

Linear Viscoelasticity

Linear viscoelasticity refers to a theory which follows the linear superposition principle, where the relaxation rate is proportional to the instantaneous stress. Experimental data shows that "classical" linear viscoelasticity (applicable to a few percent strain) represents the behavior of many materials at small strains. In this case, the instantaneous stress is also proportional to the strain. Details of the material test data fitting, to determine input data required for viscoelastic analysis (such as calculating the necessary Prony series coefficients for a relaxation curve), are discussed in Section 3.

Mechanical models are often used to discuss the viscoelastic behavior of materials. The first is the Maxwell model, which consists of a spring and a viscous dashpot (damper) in series. The sudden application of a load induces an immediate deflection of the elastic spring, which is followed by "creep" of the dashpot. On the other hand, a sudden deformation produces an immediate reaction by the spring, which is followed by stress relaxation according to an exponential law. The second is the Kelvin (also called Voigt or Kelvin-Voigt) model, which consists of a spring and dashpot in parallel. A sudden application of force produces no immediate deflection, because the dashpot (arranged in parallel with the spring) will not move instantaneously. Instead, a deformation builds up gradually, while the spring assumes an increasing share of the load. The dashpot displacement relaxes exponentially. A third model is the standard linear solid, which is a combination of two springs and a dashpot as shown. Its behavior is a combination of the Maxwell and Kelvin models. Creep functions and relaxation functions for these three models are also shown [Fung, 1981]. The Marc program features a more comprehensive mechanical model called the Generalized Maxwell model, which is an exponential or Prony series representation of the stress relaxation function. This model contains, as special cases, the Maxwell, Kelvin, and standard linear solid models.

Nonlinear Viscoelasticity

Nonlinear viscoelastic behavior may result when the strain is large. A finite strain viscoelastic model may be derived by generalizing linear viscoelasticity in the sense that the 2nd Piola-Kirchhoff stress is substituted for engineering stress, and Green Lagrange strain is used instead of engineering strain. The viscoelasticity can be isotropic or anisotropic. In practice, modified forms of the Mooney-Rivlin, Ogden, and other polynomial strain energy functions are implemented in nonlinear FEA codes. The finite strain viscoelastic model with damage [Simo, 1987] has been implemented in Marc.

Temperature Effects

Temperature effects are extremely important in the analysis of elastomers, and affect all aspects of rubber behavior, including viscoelasticity, hysteresis, and damage. Temperature has three effects: (1) temperature change causes thermal strains, which must be combined with mechanical strains, (2) material moduli have different values at different temperatures, (3) heat

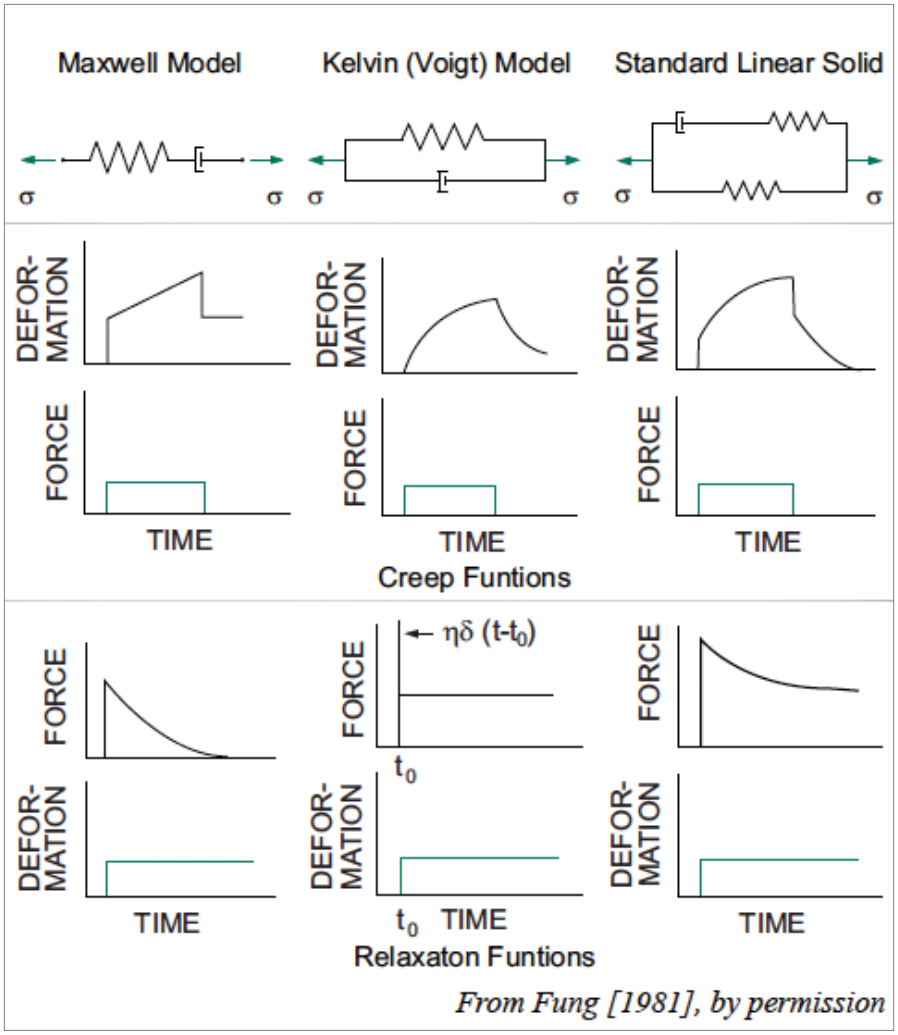

flow may occur. A modern nonlinear FEA code such as Marc accounts for heat flow and offers the capability to conduct coupled thermo-mechanical analysis. In other words, the analyst uses the same finite element model for both the thermal and stress analyses, and both thermal and force equilibrium are satisfied in each increment before the nonlinear analysis proceeds to the next increment.

Material constants associated with the strain rate independent mechanical response, such as Mooney-Rivlin, Ogden and rubber foam constants, vary with temperature, as do the coefficient of thermal expansion, Poisson's ratio, thermal conductivity, etc. The time-dependent phenomena of creep and relaxation also depend on temperature. The viscoelastic analysis is thus temperature-dependent. In contact problems, friction produces heat, which would be included in the analysis. Another important consideration is the heat generation of rubber components in dynamic applications, since after each deformation cycle some fraction of the elastic energy is dissipated as heat due to viscoelasticity. (Dynamic applications are discussed in Section 5.)

A large class of materials exhibit a particular type of viscoelastic behavior which is classified as thermo-rheologically simple (TRS). TRS materials are plastics or glass which exhibit in their stress relaxation function a logarithmic translational property change with a shift in temperature (as shown in the figure). This shift in time t as a function of temperature T is described by the so-called "shift function". An example of such a shift function is the Williams-Landel-Ferry shift. The WLF-shift function depends on the glass transition temperature of the polymer [Williams et. al., 1955]. (The Marc code allows TRS-materials for both linear and large strain viscoelasticity.) Another well-known shift function is the BKZ-shift [Bernstein, Kearsley, and Zapa, 1963]. Note that with TRS materials, the relaxation function is independent of the temperature at very small times—which implies that the instantaneous properties are not temperature dependent.

For glass-like materials, a multi-parameter viscoelastic model incorporating the memory-effect and nonlinear structured relaxation behavior [Narayanaswamy, 1970] has been implemented in Marc. The model also predicts the evolution of physical properties of glass subjected to complex, arbitrary time-temperature histories. This includes the nonlinear volumetric swelling that is observed during typical glass forming operations.

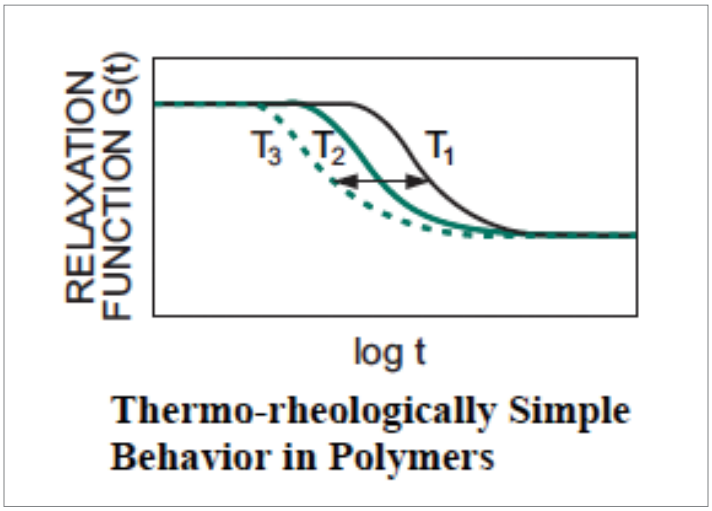

Thermo-rheologically Simple Behavior in Polymers

2.3. COMPOSITES

Rubber composites can be classified as particulate, laminated, or fibrous depending on their construction. It is well known, that such composites usually exhibit highly anisotropic response due to directionality in material properties.

The most commonly available particulate composites are filled elastomers where the carbon black particles are dispersed in a network of polymeric chains. Fillers are added to rubber products such as car tires and shock mounts to enhance their stiffness and toughness properties. Common fillers include carbon black and silica where the carbon particles range in size from a few hundred to thousands of angstroms. They influence the dynamic and damping behavior of rubber in a very complex and nonproportional manner. The unique behavior of carbon black-filled elastomers results due to a rigid, particulate phase and the interaction of the elastomer chains with this phase [Bauer and Crossland, 1990]. Unlike unfilled rubbers, the relaxation rate (in filled rubbers) is not proportional to the stress, and one may need a general nonlinear finite-strain time-dependent theory. Current research on the characterization of filled rubber shows promising results [Yeoh, 1990]. Yeoh derived a third-order strain energy density function which does not depend on the second strain invariant; features a shear modulus that can change with deformation; and can represent both tension and compression behavior equally well. Unfortunately, among the existing strain energy functions, both the polynomial as well as Ogden models are unable to capture the sharp decrease in shear modulus for filled rubbers at small strains.

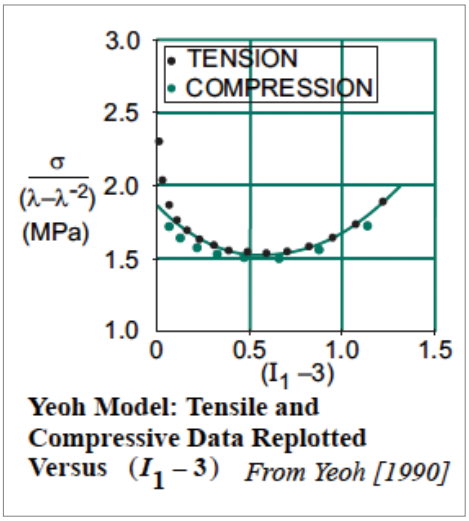

Yeoh Model: Tensile and Compressive Data Replotted Versus $(I_1 - 3)$ *From Yeoh [1990]*

On the computational side, a numerically efficient phenomenological model has been developed to analyze carbon black-filled rubber which accounts for the Mullins' effect [Govindjee and Simo, 1992]. This damage model has been extended to include the Ogden strain energy function; results agree well with experimental data for cyclic tension tests with quasi-static loading rates. Marc offers a damage model capability in conjunction with the large strain viscoelastic model for all strain energy functions. This makes it an extremely useful tool to simulate the energy dissipation or hysteresis in filled rubbers.

Laminated composites occur in rubber/steel plate bearings used for seismic base isolation of buildings and bridges where horizontal flexibility coupled with vertical rigidity is desired (right - shear strain contours). Another area of application is composite sheet metal forming where a layer of rubber may be sandwiched between two metal sheets for desired stiffness and damping characteristics. Computationally, this problem is handled by Marc using a nonlinear elasticity model within a total or updated Lagrangian framework for the rubber while resorting to large deformation

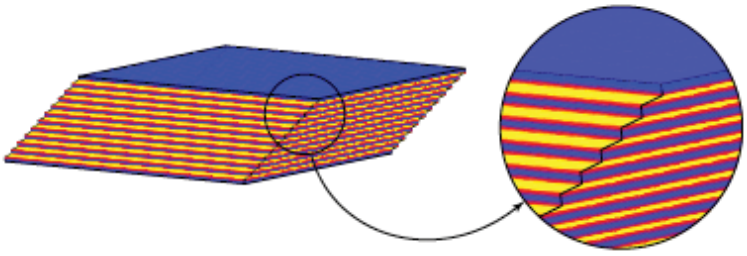

Laminated Rubber/Steel Shock Isolation Bearing in Shear *From Billings and Shepherd [1992]*

plasticity within an updated Lagrangian framework for the metallic sheets. Laminated structures can be modeled using the lower- or higher-order continuum composite elements in Marc. The standard failure criterion for composite materials can be used in analysis with brittle materials.

An important class of composites arises due to the presence of textile or steel cords in the rubber matrix [Clark, 1981]. Applications of such composites can be found in tires, air springs, shock isolators, and hoses. Such composites pose a challenge, both from a manufacturing perspective, where adhesion of the fibers to the rubber matrix can occur, as well as from a numerical point of view in which numerical ill-conditioning can occur due to stiffness differential between rubber and cords. Such cord reinforced rubber composites can be modeled using the membrane or continuum rebar elements [Liu, Choudhry, and Wertheimer, 1997].

Typical cord-rubber composites have a fiber to matrix modulus ratio of 104 - 106: 1. This gives rise to an internal constraint of near-inextensibility of cords which is analogous to the near-incompressibility of rubber. Such composites have a volume fraction of cords less than a typical stiff fiber composite (used in aerospace applications). This is primarily to provide added flexibility to the system and to prevent frictional sliding between the cords in large deformation situations. Adding further complications is the fact that the cords themselves are composed of twisted filaments. This rise to a bimodular system dependent on the tension or compression due to microbuckling of the fibers. Material modeling of such composites has traditionally been carried out by smearing or averaging out material properties over the domain of the composite structure. [Walter-Patel, 1979] have shown good correlation of the experimental data with Halpin-Tsai, Gough-Tangorra, and Akasaka-Hirano equations to derive equivalent mechanical properties for cord-rubber composites.

Marc offers several options to model the large strain behavior of cord-rubber composites. The most popular ones include modeling the composite plies as anisotropic membranes sandwiched between continuum or brick elements representing the rubber. If the composite structure is thin, anisotropic layered shell elements provide a viable option. Likewise, the rebar element, designed originally for concrete reinforced with steel rods and then extended for cord-rubber composites has recently gained popularity due to its computational economy.

On a final note, although the phenomenological theories of elastomers are quite satisfactory in the gross design of structures, they cannot be expected to accurately model microscopic effects such as debonding, cracks, and free-edge effects.

Table 1
Modulus Ratio Comparisons for Rigid and Flexible Composites

Filamentary composite system	Reinforcement modulus, E_c (GPa)	Matrix modulus, E_r (GPa)	Longitudinal ply modulus, E_1 (GPa)	Transverse ply modulus, E_2 (GPa)	Modulus ratio, E_c/E_r	Anisotropy, E_1/E_2
Glass-epoxy	75.0	3.4000	50.0	18.000	22.0	2.8
Graphite-epoxy	250.0	3.4000	200.0	5.200	74.0	38.0
Nylon-rubber	3.5	0.0055	1.1	0.014	640.0	79.0
Rayon-rubber	5.1	0.0055	1.7	0.014	930.0	120.0
Steel-rubber	83.0	0.0140	18.0	0.021	5,900.0	860.0

E_1 and E_2 are calculated at volume fractions typical of use for the different composites.

WHITEPAPER

MSC Software: Case Study - B

Car Tire

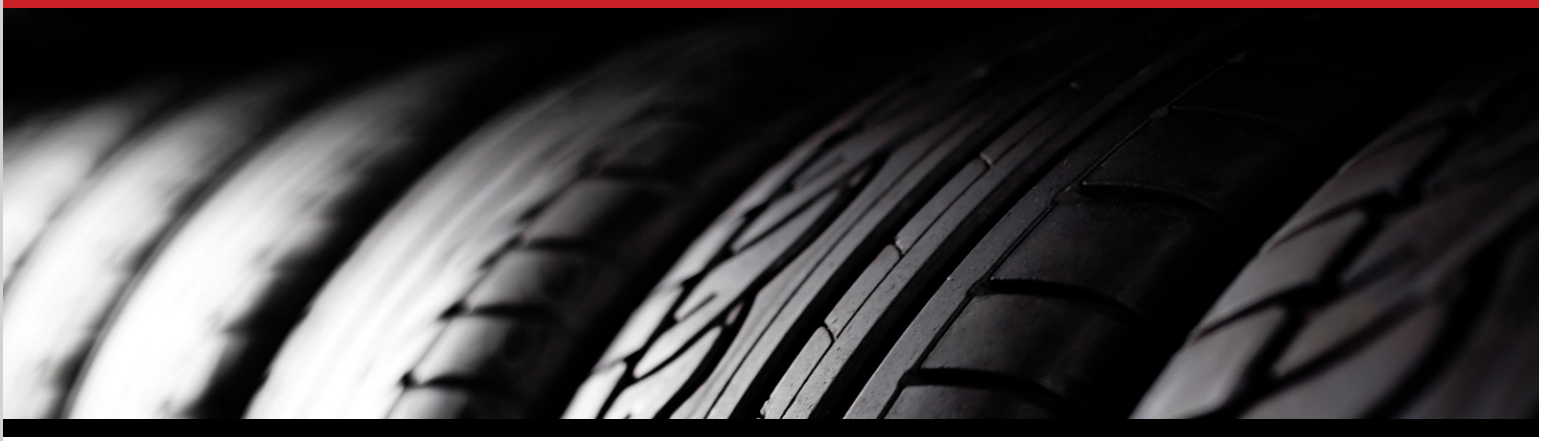

Analyzing the interaction of an automobile tire with the road is one of the most challenging problems in computational mechanics today. It is a very complex 3-D contact analysis, involving a complicated shape (tire cross section), composite materials (comprised of polyester or steel cords, steel wire beads, and rubber—leading to anisotropic behavior), uncertain loading conditions (mounting loads, inflation pressure, car weight, side impact, hitting a curb, temperature effects for a car cruising, etc.), and large deformations. Friction, dynamic, and fatigue effects are also important. All leading tire manufacturers use nonlinear FEA to help design safer and better tires...but none has, as of yet, abandoned full-scale testing. Finite element analysis allows them to minimize the number of prototypes required by eliminating designs which are not structurally correct or optimal.

The tire (right) is modeled using rubber continuum elements, a collection of 15 different isotropic and orthotropic materials. The metal wheel is modeled with continuum elements. The road is assumed to be rigid. The complete load history consists of: mounting the tire on the rim; internal pressurization up to 1.5 bar; applying the axial car load; and rolling down the road. The deformed tire shape is shown, and the contours are of the displacement magnitude as the tire begins rolling to the left. A good tire model is, by definition, very complex and typically consists of hundreds of thousands of 3-D elements.

Notes: In addition to the complexities of tire analysis mentioned here, car and tire manufacturers also need to worry about: occasional "buckling" of the bead region; tire wear for different tread designs; noise transmitted to the passenger cabin; ride comfort; tire puncture by a nail or glass; and traction effects due to rain, snow, and ice. Passenger safety, manufacturability at reasonable cost, and tire life are the most important design objectives.

Contact Bodies and Mesh

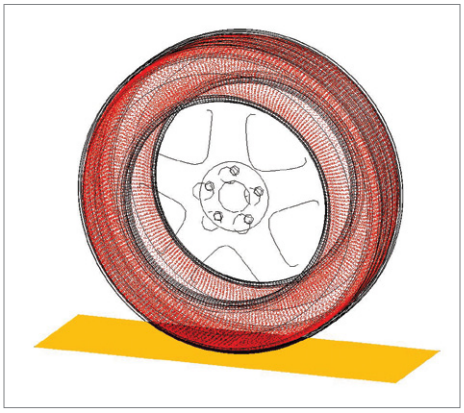

Orientations

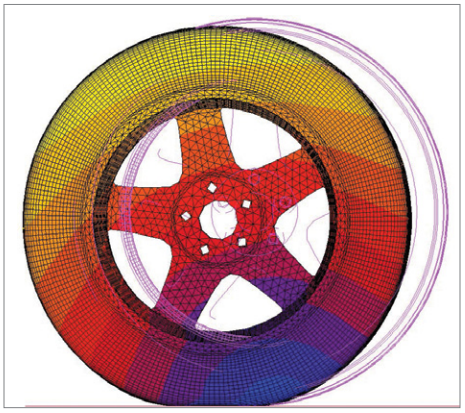

Displacement Contours

2.4. HYSTERESIS

Under cyclic loading, rubber dissipates energy—due to hysteresis effects. The steady-state response is quite different from the initial response. Filled rubber undergoes so-called stress-induced softening (sometimes referred to as damage), a phenomenon caused by a breakdown of crosslinks and a progressive detachment of rubber molecules from the surfaces of reinforcing fillers. Although rubber will stiffen under load in certain situations, here we will only discuss the more common case of rubber softening. A typical one-cycle force-extension plot for rubber in biaxial tension is shown on the right.

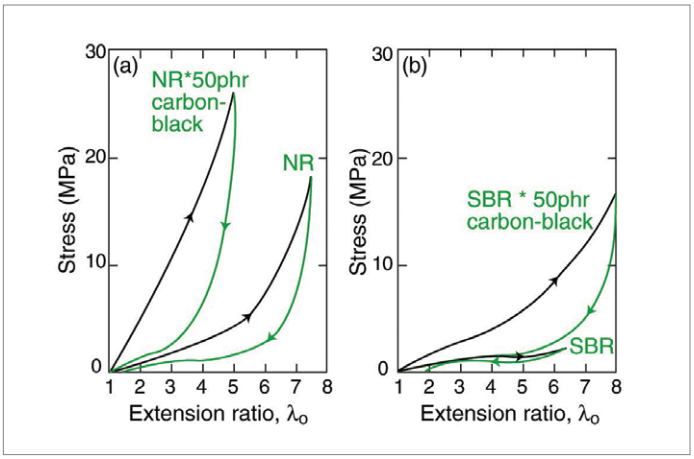

Fracture Behavior of Polymers

The five primary, underlying mechanisms responsible for hysteresis of rubber are:

1. Internal Friction

The internal friction is primarily a result of rearrangement of the molecular structure under applied load and subsequent sliding of chains, past each other. The phenomenon of internal friction or internal viscosity is highly temperature dependent and its temperature dependence may be described by the concept of flow viscosity. The flow viscosity, η_v, decreases as temperature increases and at temperature $T > T_g$, it is related to its value at the glass transition temperature, T_g, typically given by the Williams-Landel-Ferry equation:

$$\log \frac{\eta_v(T)}{\eta_v(T_g)} = \frac{-C_1(T - T_g)}{C_2 + T - T_g}$$

An increase in temperature results in increased chain mobility, thereby, leading to decreased viscosity and reduced hysteresis. Presence of particulate filler, for example, carbon black, leads to decreased segmental mobility and hence increased viscosity and increased hysteresis.

2. Strain-induced Crystallization

Large extension and retraction of elastomeric material gives rise to formation and melting of crystallized regions. Such a strain-induced crystallization produces hysteresis effects. During the retraction phase, the stress relaxation rate usually exceeds the rate at which the molecular chains disorient leading to an extended period of crystallization. In this regard, an unfilled natural rubber exhibits more hysteresis than its unfilled synthetic counterpart as shown in the figure.

3. Stress Softening

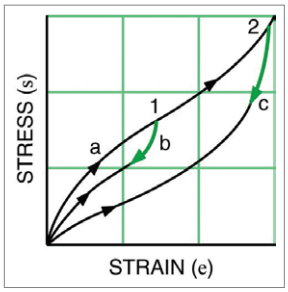

Cyclic Tension Test Demonstrating Mullins' Effect

Modification and reformation of rubber network structures in the initial loading stages can show a lower stiffness and changes in damping characteristics. This strain-induced stress softening in carbon black-filled rubbers is called the Mullins' effect [Mullins-1969; Simo-1987; Govindjee and Simo, 1992] although, such a phenomenon has been observed in unfilled rubbers also. It manifests itself as history-dependent stiffness. The uniaxial stress-strain curve remains insensitive at strains above the previous achieved maximum, but experiences a substantial softening below this maximum strain. The larger the previously attained maximum, the larger the subsequent loss of stiffness. In a cyclic test, the material is loaded in tension to a strain state labeled "1" along path "a".

If the material is again loaded, the stress-strain curve now follows path "b" to point "1" and not path "a". If additional loading is applied, path "a" is followed to a point labeled "2". Upon unloading, path "c" is followed, thereby resulting in an even greater loss of stiffness in the material. Features contributing to the stress-softening behavior include the modification and reformation of rubber network structures involve chemical effects, microstructural damage, multi-chain damage, and microvoid formation. These mechanisms are considerably enhanced by strain amplification caused by rigid particles in filled rubbers.

4. Structural Breakdown

In a filled rubber with carbon black filler particles, the carbon black particles tend to form a loose reticulated structure because of their surface activity or mutual interactions. They are also interlaced by the network of rubber chain molecules which are crosslinked during vulcanization. The breakdown of these aggregates, and of the matrix/filler interfacial bonds due to loading, gives rise to hysteresis.

5. Domain Deformation

Viscoelastic stress analysis of two-phase systems [Radok and Tai, 1962] has shown that dispersed inclusions or domains in a viscoelastic medium contribute to an increase in the energy loss even when the domains are themselves perfectly elastic in nature. In some instances, however, the domains are themselves capable of exhibiting energy dissipating mechanism. Certain elastomers also contain domains of dispersed hard inelastic inclusions. Such rubbers exhibit an inelastic deformation leading to permanent set due to shear yielding and typically show very high levels of hysteresis.

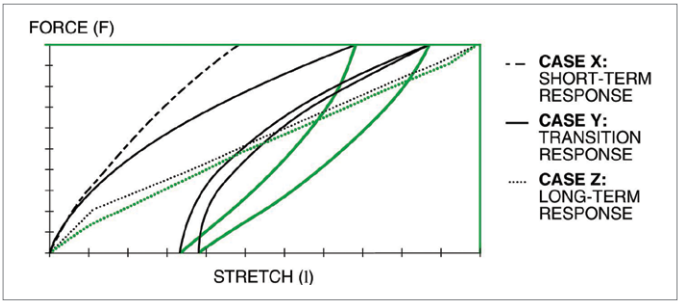

Hysteresis Effects in Rubber

Finally an example of hysteresis due to large-strain viscoelasticity is demonstrated here for three rubber samples with identical static behavior but different time-dependent behavior [Konter et al., 1991]. A series of identical load histories with constant time steps are applied: first, loading in 10 steps of 0.1 second; next, unloading of 10 steps of 0.1 second; then, loading another 10 steps of 0.1 second, etc. Calculations show very different behavior for the three samples. Case X exhibits a "short term response" behavior—with a high stiffness. Case Y shows a "transition" type of behavior, with an initial increase in displacement followed by a cycle around a "permanent set". (This permanent set is caused by rubber network modification and reformation, which is primarily developed during the initial loading.) Case Z exhibits a typical "long term response" behavior—with a lower stiffness.

2.5. OTHER POLYMERIC MATERIALS

Many of the concepts used to analyze rubber behavior are also applicable to glass, plastics, foams, solid propellants, and biomaterials [Harper, 1982]. These include: large deformations, strain energy density functions, near incompressibility, and viscoelastic effects. Here, we'll briefly note some important considerations in the modeling and design/analysis of these materials.

BIOMATERIALS include human tissues and polymeric materials used in modern medical/dental implants and devices (for example, cardiac pacemaker seals, filled dental composite resins). Plastics and other synthetic polymeric materials are viscoelastic. Human tissues may also be treated as viscoelastic materials; these include blood vessels, heart muscles, articular cartilage, mucus, saliva, etc. [Fung, 1981]. They creep and relax. Many of the concepts introduced in this White Paper are also applicable to biomechanics studies. These include, for instance: curve-fitting of test data to determine material parameters for FEA, viscoelastic modeling, response of a viscoelastic body to harmonic excitation, large deformations, hysteresis and softening; and so forth. The figure shows typical room-temperature stress-strain curves in loading and unloading for four species. Notice that, in all four cases, softening occurs and the unloading behavior is different from the loading behavior (as in the case of rubber).

CURVE	ANIMAL	L_0(cm)	STRAIN RATE (cm/min)
A	RABBIT	2.39	0.5
B	DOG	1.93	0.5
C	GUINEA	2.04	0.5
D	HUMAN	1.47	1.0

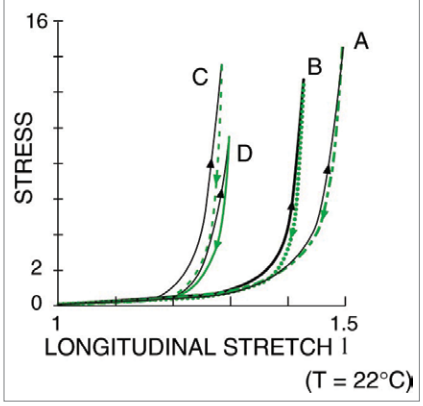

Typical Stress/Strain Curves in Loading and Unloading for Four Species
From Fung [1981], by permission

FOAMS, often made of polyurethane, are soft and spongy. Techniques now exist for making three-dimensional cellular solids out of polymers, metals, ceramics, and even glasses. Man-made foams, manufactured on a large scale, are used for absorbing the energy of impacts (in packaging and crash protection) and in lightweight structures (in the cores of sandwich panels, for instance). Unlike rubber, foam products are highly compressible, and are porous with a large portion of the volume being air. Elastomeric foams are fully elastic (resilient), metal foams may have plastic yield, and ceramic foams are brittle and crushable. Resilient foams are used for car seats, mattresses, shipping insulation materials, and other applications which undergo repeated loading where light weight and high compliance is desirable. Some foams (for example, rigid polymer foams) show plastic yielding in compression but are brittle in tension

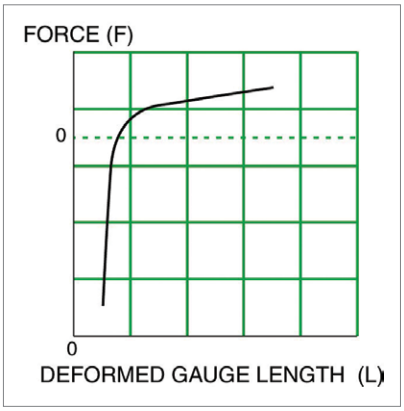

Blatz Ko Model for Foams

Crushable foams are used widely in shock-isolation structures and components. These are sometimes analyzed by "foam plasticity" models. In compression, volumetric deformations are related to cell wall buckling processes. It is assumed that the resulting deformation is not recoverable instantaneously and the process can be idealized as elastic-plastic. In tension, these cell walls break easily, and the resulting tensile strength of the foam is much smaller than the compressive strength. Strain rate sensitivity is also significant for such foams.

GLASS is brittle, isotropic, and viscoelastic. Crack initiation and propagation are important concerns (even though most glass products are not ordinarily used as load-carrying members). Like concrete and plastics, glass creeps with time.

The proper FEA of glass products must pay attention to several important characteristics of glass when considering various forming processes and environmental conditions. (1) Glass exhibits an abrupt transition from its fluid to its glassy state—known as the glass transition temperature.

(2) Transient residual stresses are developed during manufacturing, thus requiring a time-dependent analysis. (3) For safety reasons, many common glass products (such as car windshields and show doors) are tempered: in which the glass is intentionally heated, then cooled in a controlled manner to develop a thin surface layer under compressive stress, in order to resist crack propagation and tension-induced cracking. (4) For optical applications such as lenses and mirrors, the curvature of the surface and its birefringence are of crucial importance. Here, the critical design parameter is deflection, not stress. (5) In hostile environments, such as those faced by solar heliostats in deserts, the adhesive bond cementing the mirror to its substrate is highly susceptible to deterioration by ultraviolet radiation, intense heat, moisture, etc.—usually leading to a change of the mirror's intended curvature or flatness after continued exposure. (6) Many glass products in their service life experience a combination of thermal and mechanical loads, thus requiring a coupled thermo-mechanical analysis as part of the design procedure.

PLASTICS behave similarly to rubber in some aspects, but differently in others. For instance, plastics and rubber exhibit no real linear region in their stress-strain behavior except at very small strains. Load duration and temperature greatly influence the behavior of both. Like elastomers, plastics are viscoelastic materials. Both are dependent on strain rate. Although, while the elastomers typically undergo large deformations even at room temperature, plastics usually do not.

Additional complications arise in the characterization of plastics. Two generic types of plastics exist: thermosets and thermoplastics. Thermosets (such as phenolics) are formed by chemical reaction at high temperatures. When reheated, they resist degradation up to very high temperatures with minimal changes in properties. However, at extremely elevated temperatures, this type of plastic will char and decompose. At this point, the thermal and mechanical properties degrade dramatically. Phenolic materials are often used in thermal protection systems. Thermoplastics, when heated, will soften and then melt. The metamorphosis is more continuous. The relative variation in properties is more significant for thermoplastics than thermosets for temperatures below the point at which the latter decomposes. Thermoplastics generally exhibit a broad "glass transition" range over which the material behaves in a viscoelastic manner. This behavior is contrasted with thermosets that exhibit an abrupt transition. Some plastics (such as certain polyethylenes) deform inelastically and may be analyzed with standard metal plasticity models (for example, Drucker-Prager model). One important distinction from a modeling standpoint is that plastics, unlike most metals, behave differently in tension and compression. In this respect, plastics are similar to rubber and composite materials.

The proper FEA of plastic products requires the analyst to be aware of certain important characteristics of plastics. (1) The plastic forming process (for example, injection molding) results in a deformed shape with residual stresses. Coupled thermal-mechanical analysis is necessary, and automated contact analysis becomes very important. Properties are dependent upon temperature and time. (2) "Non-equilibrium" rapid heating and cooling effects are also important. In this respect, plastics are similar to glass. For most plastics, the bulk modulus and coefficient of thermal expansion are known to be sensitive to pressure. (3) Before actual cracking, a phenomenon called crazing often occurs. This is associated with localized regions where polymer chains have become excessively stretched due to high local stress concentrations. Rupture is most often initiated there. Crazing is associated with a region of altered density which is detrimental to the desired optical or aesthetic qualities of plastic products such as transparent utensils and containers. (4) Birefringence is important, as for glass. (5) Plastics are also susceptible to damage due to hostile environments, such as ultraviolet radiation and steam. Plastic products used in sterilization and autoclave applications often fail due to steam effects. They exhibit significant reduction in ductility with continued exposure to steam. (6) In some cases, linear FEA may be satisfactory when designing plastic materials under low-level loading and low strains. However, for those problems involving large deformations, buckling/postbuckling, contact/impact, high loading, or where residual stresses are to be determined, nonlinear FEA is a must.

Snap Fit of Plastic Part

WHITEPAPER

MSC Software: Case Study - C

Constant-Velocity Rubber Boot Compression and Bending

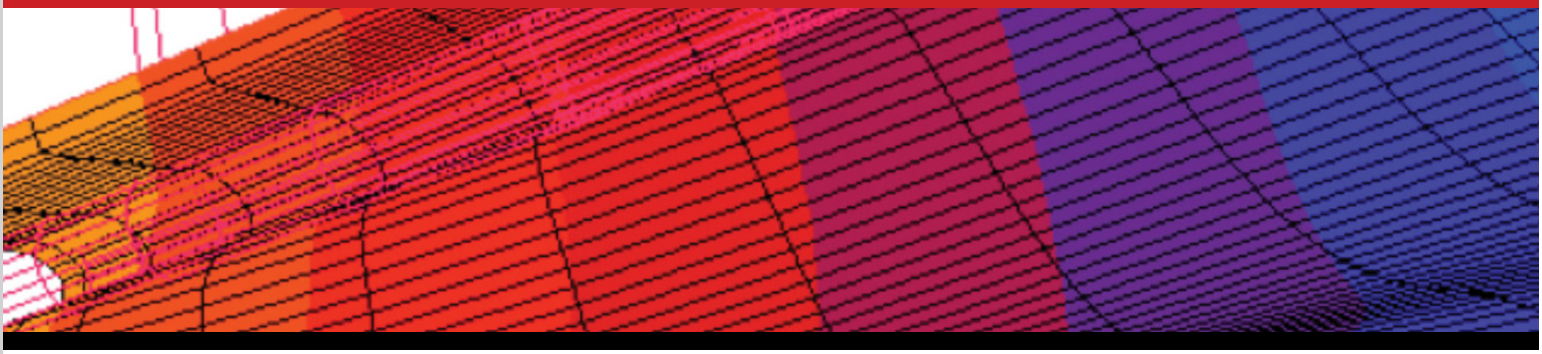

Rubber boots are used in many industries to protect flexible connections between two bodies. The boot itself should have enough stiffness to retain its shape; on the other hand, it must not have too much stiffness so as to interfere with the flexible connection. In the automotive industry, "constant-velocity" joints on drive shafts are usually sealed with rubber boots in order to keep dirt and moisture out. These rubber boots are designed to accommodate the maximum possible swing angles at the joint, and to compensate for changes in the shaft length. Proper design dictates that during bending and axial movements, the individual bellows of the boot must not come into contact with each other, because the resultant wear would produce failure of the rubber. Such undesirable contact would mean abrasion during rotation of the shaft, leading to premature failure of the joint. Local buckling can also occur in one of the bellows.

The FEA of rubber boots presents many interesting features: (1) large displacements; (2) large strains; (3) incompressible material behavior; (4) susceptibility to local buckling; and (5) varying boundary conditions caused by the 3-D contact between various parts of the boot. Proper design should also consider bellows shape optimization, fatigue life, maintainability and replaceability, and cost.

This example (panels a-d) shows the analysis of the axial compression and bending of a rubber boot. The boot is clamped on one side to a rigid surface, and on the other side to a translating and rotating shaft. Axial compression is first applied (panel b), followed by bending (panels c-d). The Cauchy stress contours on the deformed shapes are shown for the axial compression and rotation of the shaft. Once in place, the shaft rotates and the boot must rotate about the axis of the shaft in the tilted position.

Notes: One leading U. S. rubber boot manufacturer has applied such 3-D contact analysis techniques to evaluate and optimize new boot designs (one design has a longitudinal seam to facilitate installation). Improved fatigue life was the design goal, and nonlinear FEA was successfully used to minimize time and cost—and come up with a boot design which achieved an acceptable product life cycle. The analysis was correlated with test results, and showed that a modified design with a seam attained a similar fatigue life as the original design (without a seam). The new design with a seam substantially reduced the installation costs. Note that "do-it-yourself" kits using this split boot design are now available to replace worn-out boots.

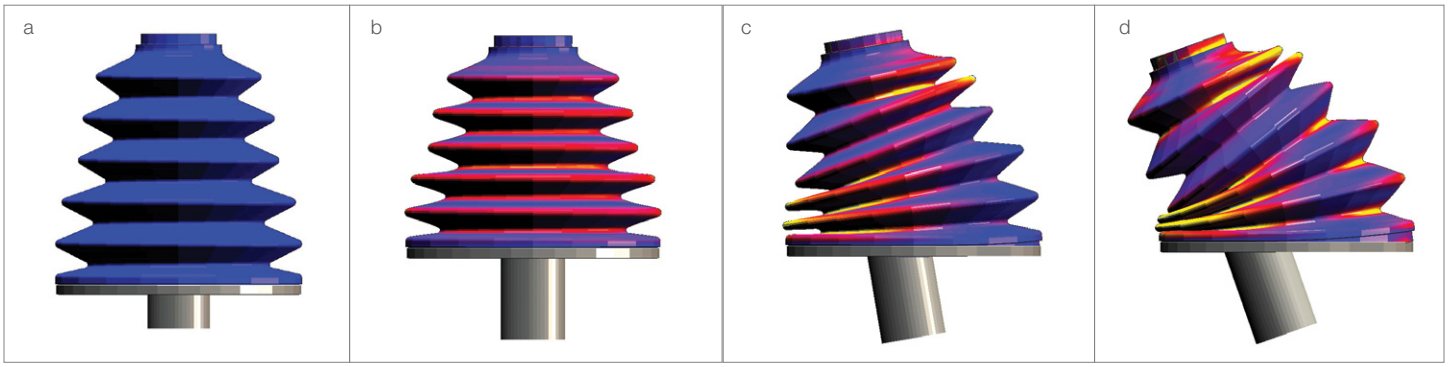

Cauchy Stress Contours

3. DETERMINATION OF MATERIAL PARAMETERS FROM TEST DATA

Successful modeling and design of rubber components hinges on the selection of an appropriate strain energy function, and accurate determination of material constants in the function. Appendix C describes the tests required to characterize the mechanical response of a polymeric material. Marc offers the capability to evaluate the material constants for nonlinear elastic and viscoelastic materials in its graphical user interface, Mentat.

Rubber Elasticity

For time-independent nonlinear elasticity, the fitting procedure may be carried out for polynomial representations of incompressible materials, the generalized Ogden model for slightly compressible materials, and the Foam model for compressible materials. Six different types of experiments are supported: uniaxial tension, uniaxial compression, equibiaxial, planar shear, simple shear, and volumetric tests. The significance of (non-equivalent) multiple tests for material modeling cannot be overemphasized. In general, a combination of uniaxial tension/compression and simple shear is required in the very least. Data from equibiaxial tension or planar shear may also be needed depending on the deformation modes of the structure. Volumetric data must be included for materials undergoing large compressible deformations, for example, foams. Also, the curve fitting in Mentat allows a combined input of more than one test to obtain the appropriate material constants.

After selecting appropriate test data for the application and adjusting the data to become comply with hyperelastic assumptions (see Appendix C), typical behavior of many elastomeric materials have stress-strain curves as shown here. This particular data set came from a silicone rubber where each of the three strain states or deformation modes (biaxial, planar shear, and tension) have decreasing stresses for the same strain level.

Mentat computes the constants of any of the ten hyperelastic strain energy functions using all the adjusted data from any of the one to six different types of experiments mentioned above simultaneously. Once the constants of the selected hyperelastic material are determined, Mentat will plot both the data and curve fit together, including any modes not tested to facilitate selecting the best curve fit. Other than a rubber band, or balloon, most rubber applications experience mixed deformation modes, and a good fit must take more than one deformation mode into consideration as we shall see.

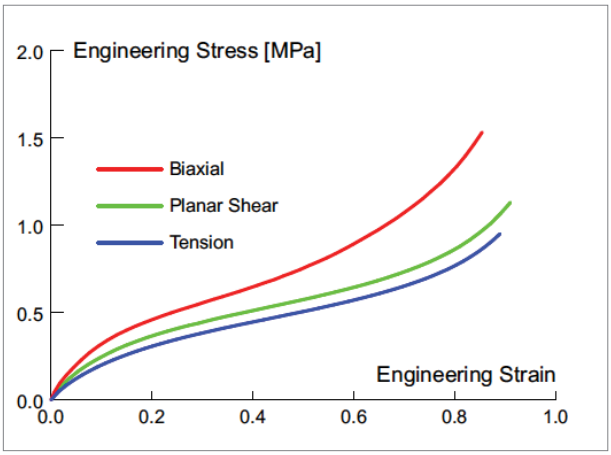

The importance of performing multiple mode tests is to assure that hyperelastic model predicts the correct behavior of other modes. The curve-fitting in Mentat shows how other (non-measured) modes would behave. The example here shows how what appears to be a great tension fit for a 2 term Ogden material greatly overpredicts the biaxial and planar response. More sophisticated hyperelastic materials seeking more constants require more modes to be tested.

From a mathematical point of view, determining the material constants for an incompressible material is relatively easy, since they follow from the least squares method in a straight forward fashion. However, the material constants may turn out to be negative and therefore physically not meaningful. The phenomenon is a numerical serendipity and not a fundamental material behavior. In this case, a constrained optimization process can be invoked, based on sequential linear programming [Press, Tenkolsky, Vetterling, and Flannery, 1992] in order to obtain non-negative constants. Forcing positive constants for the “poor” 2 constant Ogden fit here, improves its behavior, but still biaxial and planar modes are too stiff. Of course, you really don’t know unless you test the other modes.

Automated facilities are available to help the user determine these material parameters from test data. The curve-fitting program is interactive and consists of four steps: (1) data entry—where the user inputs experimental data; (2) evaluation—where the program mathematically fits the data; (3) plotting/display—where the user sees graphical verification of the results and is able to observe the behavior beyond the test range; and (4) write—where the program automatically creates a data set and the necessary coefficients for the strain energy density function of choice. Typical curve-fitting results are shown.

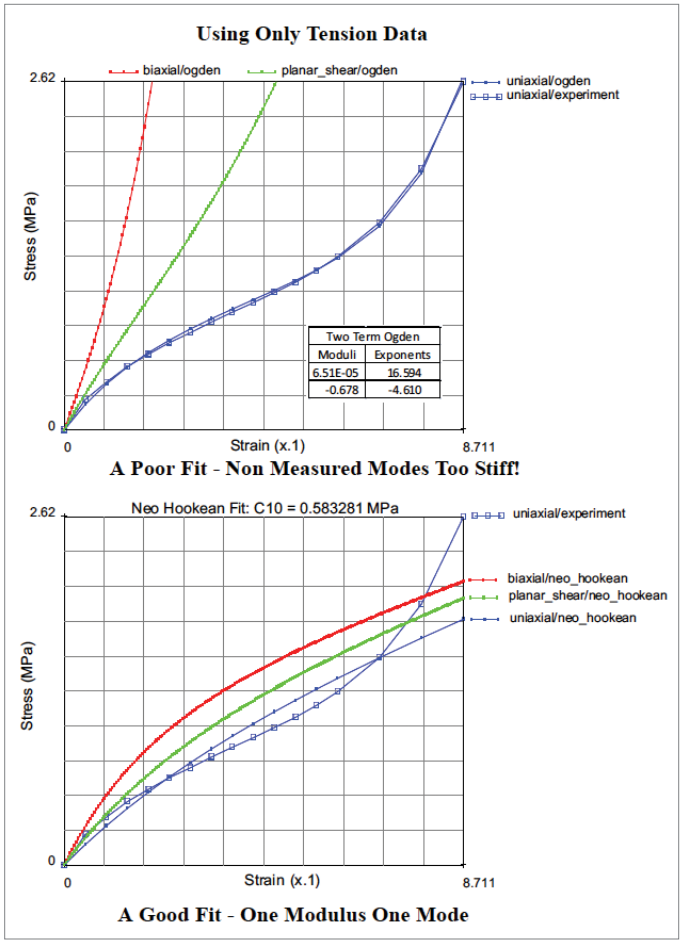

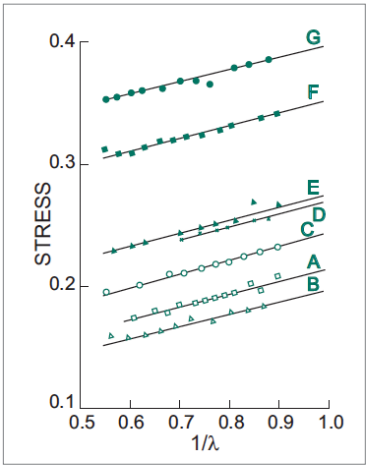

Example 1: Determination ofMooney-RivlinConstants for VulcanizedRubber in Simple Tension

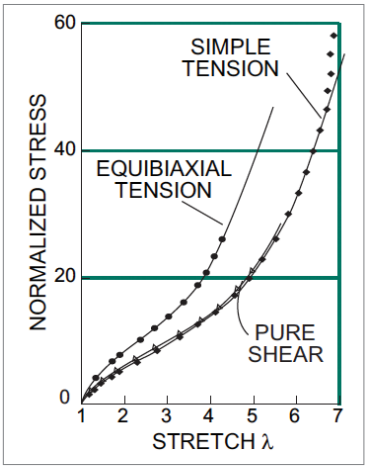

Example 2: Correlation of 3-Term Ogden Model with Treloar'sData in Simple Tension, simple Shear, and Equibiaxial Tension *From Ogden [1972]*

For the generalized Ogden as well as the Foam model (principle stretch-based models), the material constants follow from a set of nonlinear equations and the data is fitted based on the Downhill-Simpson algorithm.

Example 1: Determining Mooney-rivlin Constants

The figure on the right shows typical Mooney plots for various vulcanized rubbers in simple extension. The fitted lines are straight, with constant slope C_{01}, and intercepts C_{10}, which typically vary according to the degree of vulcanization or crosslinking.

Example 2: Determining Ogden Constants

The figure on the right shows how a 3-term Ogden model compares with Treloar's data [Treloar, 1975] in simple tension, simple shear, and biaxial tension. The Ogden constants in this case were determined to be [for details, see Ogden, 1972]:

$\mu_1 = 0.63$ MPa, $\mu_2 = 0.0012$ MPa, $\mu_3 = 0.01$ MPa

$\alpha_1 = 1.3$, $\alpha_2 = 5.0$, $\alpha_3 = 2.0$

For this example, it is clear that the 3-term Ogden model gives the best fit. Practically, more than a 3-term Ogden model is rarely used.

Example 3: Determining Rubber Foam Constants

The figure on the right shows how a 3-term rubber foam model fits a rubber foam in uniaxial compression. The coefficients were determined to be:

$\mu_1 = 1.11765$ MPa, $\mu_2 = 1.11983$ MPa, $\mu_3 = 0.125023x10^{-4}$ MPa

$\alpha_1 = 7.83173$, $\alpha_2 = 0.715832$, $\alpha_3 = 7.00243$

$\beta_1 = -5.41755$, $\beta_2 = -5.41684$, $\beta_2 = -6.85885$

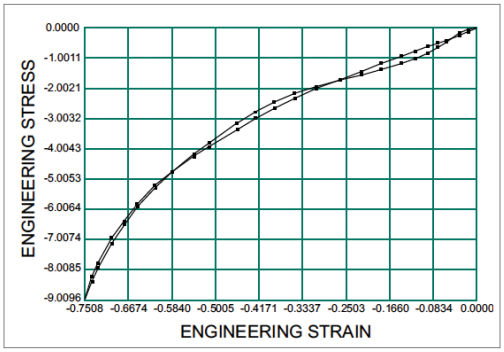

Example 3: Curve Fit to Foam Data

Viscoelasticity

The data representing a time-dependent or viscoelastic response of materials can be approximated by a Prony series, based on a relaxation or creep test. If the deformation is large, a relaxation test is more accurate. If the data is obtained from a creep test, a Prony series inversion must be performed before using it as an input to Marc. For a linear viscoelastic material, either the shear and bulk moduli, or the Young's modulus and Poisson's ratio may be expressed in terms of a Prony series. For large strain viscoelasticity, the elastic strain energy or the stress is expressed in terms of Prony series. Mentat attempts to fit the entered data based on a procedure described in [Daubisse, 1986].

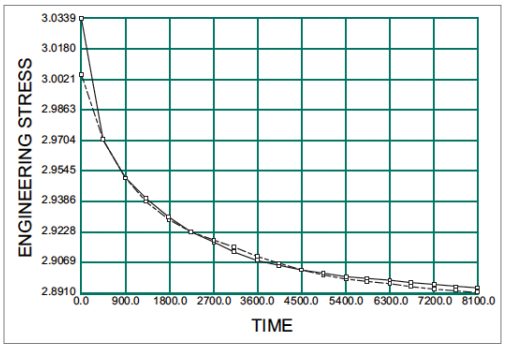

Example 4: Curve Fit to Viscoelastic Relaxation Data

Example 4: Determining Viscoelastic Constants

The figure on the right shows a typical stress-time plot for a large strain viscoelastic material in relaxation test. The Prony coefficients are obtained from fitting the relaxation test data.

4. DAMAGE AND FAILURE

The most important and perhaps the most difficult aspect of design analysis is failure prediction. Failure in rubber can occur because of flaws introduced during the manufacturing processes (for example, compound mixing, extrusion, molding, or vulcanization, etc.) or fatigue caused by service loads and/or material degradation due to environmental/mechanical/thermal conditions. Along these lines, [Simo, 1987] developed a damage model incorporated in a large-strain viscoelasticity framework to simulate the stiffness loss and energy dissipation in polymers. This model is currently implemented in Marc. Damage and Mullins' effect in filled polymers was simulated by Govindjee and Simo, using a fully micromechanical damage [1991] and continuum micromechanical damage [1992] models.

Recently, researchers have calculated tearing energy to simulate crack growth in an elastomeric material using the popular fracture mechanics concept of J-integral [Cheng and Becker, 1992]. Using the virtual crack extension method [Pidaparti, Yang, and Soedel, 1992] predicted the critical loads for crack growth. Also, the initiation and the initiation direction was found in good agreement with the experimental data for filled Styrene Butadiene Rubber. In a study of the fracture of bonded rubber blocks under compression, [Gent, Chang, and Leung, 1993] found that: (1) Under static compression, two modes of fracture are possible—circumferential tearing at or near the bonded edges, and splitting open of the free surface;

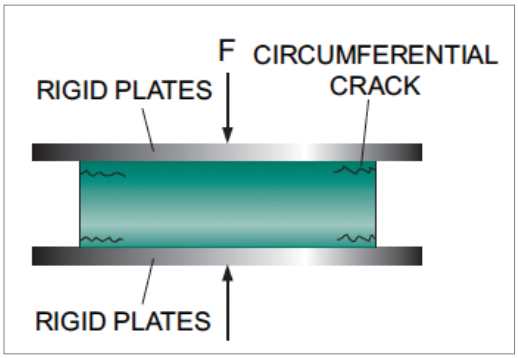

Tearing Near the Bonded Edges
From Gent et. al. [1992]

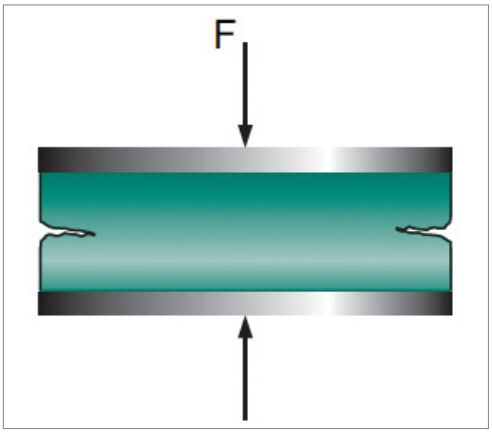

Splitting Open of the Free Surface
From Gent et. al. [1992]

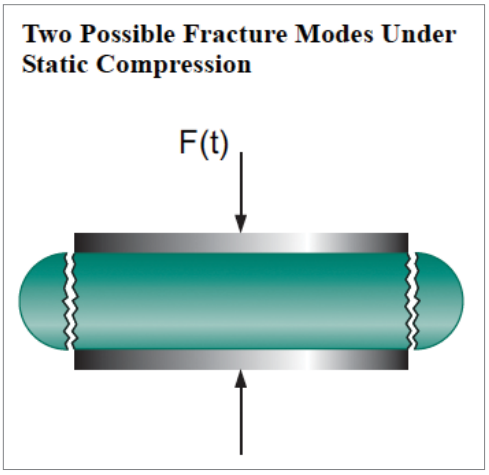

Fatigue Failure of BondedElastomer Block
From Gent et. al. [1992]

and, (2) under cyclic compression, the most likely fracture mode of the rubber is by crack propagation, breaking away the bulged volume.

For cord-reinforced composites, besides damage and fracture of the rubber matrix, the critical modes of failure are ply separation, debonding between layers of dissimilar materials, fiber pull-out due to lack of adhesion and microbuckling of cords. Besides mechanical loading, thermal and viscoelastic effects play a critical role in failure of cord-rubber composites. Frictional heating at cord-rubber interface and internal heat buildup due to hysteresis in rubber cause the temperature of the material to rise. Due to low thermal conductivity of rubber, the temperatures can rise to a very high value causing adhesion failures and microcracking in the rubber matrix. No good models exists currently in open literature to simulate the above failures.

5. DYNAMICS, VIBRATIONS, AND ACOUSTICS

A widespread use of rubber is for shock/vibration isolation and noise suppression in transportation vehicles, machinery, and buildings. These common rubber components include: snubbers, load bearing pads, engine mounts, bearings, bushings, air springs, bumpers, and so forth. Recent seismic isolation applications have seen increased usage of laminated rubber bearings for the foundation designs of buildings, highway and bridge structures (especially in the United States and Japan). These applications take advantage of well-known characteristics of rubber: energy absorption and damping, flexibility, resilience, long service life, and moldability.

A dynamic analysis is required whenever inertial effects are important, for example, high speed rolling of tires or sudden loss of contact in a snap-through buckling analysis. When inertial effects are unimportant, such as for engine mounts and building bearings, performing a dynamic analysis is unnecessary. When the viscous effects are important for such cases, a quasi-static analysis is performed to obtain the overall deformation which is followed by a harmonic analysis to obtain frequencies and mode shapes.

Damping

The nature of damping is complex and is still poorly understood. Common damping models include:

- **Proportional (Rayleigh) Damping**—assumes that damping may be decomposed as a linear combination of the stiffness and mass matrices.
- **Coulomb Damping**—or dry friction, comes from the motion of a body on a dry surface (for example, on the areas of support).
- **Viscous Damping**—occurs when a viscous fluid hinders the motion of the body. The damping forces are proportional to velocity in the equations of motion.
- **Joint Damping**—results from internal friction within the material or at connections between elements of a structural system.

Internal friction in the elastomer accounts for the damping nature of elastomeric parts. Because of the viscoelastic behavior of rubber, damping is dependent on frequency of the excitation. The presence of damping forces progressively reduces the amplitude of vibration, and ultimately stops the motion when all energy initially stored in the system is dissipated. Although it also exists in metals, damping is especially important in the design of rubber components. In the Maxwell and Kelvin models discussed in Section 2.2, damping is represented by the dashpot and is usually assumed to be a linear function of the velocity in the equations of motion. The treatment of damping in dynamics problems may be found in any book on vibrations or structural dynamics.

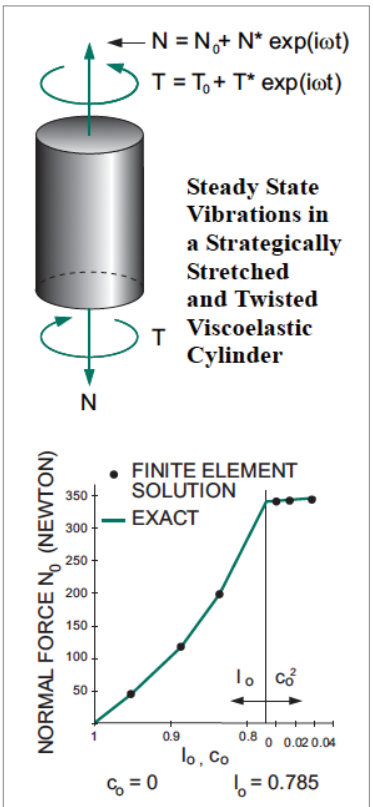

Finite Element Solution: Axial Force vs. Stretch Ratio

Modal Extraction

A popular, accurate and efficient modal (eigenvalue) extraction method for small to medium size problems in FEA codes is the Lanczos method. For full vehicle models, the automatic component modes synthesis or automated multilevel substructuring are effective for models with millions of degrees of freedom, when thousands of modes are extracted. For the case of proportional damping, real modes give useful information (the natural frequencies). In the case of nonproportional damping, complex modes result. Natural frequencies are dependent upon pre-stress and material properties; both of these would require nonlinear analysis. This factor is important in the design of isolation mounts for buildings.

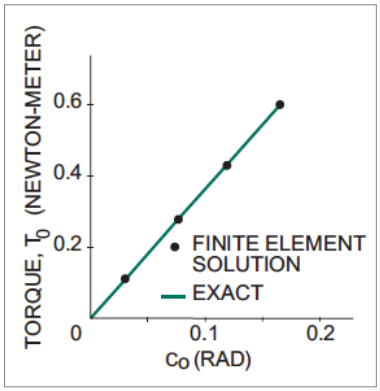

Finite Element Solution:Torque vs. Twist
From Morman and Nagtegaal [1983]

Small-amplitude Vibrations In Viscoelastic Solids: Use Of "phi-functions" and Time vs. Frequency Domain Analysis

In the analysis of an engine mount, it is often important to model small-amplitude vibrations superimposed upon a large initial deformation. The problem of small-amplitude vibrations of sinusoidally-excited deformed viscoelastic solids was studied by [Morman and Nagtegaal, 1983] using the so-called method of Phi-functions. The method was applied to improve the design of carbon black-filled butyl rubber body mounts and carbon black filled natural rubber suspension bushings in several car designs. The material was assumed to be isotropic, isothermal, incompressible, and behaving according to a "fading memory" finite-deformation linear viscoelasticity theory.

This method is available in the Marc code and uses the third-order invariant form of the James-Green-Simpson strain energy function. Morman and Nagtegaal's FEA results using Marc for the steady-state vibrations of a stretched and twisted viscoelastic cylinder which is subjected to a large initial deformation can be seen to agree well with observed results. The finite element model is a 30° wedge.

The same type of dynamic analysis of a viscoelastic body subjected to harmonic excitation may also be applied to many materials, including biomaterials such as human tissues [Fung, 1981].

Time vs. Frequency Domain Viscoelastic Analysis

In viscoelastic problems, both time and frequency domains are used. In time domain analysis, experimental data is required over the time domain of interest and a Prony series is usually used to represent the data. In frequency domain analysis, Laplace transform techniques and harmonic excitation are commonly used. The storage modulus and loss modulus are dependent upon frequency (and amplitude for filled rubbers), and one needs to be aware of the in-phase and out-of-phase concepts [Christensen, 1982]. In linear viscoelastic problems with harmonic loading, the behavior can be characterized in the frequency domain in terms of the storage and loss moduli as shown in the figure. Notice that in viscoelastic materials (assuming harmonic loading), the storage modulus typically increases with frequency, but the loss modulus first increases with frequency and then decreases to zero. As the frequency increases, the state of the rubber changes from an elastomer to a glass, with the maximum in the loss modulus signaling the transition to the glassy state. In unfilled rubbers, the storage and loss moduli are dependent on the frequency, but the former is largely independent on the strain amplitude. In filled rubbers, the storage modulus depends significantly on the strain amplitude.

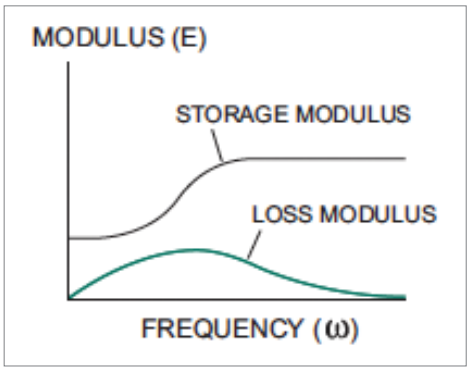

Frequency-Dependent
Storageand Loss Moduli

Direct Time Integration Methods

In transient nonlinear dynamics, both implicit and explicit direct integration methods are available for solving the equations of motion. Explicit methods include Central difference while the implicit schemes include Newmark-beta, Wilson-theta, Hilber-Hughes-Taylor, and Houbolt methods. The choice of whether to use an implicit or explicit method is very subtle and depends on: the nature of the dynamic problem and the material; the type of finite elements making up the model; and the magnitude of the speed of sound in the material.

Implicit Methods—In an implicit method, the nonlinear matrix equations of motion are solved at each time step to advance the solution. Treatment of boundary nonlinearities must occur within a time step. Large time steps may be used in implicit, dynamic analysis. Popular implicit methods (offered in several FEA codes) include: the Newmark-beta method, single-step and multi-step Houbolt, Hilbert-Hughes-Taylor, and the generalized Alpha method. These methods have different behavior in terms of stability, accuracy and damping. For oscillatory behavior, the time step should be a fraction of the period. For many problems, the adaptive time stepping procedure can be used advantageously.

As for the use of dynamic methods in viscoelastic analysis, no additional damping should be introduced because viscoelastic effects are already included in the material properties.

Explicit Method—In this method, the solution is advanced without forming a stiffness matrix, which makes the coding much simpler, reduces storage requirements, and improves computational efficiency. Explicit methods are conditionally stable for undamped linear systems. For a given time step, an explicit operator requires fewer computations per time step than an implicit one.

Explicit methods possess some known disadvantages, and it is important for users to bear in mind that a definite stability limit exists, which means that sometimes extremely small time steps may be required—resulting in higher computer costs. In nearly incompressible problems, the speed of sound in the material approaches infinity, and hence an extremely small time step is required. A common solution to overcome these numerical difficulties using explicit methods is to conjure up a scaled mass matrix—which is very often assumed to be diagonal. Finally, if Lagrange multipliers are included in the analysis, special formulations are required because they do not have any associated mass.

Coupled Acoustic-structural Analysis

Coupled acoustic-structural analysis is of great interest to the automobile industry. Typical application areas would include—determination of sound transmission in an enclosed deformable structural cavity; for example, interior noise level in a car compartment. A typical case is modeling the deformation of an automobile door seal by the glass window in order to analyze the static deformation (Case Study E) and conduct acoustic harmonic analysis. The eigenfrequencies, mode shapes, and pressure amplitude in the compartment thus calculated can be used to design better door seals. A coupled acoustic-structural analysis capability also exists in Marc.

In a coupled acoustic-structural analysis (see figure), both the acoustic medium and the structure are modeled. In this way, the effect of the acoustic medium on the dynamic response of the structure and of the structure on the dynamic response of the acoustic medium can be taken into account. Such a coupled analysis is especially important when the natural frequencies of the acoustic medium and the structure are in the same range. Since the interface between the acoustic medium and the structure is determined automatically by Marc based on the CONTACT option, setting up the finite element model is relatively easy since the meshes do not need to be identical at the interface. The ADAPT GLOBAL option may be used to remesh the acoustic regions when large deformations occur in the cavity walls.

This functionality is suited for modeling of coupled structural acoustics where the acoustic medium is undergoing small pressure vibrations. It is applicable to 'interior problems' (for example, deformable cavity) and can simulate a steady state harmonic response. Modeling of 'exterior problems' like acoustic radiation and scattering is not considered.

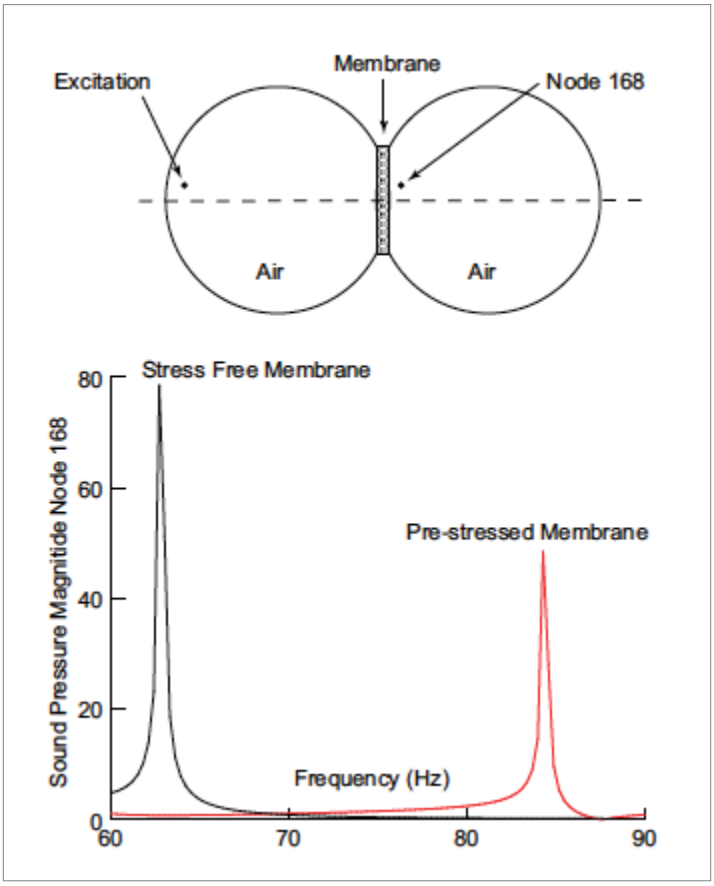

Coupled Structural - Acoustic Analysis

MSC Software: Case Study - D

Rubber Mount

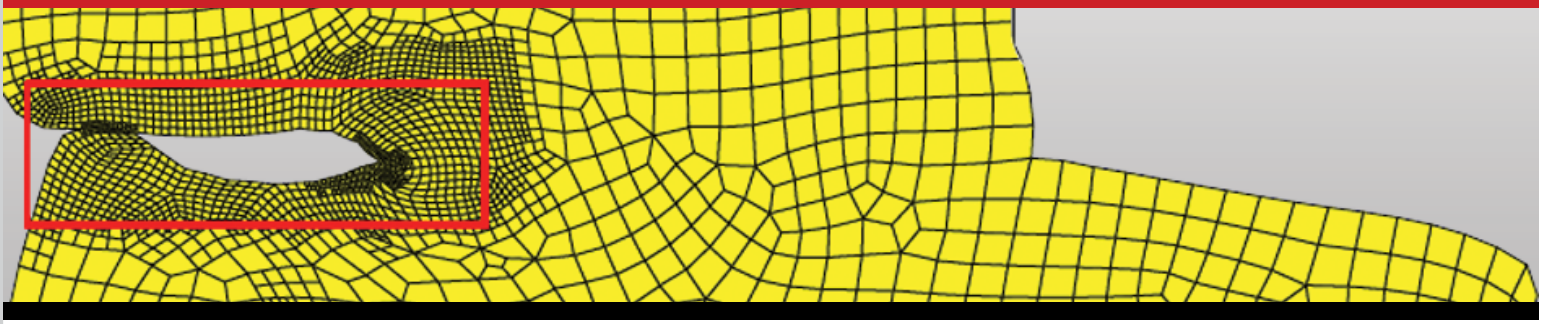

Rubber is widely used in engine mounts and suspension bushings for shock/vibration isolation and noise reduction purposes. It possesses significant damping properties which are very useful in such applications. Damping can generate heat during cyclic loading. When a piece of rubber is stretched a few times, a certain amount of stress softening occurs—which reduces its stiffness and alters its damping characteristics. Fillers in the rubber also influence the damping behavior. Rubber is viscoelastic and is usually analyzed using quasi-static methods (See more detailed discussions on rubber viscoelasticity in Section 4 and Section 5.) The usual design goal is to prolong a component's service life, implying that an optimized design should have as low stress levels as possible. Sometimes, a rubber shock mount is designed to buckle (in order to absorb a large amount of energy), followed by eventual stiffening.

This bushing example assumes a Mooney-Rivlin strain energy function. As with the other case studies, the analysis is static. Automated contact analysis is used, where the top rigid surface moves downwards, causing the rubber to contact itself. Mesh distortion is usually a problem in such analyses. The figures show the deformed geometry and equivalent Cauchy stress distributions after various increments (panels a and b). The FEA code must be able to handle such variable contact automatically. This analysis was performed both with and without adaptive meshing. One may observe that in using local adaptive meshing techniques, additional elements are automatically located in regions of stress concentrations and high stress gradients (panel c). This improves the accuracy of the solution.

Notes: In order for the stress analysis to be rigorous and complete, the engineer may need to take into account several real-life phenomena ignored in this example: material damage; viscoelastic behavior—to account for creep and relaxation effects; actual service environments—which typically include combined axial, radial, and torsional loadings, and very often, a metallic sleeve around the rubber insert; bushing preload (if any); dynamic (inertial) effects; and fracture and tearing effects.

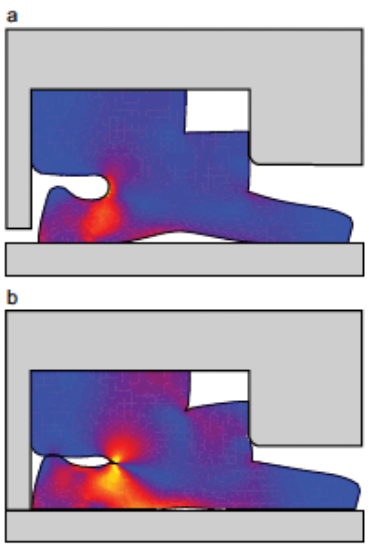

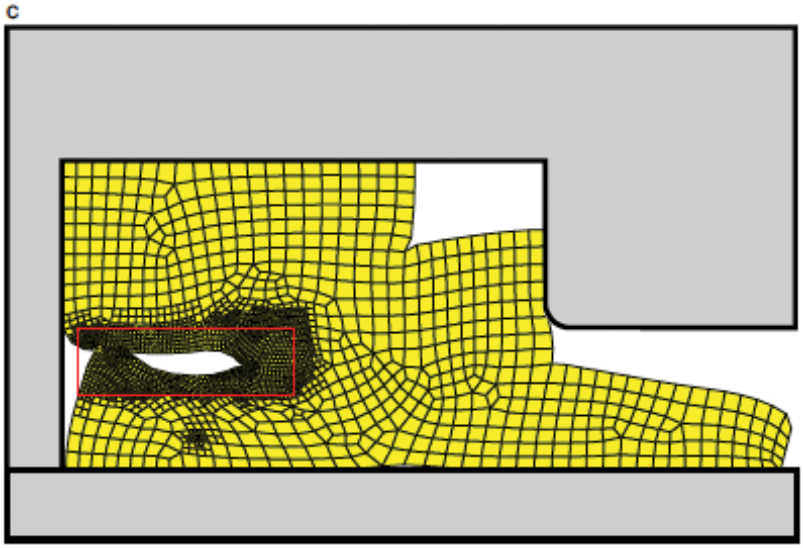

Equivalent Cauchy Stresses:

Using Local Adaptive Meshing

Chriteria Used:

1. Strain Level
2. Nodes in Contact
3. Nodes in Box (red)

6. CONTACT ANALYSIS TECHNIQUES

Rubber products always seem to involve “contact” versus “no-contact” conditions—for instance, rubber gaskets and the contact of a car tire with the road. To see applications of Marc to analyze typical 2-D rubber contact problems, see Case Studies A, D, and E. For 3-D examples, look at Case Studies B, C, and F.

Contact as a Nonlinear Constraint Problem

Contact, by nature, is a nonlinear boundary value problem. During contact, both the forces transmitted across the surface and the area of contact change. Because rubber is flexible, this change in the contact area is both significant and difficult to model using earlier methodologies (such as gap elements). The contact stress is transmitted in the normal direction. If friction is present, shear stress is also transmitted.

Mathematically, the contact problem occurs as a constrained optimization problem where contact conditions occur as inequalities described as Kuhn-Tucker conditions. Among the approaches within the finite element framework that have been used to model the frictional contact and impose the nonpenetration constraint (to prohibit the overlap of contact bodies), the most popular ones include: Penalty Methods [Peric and Owen, 1992], Langrange Multiplier [Chaudhary and Bathe, 1986], Augmented Lagrangian [Laursen and Simo, 1993], Perturbed Lagrangian [Simo, Wriggers, and Taylor, 1985], Hybrid Methods [Wunderlich, 1981], Gap Elements, Interface Elements, direct application of contact forces, and Solver Constraints.

One important point to recognize is that the use of interface elements of any kind requires the user to know a priori where contact will occur. Since rubber is flexible, guessing the location of the contact area is very difficult, thereby resulting in incorrect loads being transmitted across the surfaces. An improper choice of penalty parameter in the penalty methods can lead to either penetration (low penalty number) or numerical ill-conditioning (high penalty number). The Langrange multiplier method leads to high solution cost due to extra variables for contact pressure, in addition to the possible numerical ill-conditioning. In this regard, Marc bypasses the above objectives by the solver constraint method to solve the general 2-D/3-D multibody contact. This method allows an accurate modeling of contact without the problems associated with other methods.

Both deformable-to-rigid and deformable-to-deformable contact situations are allowed in Marc. The user needs only to identify bodies which are potential candidates for contact during the analysis. Self-contact, common in rubber problems, is also permitted. The bodies can be either rigid or deformable, and the algorithm tracks variable contact conditions automatically. Besides modeling the rigid bodies as analytical, Marc also allows the analytical treatment of deformable bodies. This improves the accuracy of the solution by representing the geometry better than the discrete finite elements. This is important for concentric shafts or rolling simulation. The user no longer needs to worry about the location and open/close status checks of “gap elements,” or about “master-slave” relationships. Also, coupled thermo-mechanical contact problems (for example, rolling, casting, extrusion, car tire) and dynamic contact problems can be handled.

Friction

Friction is a complex phenomenon. Martins and Oden have published two comprehensive studies on the physics of static and kinetic friction, and computational models [Martins and Oden, 1985, 1990]. Surface imperfections, stick-slip motions, material softening due to heat in the contact area, time- and rate-dependence of the coefficient of static friction, and the oscillatory and unstable nature of sliding should all be considered when performing sophisticated rubber contact analysis. Use of a carefully measured friction coefficient will also help to achieve success. Experience has shown that the proper simulation of friction is extremely important for the success in rubber contact analyses.

When friction is present, bodies in contact develop frictional shear stresses at the interface. As for the value of the coefficient of friction, “steel-to-steel” contact results in a significantly lower coefficient than “rubber-to-steel” or “rubber-to-rubber” contact. Experiments have confirmed that the various components contributing to friction force in rubber are:

$$F_{friction} = F_{adhesive} + F_{deformation} + F_{viscous} + F_{tearing}$$

$F_{friction}$ is caused by surface adhesion kinetics and bulk mechanical properties.

$F_{deformation}$ is due to partial irreversibility (damping loss) during the deformation of rubber.

$F_{viscous}$ represents the existence of a layer of either absorbed or liquid species between rubber and contact surface.

$F_{tearing}$ is due to the fact that some solid surfaces (due to roughness characteristics) tear off particles from rubber. This phenomenon is also responsible for the wear.

In many rubber applications, however, the design objective is to increase the friction and, hence, the traction (for example, transmission belt, car tire).

Marc offers two friction models: Coulomb friction and shear friction. Coulomb friction is where the friction force depends upon the normal force, whereas shear friction is where the friction force depends upon the shear strength of the material. Coulomb friction suits elastomeric contact, where as shear friction is more appropriate for metal forming. In addition, a user subroutine is available in Marc, permitting the user to constantly monitor the interface conditions and modify the friction effect if necessary. In this way, friction can be made to vary arbitrarily—as a function of location,

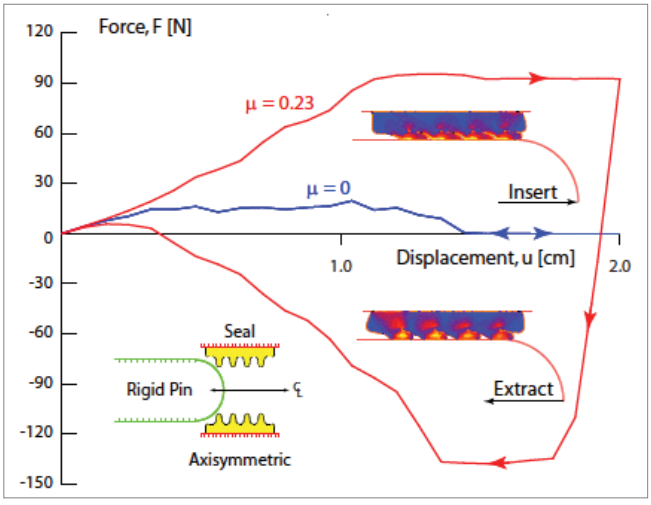

Pin Insertion and Extraction Forces with and without Friction

pressure, temperature, amount of sliding, and other variables. In order to reduce numerical instabilities in the transition between sticking and slipping, a regularization procedure is applied. Sometimes, the physics of deformation dictates modeling the regions of sticking fairly accurately (for example, driver pulley transferring torque through the belt to a driven pulley). For such cases, a stick-slip, bilinear, or arc tangent friction model based on Coulomb friction is also available. Because friction generates heat, a coupled thermo-mechanical analysis is often required in rubber contact problems.

Rigid bodies that participate in contact always have generalized force and moment components resolved to their center; these components of force, moment, and center position may be plotted over the load history. Consider a rigid pin inserted into and extracted from an axisymmetric rubber seal. Here we seek the force necessary to insert and extract the pin with and without the effects of friction. This particular problem, demonstrates this visualization of friction forces; more importantly it illustrates how a small amount of friction can dramatically affect insertion and extraction forces in rubber components. If you have ever tried to install and remove a rubber hose from a steel housing, or a steel pin from a rubber housing you may have experienced that insertion is usually easier than extraction. For instance, here friction along with the incompressibility of rubber conspire to make the extraction force magnitude of 135 N much larger than the 90 N necessary to insert the pin. Imagine if the fingers of the seal were backward facing, the extraction force would be even larger. The frictionless case (blue curve) conserves energy, whereas a significant amount of energy (2.5 J some 10x larger than energy to compress the seal) is lost for the friction case (red curve). The energy lost by the work done by friction generally dissipates in the form of heat.

Visualization of relevant contact variables, such as normal and friction forces, are available in Mentat. Here rotational motion is transferred using an elastomeric belt between two pulleys. Panel a shows the belt and pulley assembly where the right pulley is stretched placing the belt into tension (Component 11 of Cauchy stress of 0.842 MPa in panel b). The drive pulley begins to rotate transferring torque to the driven pulley via friction until the belt rotates to 180o (panel c). Friction can be visualized by the ratio of the force in the top and bottom portions of the pulley. The ratio of these two forces will yield the coefficient of friction between the belt and pulley as shown (panel c). Furthermore, the components of contact and friction forces are added in a user subroutine and displayed in panel d. The tangent of the angle between the contact force vector and the normal of the surface also yields the coefficient of friction, 0.51 (panel d).

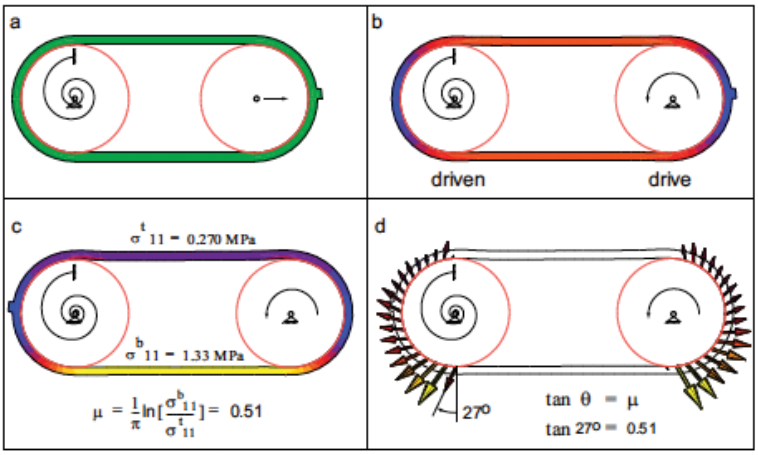

Cauchy Stress (11 component) Contours

Automatic Boundary Condition Handling for 3-D Contact Problems

"Real-world" contact problems between rigid and/or deformable bodies are three-dimensional in nature. To solve such contact problems, one must define bodies and their boundary surfaces. In Marc, the definition of bodies is the key concept in automatically analyzing 3-D contact. For rigid bodies, one can define the following surfaces: 4-point patch, ruled surface, plane, tabulated cylinder, surfaces of revolution, Bezier surfaces and NURBS. These surfaces can be converted into NURBS which have the advantage of continuity of the normal vector along the surface and the flexibility to model complex surfaces with a single mathematical description. Such a description of contact bodies is an essential requirement for robustness of solution algorithm. Virtually all common surface entities as defined by the latest IGES (Initial Graphics Exchange Standard) are included. Two examples of curved surfaces that can be used to define the shape of contact bodies are the ruled surface and the Bezier surface, as shown in the figures here.

Deformable bodies are defined by the elements of which they are made. Once all the boundary nodes for a deformable body are determined by Marc, four-point patches are automatically created and are constantly updated with the body deformation. Contact is determined between a node and all body profiles—deformable or rigid. A body may fold upon itself, but the contact will still be automatically detected; this prevents self-penetration.

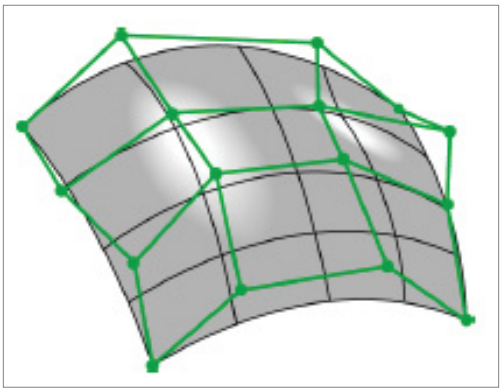

Cauchy Stress (11 component) Contours

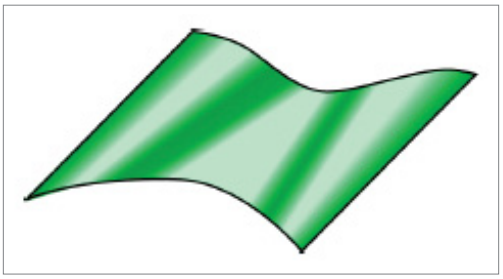

Cauchy Stress (11 component) Contours

MSC Software: Case Study - E

Car Door Seal: Automatic Multibody Contact

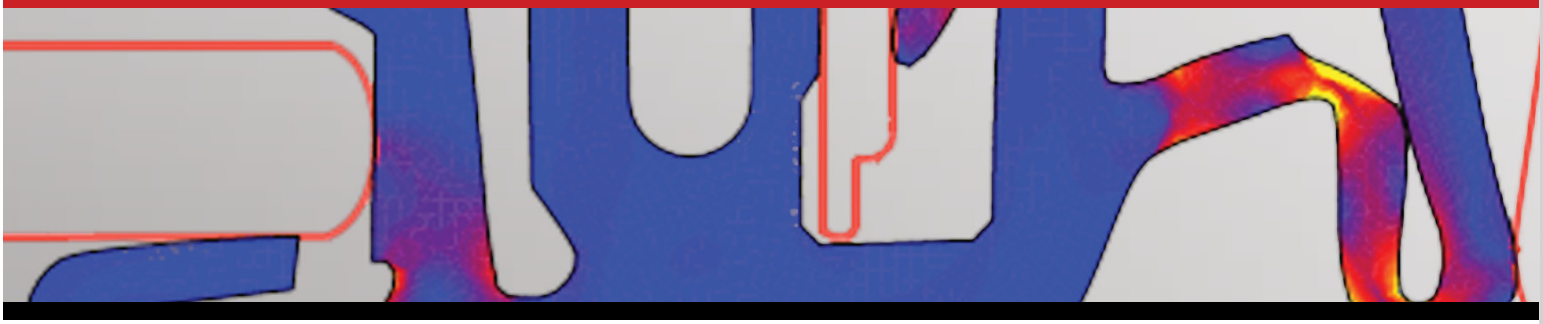

Automotive body seals are necessary due to the presence of openings in the car body such as passenger doors, windows, engine and trunk lids, and sunroofs. The requirements of static seals, such as those around windshields, are important but relatively simple. On the other hand, dynamic seals, such as door and window seals, are complex in function. They must not only maximize the seal between fixed and movable components, but must also compensate for the manufacturing tolerances of various body parts.

Material requirements for automotive seals include: resilience, weather resistance (including ultraviolet radiation effects), bonding strength, tear and abrasion resistance, surface finish, and strain resistance. Mechanical requirements include: sealing of components against water, air, dust, and noise; ease of installation; and closing/cycling effort.

Historically, the design and prototyping of automotive seals have relied on experience, empirical data, and "trial and error". Today, however, most leading seal manufacturers use nonlinear FEA to optimize their seal designs early in the design cycle.

A typical car door seal (panel a) is subjected to three loading conditions:

1. install seal onto door frame
2. door closure
3. window closure

The rubber is assumed to be isotropic, with a Mooney-Rivlin strain energy density function. Panel b shows the deformed geometry and the equivalent Cauchy stress (see Appendix B) distribution when the door frame moves downward. The window and door approach the seal simultaneously. Panel c shows the effects of door closure and panel d shows both door and window in their final position.

Notes: In this type of analysis, sliding contact and potential contact of the body with itself are important. This example illustrates how a modern nonlinear FEA code can easily handle difficulties with complex boundary conditions. An automated solution procedure which keeps track of the multi-body movements and variable contact conditions is crucial for success here. Such an analysis helps the designer to understand and improve the seal behavior by providing information about stresses, strains, reaction forces, and deformation histories. It also tells the designer where the rubber material is best used—leading to an optimum design of the car door seal for its expected dynamic loading histories.

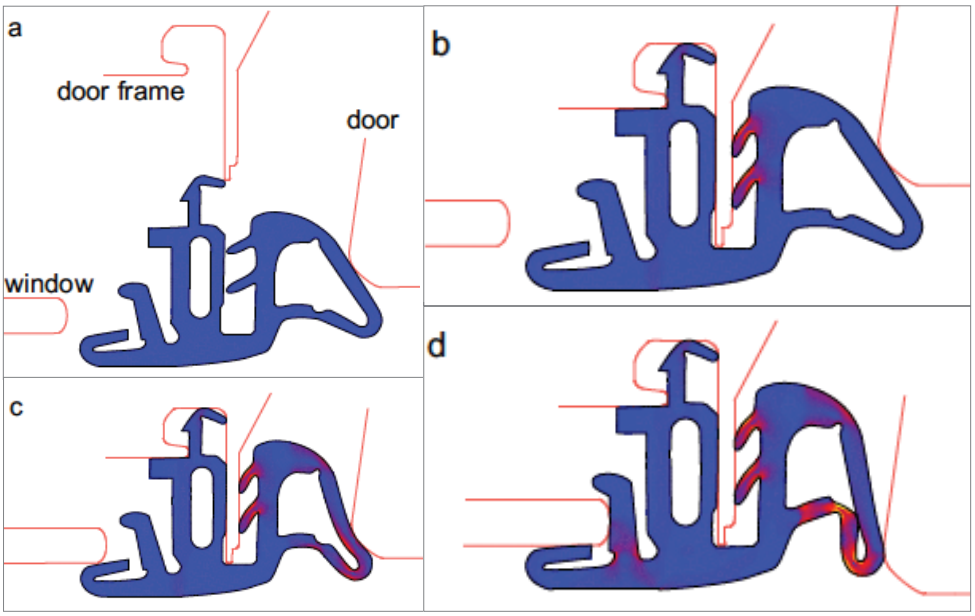

Equivalent Cauchy Stress Contours

7. SOLUTION STRATEGIES

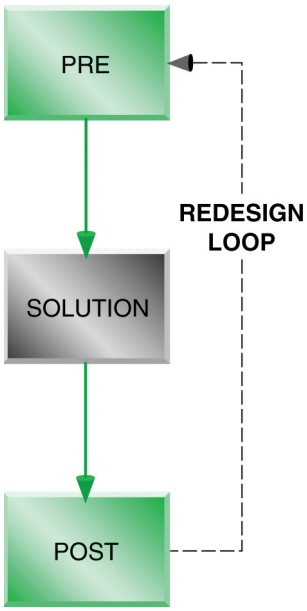

The core of a typical design process encompasses three phases: preprocessing of data, solution, and postprocessing. In the preprocessing phase, besides the data required in a typical linear analysis, a user must specify certain nonlinear analysis controls (analysis procedures, "contact" control parameters, convergence controls, etc.) and additional material properties (for example, Mooney-Rivlin and Ogden coefficients) required for a nonlinear rubber analysis.

In the solution phase, the key difference between nonlinear and linear FEA is that the solver performs the analysis in load steps (called increments). Within each increment, for implicit analysis the program seeks a solution by iteration until equilibrium is achieved, before proceeding on to the next increment. A modern nonlinear FEA code like Marc helps the user achieve success by first querying for acceptable tolerances in force, displacement strain energy, or other parameters. Then, it automatically increases or decreases the step size in order to achieve a converged solution using a minimum number of increments. Lack of convergence can take place due to input errors, improper modeling of physical phenomenon, or real physical instabilities. Therefore, the objective of a successful nonlinear analysis is to obtain an accurate, converged solution at the least cost.

Adaptive solution strategies run into three classes, the first is a procedure where if convergence is not achieved the time step is reduced, such that convergence is achieved. The applied excitation will be scaled down, or re-evaluated if the boundary condition is a function of a table. The second procedure is similar to the first, but additionally artificial damping is added to the solution. This is an effective process when rubber components are present. The third method is the use of arc-length or continuation methods (Chrisfield, Riks, Ramm, etc.), that effectively use mathematical methods to get a sense of the direction of the solution. These methods are often very successful when there is effectively one source of the external load present.

On the computational front, several key features distinguish Marc from other existing nonlinear FEA codes. Features on the materials side include, a very robust singularity-free implementation for case of equal stretches of the Ogden model, and special treatment for extremely large compressive stresses generated during deformation. Fast, efficient elements incorporating special treatment for incompressibility and hourglassing modes, and solution schemes which are able to analyze buckling and post-buckling regime.

For ease-of-use and computational savings, Marc allows a data transfer capability from axisymmetric to 3-D analysis. In many cases, the component has an initially axisymmetric geometry and is initially axisymmetrically loaded (axial motion) and, hence, is truly axisymmetric. The second stage of the problem invokes asymmetric loading (radial motion) and needs to be fully three-dimensional. This function transfers the results from the nonlinear axisymmetric model to the 3-D analysis. Large savings in computational cost can be expected. This feature can be used with lower- and higher-order displacement and Herrmann elements in static, dynamic, and heat transfer analysis. This feature can be used with both rubber elasticity and metal plasticity.

The role of graphics (pre- and postprocessing) capabilities cannot be underestimated. Rapid developments in the nonlinear finite element technology has brought the modeling of full scale industry problems within reach. Hence, it is not uncommon for the model preparation stage to be more time consuming than the actual analysis itself. The interactive graphics program, Mentat, is tightly coupled with the analysis program, Marc. Analysis with Marc can also be done via Patran. Besides a wide array of geometry modeling features, both Mentat and Patran offer a variety of mesh-generation capability in 2-D and 3-D.

Augmenting the array of visualization techniques are the animation and movie capabilities in Mentat. In addition, interfaces to other commercial CAD systems allow designers to access the nonlinear capabilities of Marc while operating in their familiar environment.

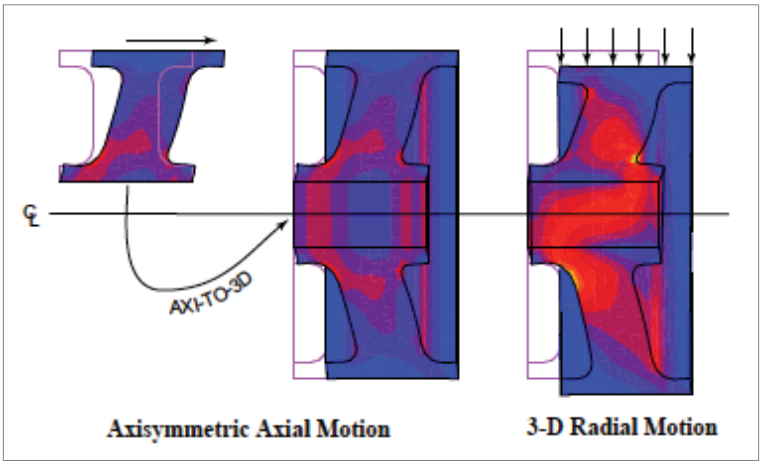

Data Transfer from Axisymmetric to 3-D Analysis

8. ADAPTIVE REMESHING

In the analysis of metal or rubber, the materials may be deformed from some initial (maybe simple) shape to a final, very often, complex shape. During the process, the deformation can be so large that the mesh used to model the materials may become highly distorted, and the analysis cannot go any further without using some special techniques. Global adaptive remeshing in Marc is a useful feature to overcome these difficulties.

When the mesh becomes too distorted because of the large deformation to continue the analysis, the analysis is stopped. A new mesh is created based on the deformed shape of the contact body. A data mapping is performed to transfer necessary data from the old, deformed mesh to the new mesh. The contact conditions are redefined, and the analysis continues.

Now the above steps are done automatically (see figure). Based on the different remeshing criteria you specified, the program determines when the remeshing is required. Remeshing can be carried out for one or more contact bodies at any increment. Different bodies can use different remeshing criteria.

Besides global adaptive remeshing, Marc also offers an h-method based adaptive mesh refinement capability called local adaptive remeshing (an automated process in which mesh is repetitively enriched until the error criterion is satisfied) for both linear as well as nonlinear analysis. Several error criteria are available to the user for subdividing the mesh adaptively. This is demonstrated in Case Study D.

A successful rubber analysis requires: a state-of-the-art nonlinear FEA code with automated contact analysis capabilities; availability of the necessary test data and friction coefficients; an experienced user; careful evaluation and application of the analysis results; and good pre- and postprocessing software which is closely coupled to the solver.

Here the automatic remeshing of a rubber seal demonstrates what is called global adaptive remeshing. The original rectangular rubber seal only uses one element to begin (panel a). As the material is pushed into the horizontal channel (panels b - f) the automatic global adaptive meshing option automatically generates new meshes as many times as needed (38 remeshes here) until the seal fills the horizontal channel. Although this illustrative problem is two dimensional, global adaptive remeshing can also be done in three dimensions.

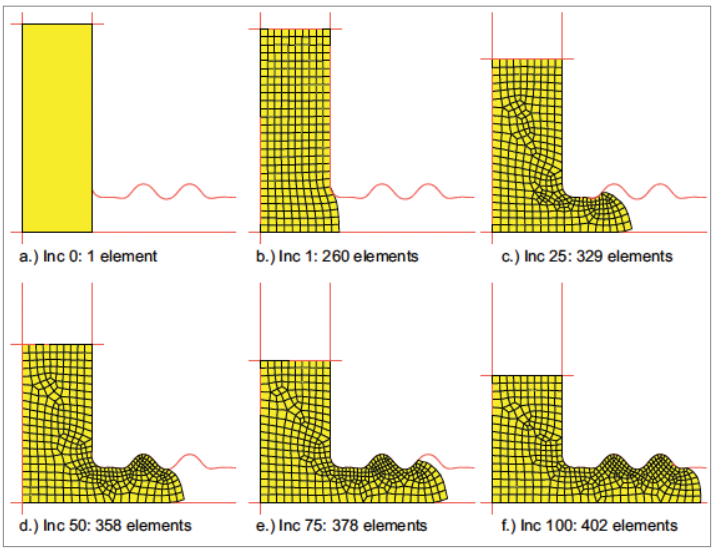

Global Adaptive Remeshing of a Rubber Seal

WHITEPAPER

MSC Software: Case Study - F

Downhole Oil Packer

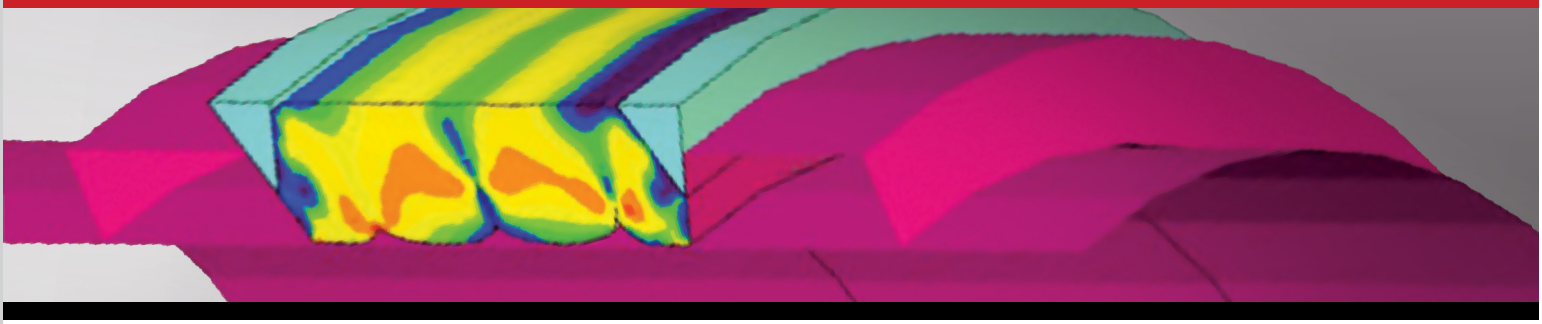

Downhole packers seal off the region between casing and production tubing helping prevent flow of corrosive fluids upstream. Because of their location underground, they are subjected to harsh environmental conditions and high temperatures and pressures, making physical testing difficult and expensive. Simulation provides a superior alternative both in terms of cost advantage and testing safety. However, simulation of these products presents a challenge as their designs incorporate multiple nonlinearities: material, large deformations and strains, contact between multiple components and self-contact, and friction, to name a few.

In this case study, model of a fictitious packer assembly is analyzed demonstrating the benefits of automatic remeshing. The simplified packer design shown here contains packing elements, loaded and fixed cones, left and right v-rings and the casing walls. While packers are three dimensional, many are very nearly axisymmetric and may be simulated using an axisymmetric finite element model as shown here. The packing element is an elastomer, the v-rings are made of steel and the cones and casing are assumed to be rigid.

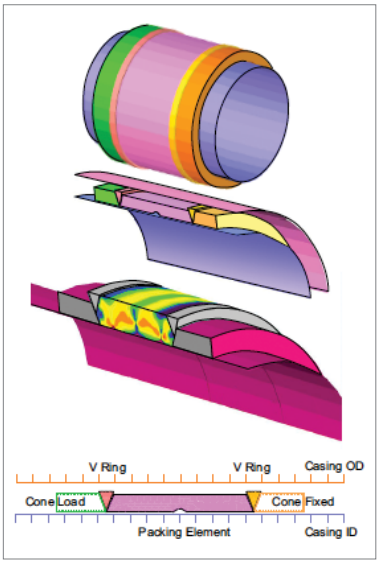

The packer is compressed by the loads on the cone until it reaches 100% of its setting and fills the volume between the inner and outer walls. During this process, all the components of the packer assembly experience contact, including self-contact of the packer elements. Because of the high pressures on the packer, the original finite element mesh becomes too distorted; automatic global adaptive meshing is activated in this analysis whereby new meshes are automatically generated as many times as needed. Use of this advanced capability of Marc leads to a successful completion of the analysis, which would otherwise have been a very challenging problem to solve.

Once the packer seats, the maximum stress and strain in the packer may be examined to determine possible failure locations. Total equivalent strain contours are shown here for 25%, 50%, and 100% of the compression set. Subsequently, a system pressure is applied to the packer (left end at red arrow) to analyze packer performance at operating pressures. In this case, a pressure subroutine assures that the pressure loading will advance only along the downstream direction as the packer separates from the outer casing. As the packer continues to deform, automatic remeshing facilitates quality mesh enabling superior convergence and accuracy. For larger pressures, more volumetric compression of the rubber packer occurs, as shown in increased blue and green colored regions in the total equivalent strain contours. At operating pressure, about 50% of the packer separates from the outer casing; subsequent studies can determine if the seal continues to operate within tolerances under material relaxation and creep.

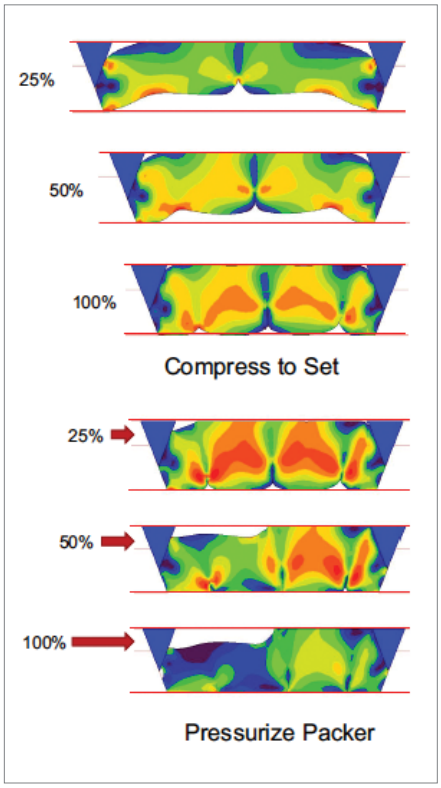

Marc capabilities used: Elastomer material properties, Rigid-deformable contact, deformable-deformable contact, Self-contact, User subroutine for customized pressure loads, Automatic global remeshing.

DATA PREPERATION

- FE model (nodes, elements)
- material properties
- loads
- boundry conditions

Linear FEA

PREPROCESSING

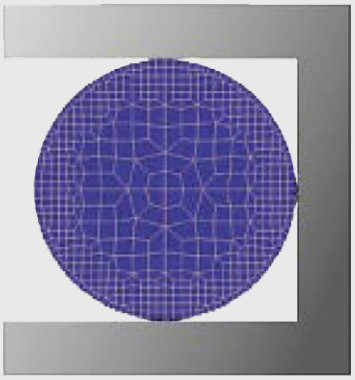

Nonlinear FEA

(same as for linear FEA)

Nonlinear Analysis controls required

Material data to represent nonlinear behavior required, e.g.:

“Material Constants for strain energy functions”

Solution

Incremental Loop

- Update Configuration
- Update Contact Conditions

Iteration Loop

Rezoning

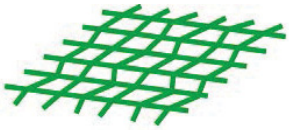

OUTPUT

- displacements
- strains
- stresses
- strain energy density

POSTPROCESSING

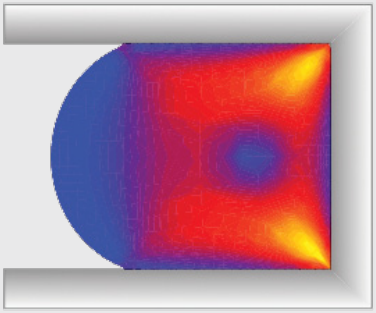

- thermal strains
- creep strains
- plastic strains
- Cauchy stresses
- failure criteria

- contact forces distribution
- strain rates
- history plots
- derived variables

RESULTS EVALUATION

- deformed geometry
- strain distributions
- stress distributions
- tempaturature distributions

9. CURRENT TRENDS AND FUTURE RESEARCH

Nonlinear FEA of elastomers has come a long way in the past twenty five years. Previous difficulties in the 1970-1985 period with handling complex contact boundary conditions have now been solved, recently, significant progress also has been made in 2-D and 3-D automated adaptive meshing, and these automated procedures are now being used in the design/analysis of rubber components. Areas which still require further research and development include:

- Global and local adaptive meshing for nonlinear FEA (especially for 3-D problems)
- Coupling of design optimization methods with nonlinear FEA
- Methods for dealing with crack or void initiation and propagation in elastomers
- Improved modeling of friction effects
- Material instabilities–for example., surface folds and wrinkling
- Viscoelastic effects in filled rubbers
- Improved plastics and other polymer models (to model large elastic as well as inelastic deformations)
- Coupled processes involving interaction between mechanical, chemical, thermal, and electrical phenomena.

Sometimes rubber seals have closed air pockets, or in the case of air springs the closed cavity is actively pressurized. Here the crush force increases dramatically and the deformed shape of the tube changes as well when the cavity of air is closed. The compression of the air inside the closed cavity of the tube plays an important role in the analysis.

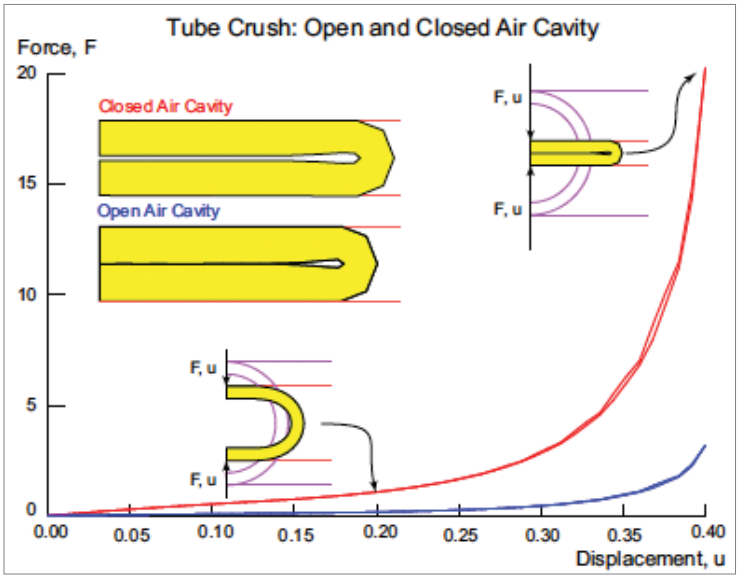

Elastomeric Tube Crush

10. USER CONVENIENCES AND SERVICES

MSC Software offers an array of tools and services to help the customer design their products efficiently:

Material Characterization. Very often, obtaining the correct material parameters for analysis from test data is the major obstacle to a successful simulation. In such cases, Marc can refer the customer to materials testing firms which specialize in this type of testing (the same firm can also be used for testing the structural integrity of the finished elastomeric product). The required tests to characterize a material are given in Appendix C (Courtesy: Akron Rubber Development Lab and Axel Products, Inc.). In addition, a curve fitting procedure is required to determine the coefficients of the selected model. Details of the curve fitting program in Mentat, used along with Marc, are described in Section 3.

Training. Attendees Performing Analysis Using MSC Software. MSC Software offers training with a wide variety of workshops, including MAR 103 "Experimental Elastomer Analysis". This is a hands-on workshop covering material testing, material modeling and finite element analysis of elastomers. Instructors from MSC Software and Axel Products, Inc. present an integrated testing and analysis workshop featuring the experimental facilities of Axel Products, Inc. and the MSC Software Corporation. Attendees perform elastomer experiments using laboratory instruments to create data appropriate for use in building elastomer material models in FEA. Material models are then developed and examined on workstations running the Marc software.

MAR 103 Experimental Elastomer Analysis Training Class in Action

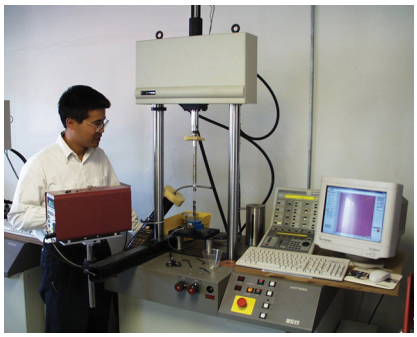

Customer Support. Recognizing the complex nature of FEA of elastomers, MSC Software Corporation offers prompt and professional customer support. For rubber FEA, the user should expect help from a knowledgeable support person or, in some complicated cases, the particular developer who created that part of the analysis capability. The availability of competent support is often crucial to success in nonlinear FEA.

Consulting. Most nonlinear FEA software developers, such as MSC Software Corporation also offer consulting services to assist an organization in performing rubber FEA. This service is especially valuable for a company that either does not possess an FEA capability or their in-house engineers do not have nonlinear analysis expertise. The scope of such consulting work usually includes the development of a model(s), analyzing the rubber problem, writing a final report, and sometimes, an oral presentation of the key results.

Documentation. In addition to the reference documentation; MSC Software Corporation also offers tutorial documentation. The latter allows new users to try a rubber analysis similar to their own, and become familiar with the recommended procedure before venturing into a difficult rubber contact problem using a large 3-D model.

Error Checks And Warning Messages. FEA programs all contain built-in input error checks. In rubber FEA, the program checks for items such as: the completeness of input coefficients for a certain strain energy density function, contact body definition correctness, consistency of the nonlinear analysis controls (tolerances, step size, etc.), friction definition, whether a user subroutine is used and if the required data for that subroutine is completely defined, etc. To help detect potential instability problems, the code also issues warnings to the user during the analysis about possible snap-through, negative eigenvalues, non-positive definiteness, etc.

User Subroutines. These are a must in nonlinear FEA that involve complex geometric, material, and boundary nonlinearities (such as in rubber and metal forming problems). They allow the user to define arbitrary variations of material properties, loads, and boundary conditions as a function of time, space, and temperature or some other state variable. User subroutines give the flexibility to users to tailor the nonlinear analysis specifically to their exact problem requirements. The coding and accuracy verification of user subroutines is best left to the experienced user. In rubber FEA, user subroutines can be used, for instance, to define the dependence of friction coefficient or some other material property on time, temperature, or location. More importantly, they can be also used to define a new material model.

11. CONCLUSION

In the final analysis, the FEA of elastomeric or viscoelastic structures is a nontrivial undertaking. This White Paper has presented a lot of information about what one should know about analyzing rubber. But, where does one go from here? By that, we mean what types of questions should be asked when selecting a code for rubber FEA?

- Does the FEA code contain the proper material models? Which is the proper model?
- Are there suitable finite elements for incompressible analysis?
- Does the code have modern automated contact analysis capabilities?
- Does the code offer the best choice of elements, material models, solution algorithms, and convergence criteria for your situation?
- Does the code developer have an extensive track record in analyzing applications similar to yours? If so, the developer should possess examples and verification problems similar to your application.

All these questions relate to the quality of the nonlinear FEA code and the support. After the code has been selected, the user should bear in mind that there are other additional considerations which help to ensure success. These are “tricks of the trade” that come with experience in analyzing rubber parts. For instance, some important considerations about model definition include: mesh refinement, specification of the incremental load schedule, and tolerance selection in the convergence criterion used. These subtleties very often mean the difference between success and failure.

Modeling of real world rubber parts is often complicated by a lack of good material data, boundary conditions, and knowledge of the actual field service conditions. Finally, a professional engineering judgment must be applied to interpret the numerical simulation results.

APPENDIX A
Physics of Rubber

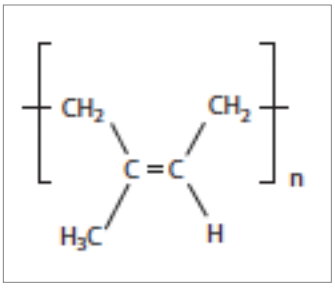

cis-polyisoprene

Early applications of a material which came to be known as natural rubber (NR) with C_5H_8 , cis-polyisoprene, as a basic monomer unit involved a product derived from the Hevea Brazieliensis tree. Other varieties of NR came from balta, guayule, and gutta-percha. The superior heat dissipation properties under cyclic loading, resilience, electrical insulation, high tensile strength, and wear resistance make NR an attractive choice over the synthetics in many applications even today. Some common uses of NR can be found in golf-ball covers, cable insulation, tires, etc.

However, the desire to improve certain properties like resistance to environmental factors such as ozone degradation and ultraviolet rays, aging, and protection against industrial oils, led to the discovery of synthetic rubber. The advent of World War II saw an increased interest and necessity of the development of synthetic rubber compounds. Commonly known synthetic rubbers are Neoprene, Isoprene, Styrene-Butadiene, Butyl, Nitril, Acrylic, Butadiene, and Urethanes. The basis of modern synthetic rubbers lies in synthesis of macromolecules by way of step-growth or chain-growth polymerization.

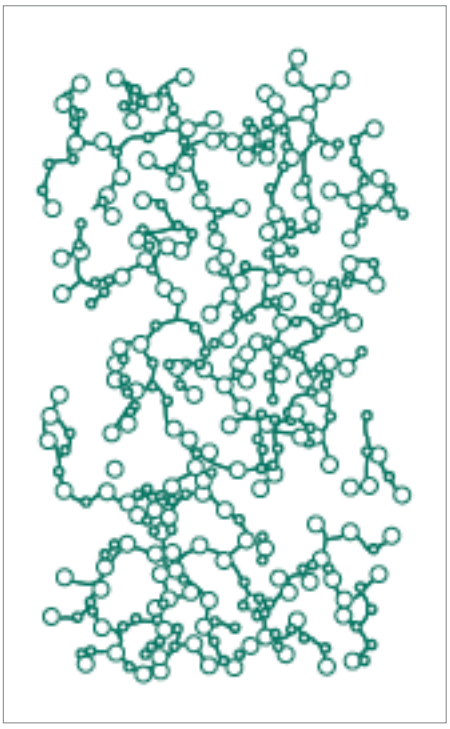

Typical Polymer Molecules

Rubber products are manufactured via a vulcanization process. In an unvulcanized (green) state, rubber does not have the desired tensile strength, is sticky and deforms permanently under large deformations. Rubber is vulcanized at high temperatures with addition of sulfur, accelerators, and curatives under application of pressure. The sulfur and carbon atoms, together with metal ions and organic radicals, form the crosslinks between polymer chains. This crosslink network determines the physical properties and is controlled by vulcanization time and temperature. Mechanically, the process manifests itself by an increase of retractile force and a possession of “rubbery” properties such as increased elasticity.

After prolonged exposure to the sun, rubber parts become discolored, brittle, and exhibit crazing and stress cracks. To inhibit these ultraviolet radiation effects, rubber manufacturers typically use “stabilizers” (for example, carbon black, an excellent absorber) and “masks” (for example, urethane-based paint). These are used, for instance, in exterior rubber gaskets and seals for cars. In the United States, federal regulations require that exposed rubber components must withstand exposure to ultraviolet radiation for approximately five years. The most damaging effect is due to ozone, which causes exposed rubber to become brittle. To simulate these effects and to improve the design of rubber parts, manufacturers subject specimens to xenon (or carbon) arcs, where the specimen is typically stretched 20% at certain prescribed temperatures.

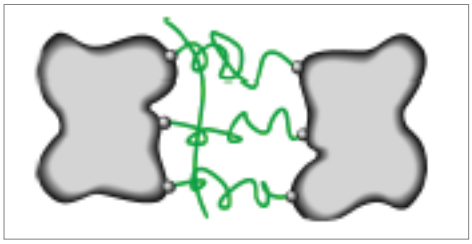

Carbon Black Filled Rubber
From Govindjee and Simo [1991]

Fillers play an extremely important role in the manufacturing of rubber to impart the desired properties. On one hand, several properties of unfilled rubbers such as hardness, abrasion resistance, tensile, tear strength [Mark, Erman, and Eirich, 1994] and a possible redistribution of rubber network stresses can be enhanced by use of carbon black and silica. On the other hand, the viscoelastic response and hysteresis losses are greatly enhanced by fillers (since the material properties depend on the strain history). There is, nevertheless, a correlation between the above two characterizations of carbon black. It is hypothesized that carbon black particles act as stress concentrators and originators of microscopic flaws which precede a gross macroscopic tearing. However, stress relaxation and creep reduce the stress concentration at the crack tip. The increased stresses at the particles produce molecular orientation or alignment; thereby, blunting the crack tip and diverting the tear from a rapid fracture. Other fillers like wax, paraffin, and mineral oil are added to increase the heat dissipation capability.

The distinctive features of rubber elasticity have a thermodynamical basis:

$$F = \left(\frac{\delta E}{\delta L}\right)_T - T\left(\frac{\delta S}{\delta L}\right)_T$$

Thus, at equilibrium, the force (F) exerted on stretching a rubber strip equals the rate of change of internal energy (E) and entropy (S) with length (L) for a given temperature (T). It has been concluded from experiments that rubber elasticity manifests itself in the second term of the above equation, except at low elongations (<10%) at which the thermal expansion masks the entropy effect resulting in thermoelastic inversion or at very large elongations, at which molecular chain orientation and strain-induced crystallization occurs.

Rubber is composed of long chain of molecules, oriented randomly due to thermal agitation of their segments. Breakdown of chains, due to straining, results in damage and stiffness reduction of the elastomer. Entangled chains have significant impact on the viscoelastic properties such as creep and stress relaxation and melt viscosity.

The following table shows how some mechanical properties of rubber compare with other materials:

Material	Young's Modulus (MPa)	Bulk Modulus (MPa)	Shear Modulus (MPa)	Poisson's Ratio
Rubber (typical range)	0.76-7.60	3,000-3,5000	0.35-1.38	~0.50
Lightly Vulcanized Rubber	1.40			
Mild Steel	207,348	158,967	79,483	0.29-0.3
Aluminum Alloys	69,116	67,733	23,499	0.31
Glass	55,292	36,631	22,117	0.25
Concrete	27,646			0.18
Oak	10,021			
Human Bone *(along osteones)*	10,021			
Polyurethane Foam	3.11	2.		
Plastics:				
Polyethylene	138-380	89-255	55.-152	0.25
Phenolic Laminate	8,501			0.25
Polycarbonate	2,384			0.35
Cast Acrylic	3,110			0.35
Cellulose Acetate	1,520			
Vinylchloride Acetate	3,179			

APPENDIX B
Mechanics of Rubber

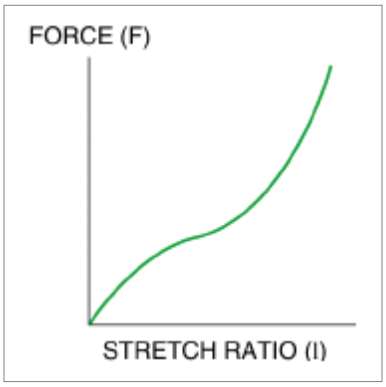

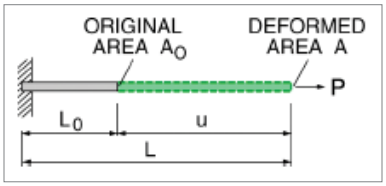

Stress and Strain Measures

In large deformation analysis of elastomers, two equivalent methods may be used to describe material behavior, the total Lagrange or the updated Lagrange procedure. When using the total Lagrange, the original configuration is the material reference frame, whereas updated Lagrange, the current deformed configuration is the material reference frame. In such cases, most nonlinear FEA codes such as Marc use a strain measure called the Green-Lagrange strain, E [Fung, 1965], which for uniaxial behavior is defined as: $E = 1/2(\lambda^2 - 1)$ and a corresponding "work conjugate" stress called the 2nd Piola-Kirchhoff stress, S_2; $S_2 = P / A(L_0 / L)^2$. Although the 2nd Piola-Kirchhoff stress is useful for the mathematical material model, it has little physical significance and is difficult to use for the interpretation of results. Therefore, the engineer resorts to either the Cauchy (true) stress, σ; $\sigma = P / A$ with energetically conjugate strain measure the logarithmic (true) strain, ε; $\varepsilon = \ln(L / L_0)$ or one can utilize the familiar engineering (Biot) stress, S_1; $S_1 = P / A_0$ with energetically conjugate strain measure being engineering strain, $e = L / L_0$. As an alternative one can use the updated Lagrange formulation, where stress and strain measures are with respect to the current deformed configuration. Then the Cauchy stress and logarithmic strain are naturally used. It should be noted that the Green Lagrange strain is often expressed with respect to the deformation gradient, $F = \partial x / \partial X$ where x and X refer to the deformed and original coordinates of the body. Marc provides all of these strain and stress measures to the analyst. It is important to note that at small strains, the differences between various measures of stresses and strains are negligible.

Numerical Treatment of Incompressibility

This part explains the principles underlying the behavior and numerical treatment of incompressible materials. (For more details, see any of the finite element textbooks—for example, [Hughes, 1987]—listed in the Suggestions for Further Reading.) Incompressibility is one of the most troublesome areas in the finite element analysis of elastomers. Modern computational mechanics practice in the analysis of incompressible materials is to suppress the volumetric component of the strain field by appropriately selected variational principles.

Incompressible Elasticity

A simple way to understand why incompressibility results in numerical problems is to examine the familiar elasticity relationship:

$$\frac{\text{Bulk modulus } (K)}{\text{Shear modulus } (G)} = \frac{2(1+v)}{3(1-2v)}$$

For nearly incompressible materials, Poisson's ratio v approaches 0.5, and the bulk modulus becomes large relative to the shear modulus. In the limit, when the material is completely incompressible ($v = 0.5$), all hydrostatic deformation is precluded. In this limiting case, it is, therefore, not possible to determine the complete state of stress from strain only. This indeterminacy difficulty applies not only to isotropic materials, but also to orthotropic and anisotropic materials.

Most rubbery and polymeric materials are not completely incompressible. Typical values of Poisson's ratio are in the range of 0.49 to 0.49999. It is important to note that the use of these values in finite element codes that have not been tailored for incompressibility analysis will lead to very serious numerical errors, caused by the ill-conditioning resulting from the division by a value which is nearly zero. More importantly, "mesh locking" may occur when using conventional displacement based formulations. Filled elastomers, however, often have Poisson's ratios of approximately 0.49 and may be considered "nearly incompressible". Whenever the material is nearly or completely incompressible, special finite element formulations must be used to obtain reliable results, as explained in the following subsections.

Mesh Locking and Constraint Counting

Whether a particular finite element code is suitable for analyzing incompressible problems depends on the type of element used and its formulation. For instance, standard lower-order quadrilateral isoparametric elements found in many FEA codes exhibit extremely poor performance in analyzing incompressible or nearly incompressible problems and exhibit a pathological behavior called mesh locking. "Mesh locking" refers to the inability of an element to perform accurately in an incompressible analysis regardless how refined the mesh is, due to an over-constrained condition and insufficient active degrees of freedom. Specifically, if a standard element is distorted into an hourglass mode, it will lock as the bulk modulus becomes infinite. Note that the element locks despite the fact that its area has remained constant, resulting in the prediction of too small of a

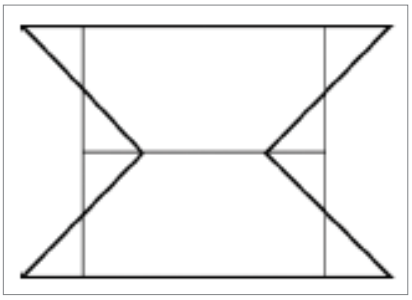

2-D Hourglassing Mode

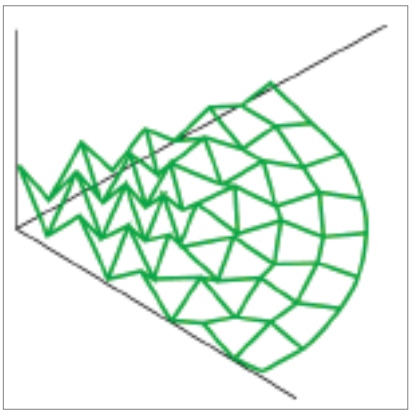

3-D Hourglassing "Eggcrate" Mode

displacement and too large of a stress. Hence, the locking is a peculiarity of the finite element discretization, and special techniques have been used to improve the behavior of the elements. Some effective analytical approaches to overcome mesh locking are discussed in the next subsection.

To check whether an element will lock, a method called constraint counting has proven to be quite effective [Nagtegaal, Parks, and Rice, 1974]. The constraint ratio r is defined as the ratio of the active degrees of freedom to the number of constraints. Optimal constraint ratios are r = 2 for two-dimensional problems, and r = 3 for three-dimensional problems. A tendency to lock occurs if r is less than these values. While constraint ratios are a helpful engineering tool, they do not ensure convergence. A mathematically rigorous approach instead makes use of the so-called Babuska-Brezzi stability condition [Hughes, 1987]. Before embarking on an incompressible analysis, therefore, the user must exercise extreme care and fully understand the limitations of the elements to be used.

Overview of Analytical Approaches

Modern analytical techniques used in treating incompressibility effects in finite element codes are based on the Hellinger-Reissner and Hu-Washizu variational principles [Zienkiewicz and Taylor, 1989]. Well-known applications of these principles include assumed strain methods, such as: the mixed method of [Herrmann, 1965]; the constant dilatation method of [Nagtegaal, Parks, and Rice, 1974]; the related B-bar methods of [Hughes, 1980] and [Simo, Taylor, and Pister, 1985]; the Hu-Washizu methods of [Simo and Taylor, 1991]; the mixed assumed strain methods used with incompatible modes by [Simo and Rifai, 1990]; and selective-reduced integration methods. Another class of approaches is the so-called assumed stress methods, which are used by researchers such as T.H.H. Pian and S.N. Atluri and their co-workers.

Mixed methods usually have the stresses, strains, dilatancy, or a combination of variables as unknowns. The earliest mixed method is the so-called Herrmann formulation. A modified form of the Hellinger-Reissner variational principle is used to derive the stiffness equations. A pressure variable (energetically conjugate to the volumetric strain) is introduced in the form of a Lagrange multiplier. Herrmann's approach has been used since the mid-1960s and 1970s in FEA codes such as Marc, TEXGAP, and various in-house codes developed by leading solid rocket propellant manufacturers.

The constant dilatation method of [Nagtegaal et al., 1974] decouples the dilatational (volumetric) and distortional (isochoric) deformations and interpolates them independently. Appropriately chosen functions will preclude mesh locking. The B-bar method of Hughes is a generalization of this method for linearized kinematics. Selective-reduced integration under integrates the volumetric terms. However, all these methods can be shown to be equivalent under certain conditions [Malkus and Hughes, 1978].

Stability

Instabilities that arise in the FEA of elastomers can be either "physical" or "numerical". Physical instabilities include buckling of a structure. Possible onset of buckling may be characterized by a limit point when the rubber structure can snap-through from one equilibrium configuration to another, or a bifurcation point which is characterized as an intersection of two equilibrium paths. Other types of instabilities would include necking of a sheet; or sudden folds or wrinkles which occur due to high compressive stresses near a surface. Marc has extensive post buckling capability to analyze rubber-to-rubber contact beyond the initial stage of folding. These instabilities which result in a sudden change in stiffness pose a severe test of a code's solution algorithm.

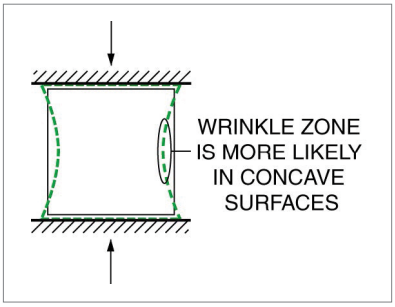

Surface Instability

[Padovan et al., 1991] have studied the occurrence of physical instabilities associated with surface wrinkles and local bifurcations in seals and gaskets. Typical mesh densification results are shown for those elements bordering the folds. In studying surface instabilities of oil well valve rubber packings, Padovan has found that strains will reach 400 to 450 percent and that low cycle fatigue becomes important. With valve closure, a hierarchy of folds appears: single folds, folds of folds, and multiple foldings. In those cases where folds occur near a rigid or very stiff boundary, refining the model would not help to achieve a converged solution!

Cord-rubber composites present yet another example of instability that may arise due to treatment of internal constraints, that is, near inextensibility of the fibers. In fact, buckling and warping of surfaces of a reinforced material may result from the loading, which if applied to unconstrained material, would cause no instability at all [Beatty, 1990]. Inflatable cord-reinforced rubber products present an example of structure whose stability limits are governed by air pressure and construction parameters in addition to the material properties.

Numerical instabilities include: instabilities in the mathematical description of the material law, and instabilities in the numerical enforcement of the incompressibility constraint. The material model must satisfy certain restrictions on its elastic moduli [Rivlin, 1980] to produce physically acceptable modes of deformation. In short, the material must satisfy the Drucker Stability criterion that the change of energy in a closed cycle is non-negative. For isotropic, incompressible materials, the Drucker Stability criterion is expressed as:

$$\sum_i \sum_j d\sigma_{ij} d\varepsilon_{ij} \geq 0$$

For elastic materials without energy dissipation, the above criterion reduces to an equality. Marc material parameter evaluation solves a constrained optimization problem to assure the stability of energy functions. [Tabaddor, 1987] has shown the existence of multiple solutions with more than one stable solutions in pure, homogeneous modes of deformation using perturbation method. These instabilities do not usually occur in the actual structure and are often the result of the mathematical abstraction of the real material. The numerical algorithms in Marc enable the user to avoid these instabilities.

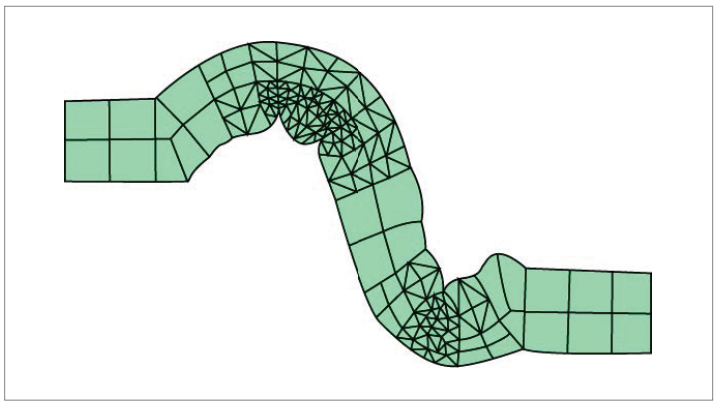

Mesh Densification During Folding
From Padovan et. al. [1991]

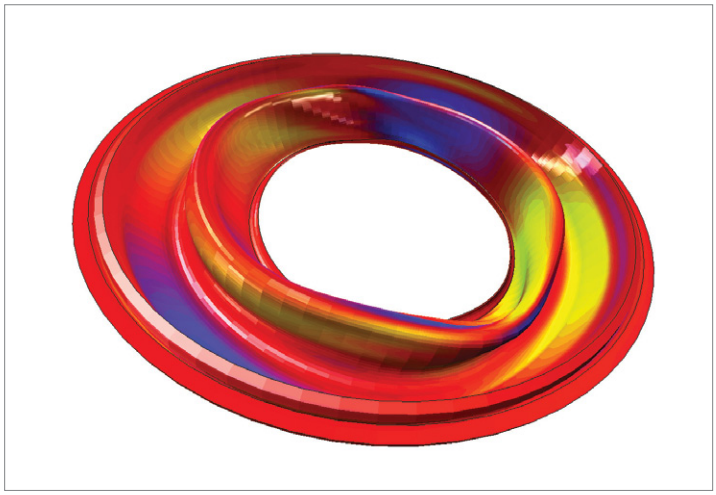

Wrinkling of Seal

APPENDIX C
Material Testing Methods

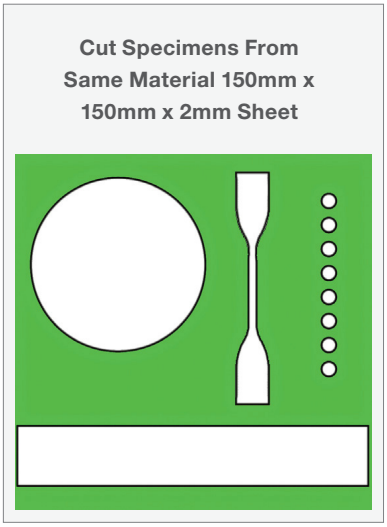

Specimen Cutouts

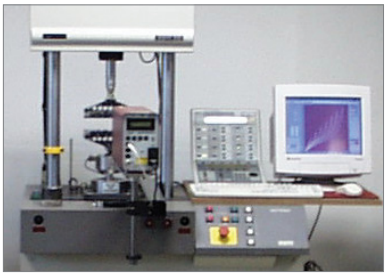

Testing Machine

axel physical testing services Mar103 MSC Software

The testing described herein is to define and to satisfy the input requirements of hyperelastic material models that exist in nonlinear finite element software like Marc. Although the experiments are performed separately and the strain states are different, data from all of the individual experiments is used as a set. This means that the specimens used for each of the experiments must be of the same material. This may seem obvious but if the specimens are specially molded to accommodate the differing instrument clamps for different experiments, it is possible that you may be inconsistently testing the material. Remember to cut specimens from the same material as the application.

The testing of elastomers for the purpose of defining material models is often mis-understood. There are several standards for the testing of elastomers in tension. However, the experimental requirements for analysis are somewhat different than most standardized test methods. The appropriate experiments are not yet clearly defined by national or international standards organizations. This difficulty derives from the complex mathematical models that are required to define the nonlinear and the nearly incompressible attributes of elastomers, and hence the experimental procedures are very intimately tied to elastomeric material model development.

Physical Measurements

Basic physical measurements discussed here are limited to force, length, temperature and time. Force is usually measured by a load cell. The load cell actually measures changes in resistance of strain gages placed in a bridge on a metal shape that deforms slightly as the specimen is loaded. The change of resistance is calibrated to report force. The load cell can be seen at the top of the specimen in the right top figure. The output from the load cell enters the data acquisition system in the computer along with the initial specimen area. The recorded force is divided by the initial specimen area automatically by the data acquisition system. Length or position is best measured by a non-contacting device such as a video extensometer as show in the middle right figure. The video extensometer senses differences in color between two marks on the specimen. The length between these two marks is continuously recorded by the data acquisition system. Another non-contacting technique is the use of a laser extensometer. The laser sends out a planar light which is reflected back from reflector tags attached to the specimen as shown in the bottom right figure. At the start of the test, the initial gage length is entered into the data acquisition system, and as the test progresses the change in gage length is recorded by the data acquisition system. Time is recorded by the data acquisition system that synchronizes the force and length measurements. The data recorded can be output in ascii files that contain the engineering stress, engineering strain and time that are later used for the hyperelastic material model fitting.

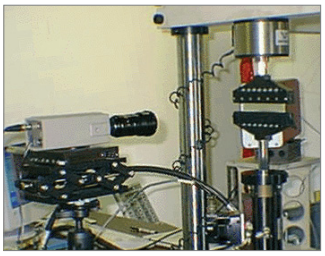

Video Extensometer

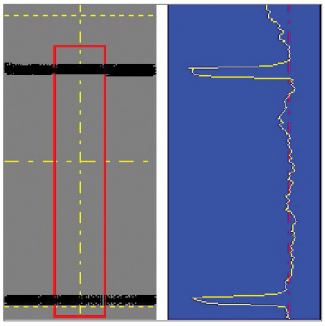

Video Extensometer Readings

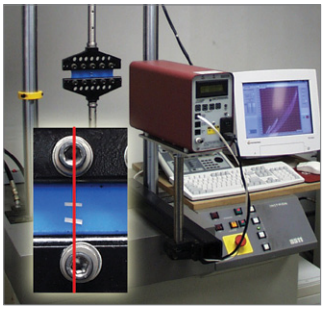

Laser Extensometer with Tags on Specimen

In the following tests, the material, temperature, strain range, strain rates, and preconditioning should be determined by the application to be modeled.

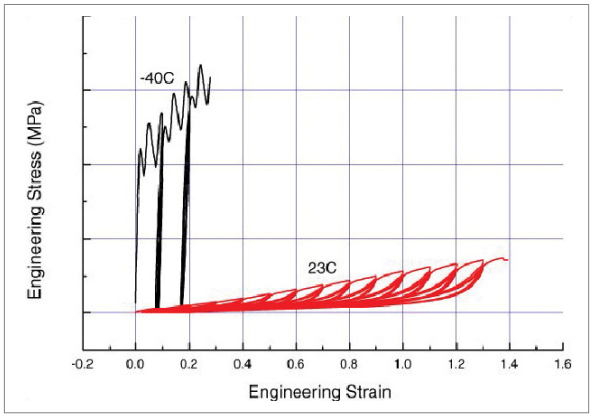

Dramatic Change in Properties with Temperature

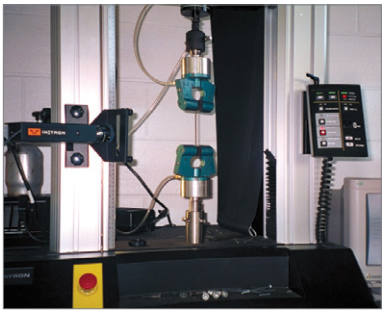

Tensile Machine

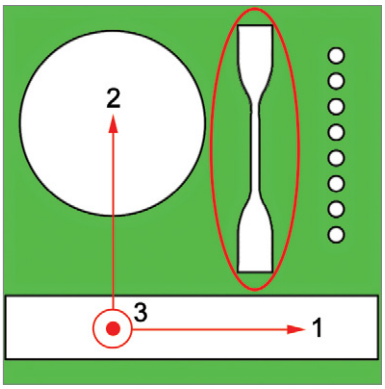

Tensile Specimen

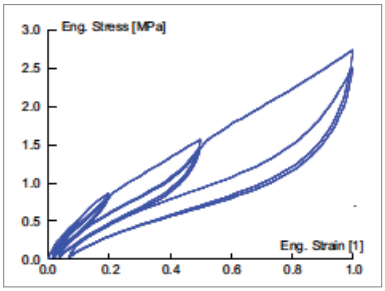

Specimen Response

Uniaxial Tension Test

a. Deformation state:

$$\lambda_2 = \lambda = L / L_0\,,\ \lambda_1 = \lambda_3 = \sqrt{A / A_0}$$

b. Stress state:

$$\sigma_2 = \sigma = P / A_0\,,\ \sigma_1 = \sigma_3 = 0$$

Simple tension experiments are very popular for elastomers. The most significant requirement is that in order to achieve a state of pure tensile strain, the specimen be much longer in the direction of stretching than in the width and thickness dimensions. The objective is to create an experiment where there is no lateral constraint to specimen thinning. One can perform finite element analysis on the specimen geometry to determine the specimen length to width ratio. The results of this analysis will show that the specimen needs to be at least 10 times longer than the width or thickness. Since the experiment is not intended to fail the specimen, there is no need to use a dumbbell shaped specimen that is commonly used to prevent specimen failure in the clamps. There is also not an absolute specimen size requirement. The length in this case refers to the specimen length between the instrument clamps. Specimen clamps create an indeterminate state of stress and strain in the region surrounding the clamp in the process of gripping. Therefore, the specimen straining, L/L0, must be measured on the specimen, but away from the clamp, where a pure tension strain state is occurring. A noncontacting strain measuring device such as a video extensometer or laser extensometer is required to achieve this. The load, P, is measured by a load cell. Calipers can be used to measure the instantaneous area, A, normal to the load. If this area is not measured, the material is assumed to be incompressible, V=V0.

Uniaxial Compression Test (Simple Compression)

a. Specimen size: 25.3 mm diameter x 17.8 mm thickness

b. Deformation state:

$$\lambda_2 = \lambda = L / L_0\,,\ \lambda_1 = \lambda_3 = \sqrt{A / A_0}$$

c. Stress state:

$$\sigma_2 = \sigma = P / A_0\,,\ \sigma_1 = \sigma_3 = 0$$

Uniform states of strain are desired and this is especially difficult to achieve experimentally in compression. There are two basic reasons that make the compression test difficult. For the compression button depicted the first difficulty is making the button so that it becomes thick enough to measure the gage length. This may require a molded specimen, rather than extruded or poured sheet. Hence the wrong material may be tested. Secondly, because there is friction between the test specimen and the instrument platens, the specimen is not completely free to expand laterally during compression. Even very small friction coefficient levels such as 0.1 between the specimen and the platen can cause substantial shearing strains that alter the stress response to straining. Often, the maximum shear strain exceeds the maximum compression strain! Because the actual friction is not known, the data cannot be corrected.

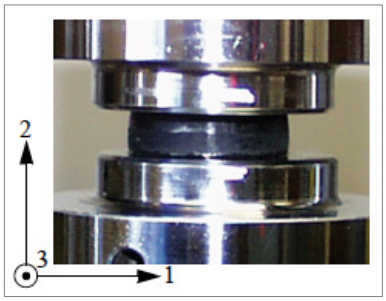

Compression Machine

Specimen Sizes

Other compression tests include the split Hopkinson pressure bars designed for soft materials such as polymers and elastomers which measures high strain rate data.

For incompressible or nearly incompressible materials, equal biaxial extension of a specimen creates a state of strain similar to pure compression. Although the actual experiment is more complex than the simple compression experiment, a pure state of strain can be achieved which will result in a more accurate material model. The equal biaxial strain state may be achieved by radial stretching a circular or square sheet.

Biaxial Tension Test (Circular)

a. Deformation state:

$$\lambda_1 = \lambda_2 = \lambda = L / L_0\,,\ \lambda_3 = t / t_0$$

b. Stress state:

$$\sigma_1 = \sigma_2 = \sigma\,,\ \sigma_3 = 0$$

The equal biaxial strain state may be achieved by radial stretching a circular disc. The nominal equibiaxial stress contained inside the specimen inner diameter is calculated as: $\sigma = P / A_0$ where: $A_0 = \pi D t_0\,,\ D$ is the original diameter between punched holes, P is the sum of radial forces, and t_0 is the original thickness. Since the deformation state is uniform in the plane of the sheet, the radial components of stress and strains are constant with the polar and in-plane rectangular components of stress being the same value. In other words, if a square or circle are drawn on the

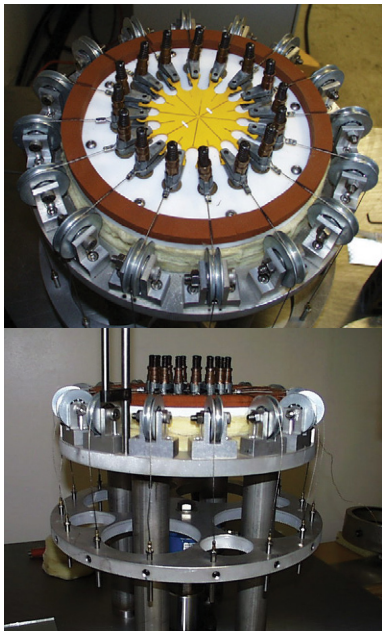

Biaxial Machine

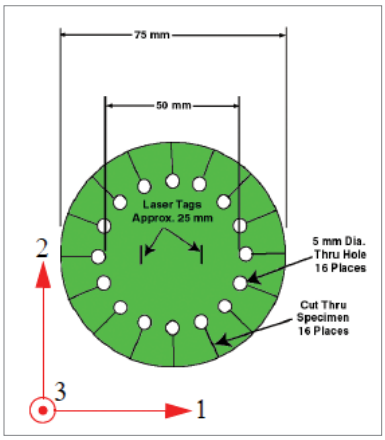

Biaxial Specimen

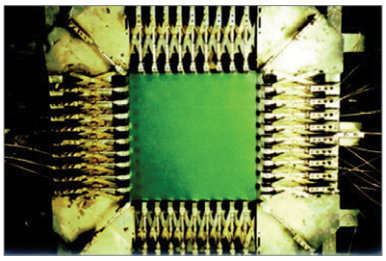
Biaxial Machine

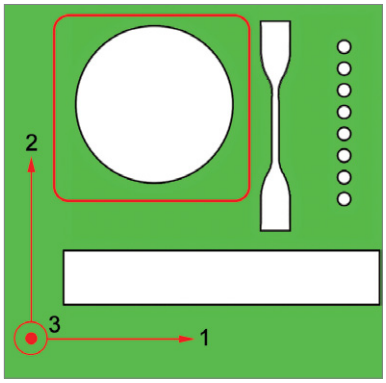

Biaxial Specimen


Planar Shear Test With
Laser Reflection Tags

specimen, they deform into a larger square or circle as the specimen is stretched. Once again, a non-contacting strain measuring device must be used such that strain is measured away from the clamp edges. Finally if the instantaneous thickness, t, is not measured, the material is assumed to be incompressible, $V = V_0$. For more details about this test and specimen, see:

http://www.axelproducts.com/downloads/BiaxialExtension.PDF

Biaxial Tension Test (Rectangular)

a. Deformation state:

$$\lambda_1 = \lambda_2 = \lambda = L / L_0 \,,\ \lambda_3 = t / t_0$$

b. Stress state:

$$\sigma_1 = \sigma_2 = \sigma \,,\ \sigma_3 = 0$$

The equal biaxial strain state may also be achieved by radial stretching a square sheet. The nominal equibiaxial stress contained inside the specimen calculated as: $\sigma = P / A_0$ where: $A_0 = Wt_0$, and W is the width and height of the specimen, P is the average of the forces normal to the width and height of the specimen, and t_0 is the original thickness. Once again, a non-contacting strain measuring device must be used such that strain is measured away from the clamp edges. Finally if the instantaneous thickness, t, is not measured, the material is assumed to be incompressible, $V = V_0$.

Planar Shear Test

a. Deformation state:

$$\lambda_1 = 1 \,,\ \lambda_2 = \lambda = L / L_0 \,,\ \lambda_3 = t / t_0$$

b. Stress state:

$$\sigma \neq 0 \,,\ \sigma_2 = \sigma \,,\ \sigma_3 = 0$$

The planar shear experiment used for analysis is not what most of us would expect. The experiment appears at first glance to be nothing more than a very wide tensile test. However, because the material is nearly incompressible, a state of planar shear exists in the specimen at a 45 degree angle to the stretching direction. The most significant aspect of the specimen is that it is much shorter in the direction of stretching than the width. The objective is to create an experiment where the specimen is perfectly constrained in the lateral direction such that all specimen thinning occurs in the thickness direction. This requires that the specimen be at least 10 times wider than the length in the stretching direction. This experiment is very sensitive to this ratio. A non-contacting strain measuring device must be used to measure strain away from the clamp edges where the pure strain state is occurring (top right figure). If the instantaneous thickness, t, is not measured, the material is assumed to be incompressible, $V = V_0$. Below illustrates how analysis can be used to verify experimental assumptions. Modeling the actual specimen shows that $\lambda_1 = 1$ to within 30 parts per million as the specimen deforms.

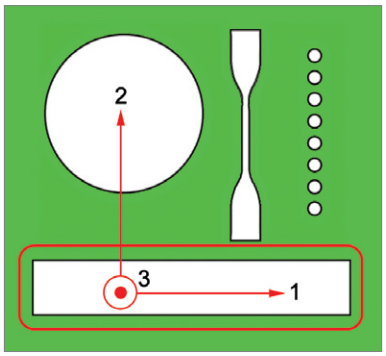

Planar Shear Specimen

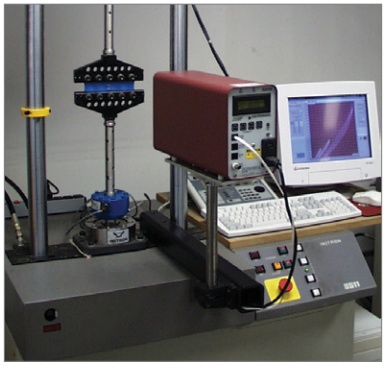
Laser Extensometer

axel physical testing services Mar103 MSC Software

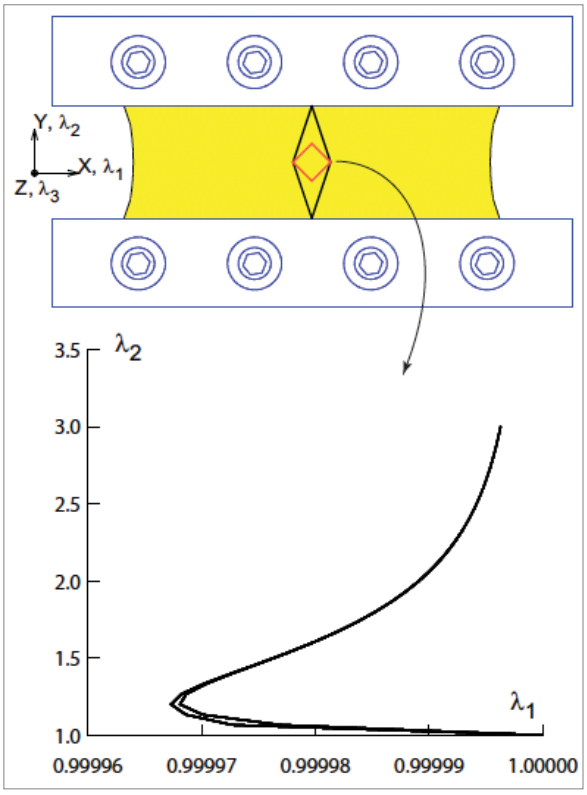

Simple Shear Test

a. Deformation state:

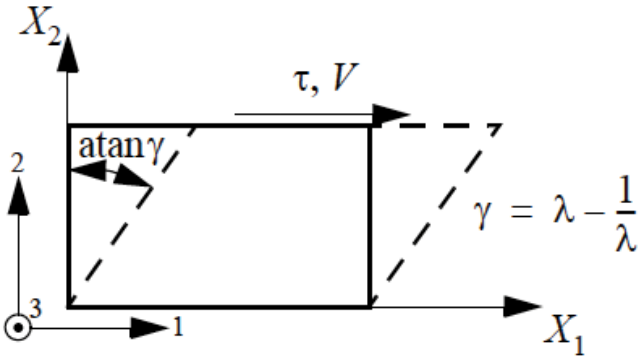

$$\lambda_1 = \sqrt{1+\frac{\gamma^2}{2}+\gamma\sqrt{1+\frac{\gamma^2}{4}}}$$

$$\lambda_2 = \sqrt{1+\frac{\gamma^2}{2}-\gamma\sqrt{1+\frac{\gamma^2}{4}}}$$

$$\lambda_3 = 1$$

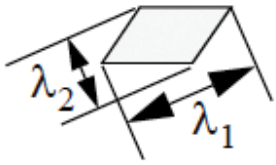

b. Stress state:

$$\sigma_{12} = \tau = V / A_0$$

The dual lap simple shear test is used in the tire industry. As a result of low shear strains, the end plates do not move in the vertical direction in this test. The quad lap simple shear test is used by the bearings industry. Since the material shear requirements are much higher, the end plates in the quad lap shear test are allowed to move in the vertical direction due to development of very high normal stresses (in mechanics, this phenomenon is termed as Poynting Effect). This test does not allow for the measurement of compressibility and as such this the volumetric compression test can be performed or the material assumed to be incompressible.

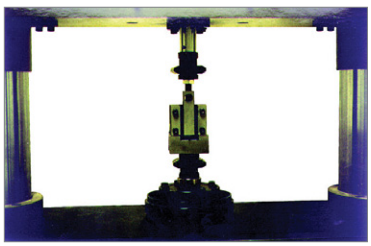

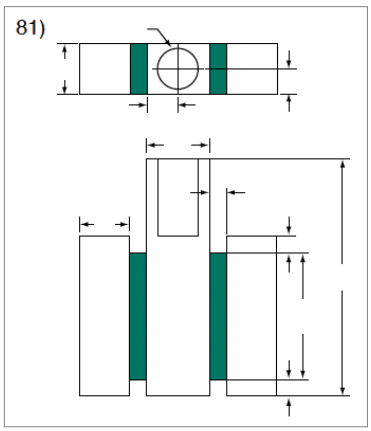

Dual Lap Shear Test

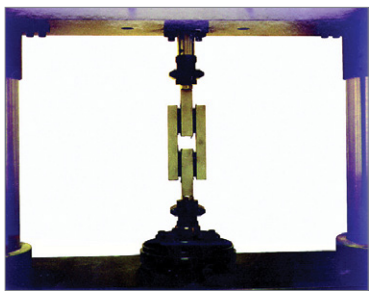

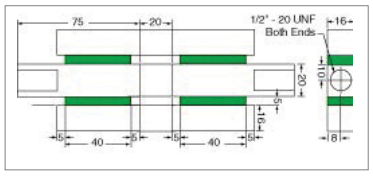

Quad Lap Shear Test

Volumetric Test

a. Specimen size: 3 mm diameter x 2 mm thickness. Eight buttons stacked and lubricated with silicone oil.

b. Deformation state:

$$\lambda_1 = 1,\ \lambda_2 = 1,\ \lambda_3 = L / L_0$$

c. Stress state:

$$\sigma_1 = \sigma_2 = \sigma_3 = -\left|P / A_0\right|$$

A_0 is the cross-sectional area of the plunger and P is the force on the plunger. Information regarding the bulk modulus can also be obtained by measuring relative areas in an uniaxial tensile or biaxial test. In this case, volumetric tests need not be performed. Otherwise this volumetric test may be performed. Furthermore, if a bulk modulus is not supplied, Marc will estimate it. For example, when using Mooney-Rivlin forms of the strain energy density, Marc estimates the bulk modulus as $K = 10000(C_{10} + C_{01})$. Whereas for Ogden models, Marc estimates the bulk modulus as:

$$K = \sum_{n=1}^{N} \left|\mu_n \alpha_n\right|$$

Plotting volumetric along side simple compression expresses rubber's incompressibility.

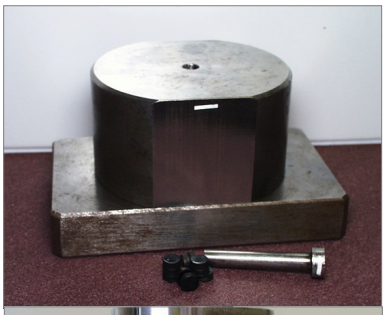

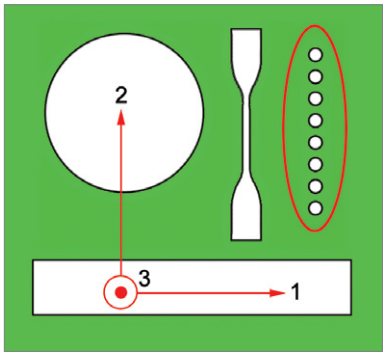

Volumetric Compression Test

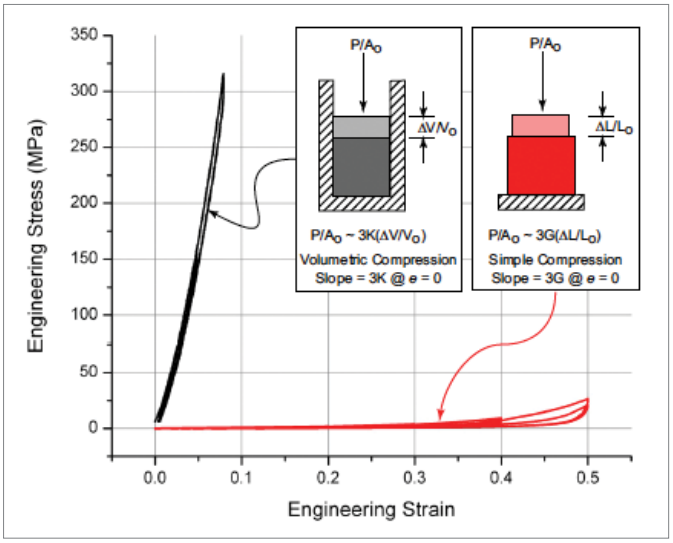

K >>> G for Rubber

For materials where compressibility is very significant, for example, foams, volumetric tests may be performed by using a pressurized incompressible fluid such as water and the corresponding deformation and stress states are:

a. Deformation state:

$\lambda_1 = \lambda,\ \lambda_2 = \lambda,\ \lambda_3 = \lambda$

b. Stress state:

$\sigma_1 = \sigma_2 = \sigma_3 = -p$

where: $\lambda = (V / V_0)^{1/3}$, and p is the fluid pressure.

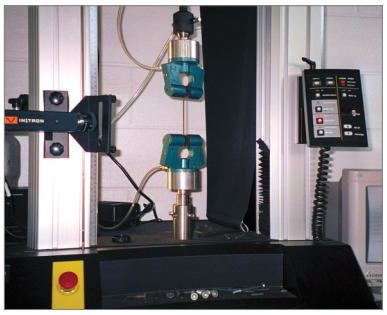

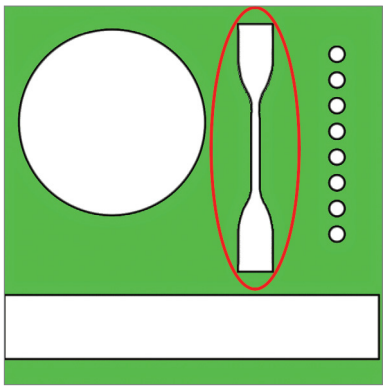

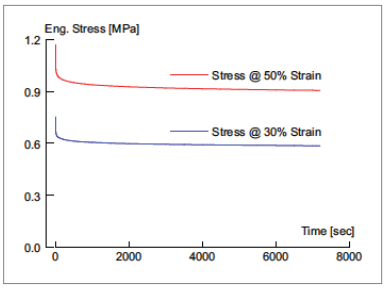

Viscoelastic Tensile Test

Viscoelastic Stress Relaxation Test

When a constant strain is applied to a rubber sample, the force necessary to maintain that strain is not constant but decreases with time, this behavior is called stress relaxation. Conversely, when a rubber sample is subjected to a constant stress, an increase in the deformation takes place with time, this behavior is called creep. Stress relaxation of a material can be measured in tension, biaxial tension, compression, or shear. Fortunately visocelastic behavior not being sensitive to the deformation mode can be determined by a tensile test being the easiest to perform. A simple loading experiment where the a specimen is stretched to a set strain and allowed to relax may be performed to provide sufficient data to model this behavior. The material data is typically fitted using a Prony or exponential series expansion. The accuracy with which this may be fitted is sensitive to the number of decades of time data. This means that the relaxation data from 0.1 second to 1 second is as valuable to the fit as the relaxation data from 1 second to 10 seconds and so on. As such, proper data collection early in the experiment can provide several decades of time data without running the experiment over several days.

The link below is a discussion of stress relaxation testing and the use of Arrhenius plots to estimate the useful lifetime of elastomeric components.

http://www.axelproducts.com/downloads/Relax.pdf

Friction

Friction Test

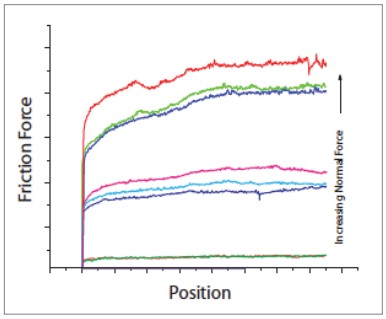

Friction Data

Because elastomers are commonly used in sealing applications, friction plays an important role in the performance of these applications. Friction is the force that resists the sliding of two surfaces relative to each other. The friction force is: (1) approximately independent of the area of contact over a wide limits and (2) is proportional to the normal force between the two surfaces. These two laws of friction were discovered experimentally by Leonardo da Vinci in the 13th century, rediscovered in 1699 by G. Amontons and latter refined by Charles Coulomb in the 16th century. Coulomb performed many experiments on friction and pointed out the difference between static and dynamic friction. This type of friction is referred to as Coulomb friction today. In order to model friction in finite element analysis, one needs to measure the aforementioned proportionally factor or coefficient of friction, μ. The measurement of μ is depicted here where a sled with a rubber bottom is pulled along a glass surface. The normal force is known and the friction force is measured. Various lubricants are placed between the two surfaces which greatly influence the friction forces measured.

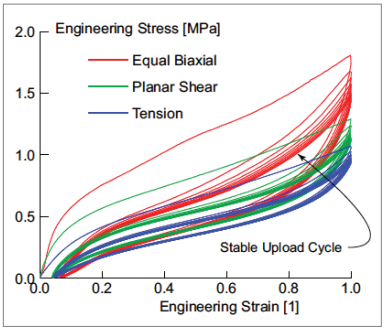

Raw Data

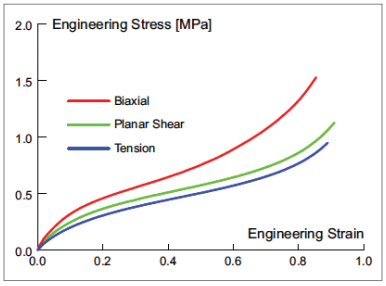

Adjusted Data

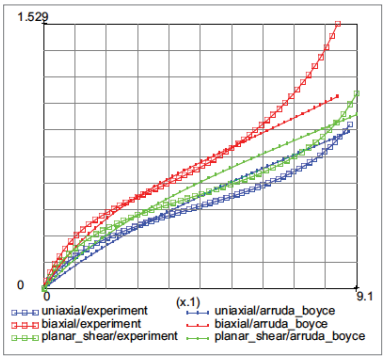

Fit for Arruda-Boyce

Adjusting Raw Data

The stress strain response of a typical test are shown at the right as taken from the laboratory equipment. In its raw form, the data is not ready for fitting to a hyperelastic material model. It needs to be adjusted.

The raw data is adjusted as shown by isolating a stable upload cycle. In doing this hysteresis is ignored. This cycle needs to be shifted such that the curve passes through the origin. Remember hyperelastic models must be elastic and have their stress vanish to zero when the strain is zero.This shift changes the apparent gauge length and original cross sectional area. Letting (σ', ε') be the raw data selected and defining $(\sigma_p, \varepsilon_p) = Min(\sigma', \varepsilon')$, then the adjusted data becomes:

$$\varepsilon = (\varepsilon' - \varepsilon_p)/(1+\varepsilon_p)$$
$$\sigma = (\sigma' - \sigma_p)/(1+\varepsilon_p)$$

There is nothing special about using the upload curve, the entire stable hysteresis cycle can be entered for the curve fit once shifted to zero stress for zero strain. Fitting a single cycle gives an average single equilibrium curve to represent the hysteresis of that cycle. Also one may enter more data points in important strain regions than other regions. The curve fit will give a closer fit were there are more points.

After shifting each mode to pass through the origin, the adjusted data curves are shown here. Very many elastomeric materials have this basic shape of the three modes, with uniaxial, planar shear and biaxial having increasing stress for the same strain, respectively. Typically examining the shifted curves, one observes that the ratio of equal biaxial to uniaxial stress is about 2. With the adjusted data, a hyperelastic fit can be generated like the Arruda-Boyce material shown here.

Acknowledgements

MSC Software Corporation is greatly indebted for the generous help provided by the Akron Rubber Development Laboratory, Inc. and Axel Products, Inc. in the preparation of this section. A more in depth presentation “Testing Elastomers for Hyperelastic Material Models in Finite Element Analysis” is available from the Axel Products web site below.Further information on material testing may be obtained from:

Akron Rubber Development Laboratory, Inc.

www.ardl.com

2887 Gilchrist Road
Akron, Ohio 44305

Tel: (330) 794-6600
Fax: (330) 794-6610

Axel Products, Inc.

www.axelproducts.com

2255 S. Industrial Hwy.
Ann Arbor MI 48104

Tel: (734) 994-8308
Fax: (734) 994-8309

APPENDIX D
Answers to Commonly Asked Questions in Rubber Product Design

1. What can one expect from the Finite Element Analysis?

The quality of the finite element results depends on several factors including computational technology in the code, experience and level of understanding of the analyst, and the interpretation of the results. Deficiencies in any of the above can lead to erroneous results or a poor design. However, an experienced analyst, who has a good understanding of the design process and the mechanics involved, can use the analysis judiciously as a verification as well as a predictive tool for better product and process design.

2. How do analysis and testing compliment each other?

Testing comes at two different levers:

i. *Material Testing*: Depending on the anticipated deformation, different types of tests can be chosen for determination of material coefficients. The quality of results is significantly affected by appropriate choice of tests and equally importantly, maintaining material stability with obtained coefficients.

ii. *Product Testing*: Several iterations in the development cycle can be bypassed if the design is first simulated by analysis. Only incremental changes will then be necessary to fine tune the prototype.

3. How do you know the answer is correct in a nonlinear Finite Element Analysis?

Previous experience, laboratory testing, code verification against analytical solution and simpler problems, and, above all, the intuition and engineering judgement of the analyst are the key factors in obtaining an accurate answer.

4. Why is Finite Element Analysis necessary along with testing?

Analysis does not replace component testing, but it will significantly reduce the product testing for performance and integrity. Several parametric sensitivity analysis before the mold design stage can significantly reduce the development cycle of the product. Typically, analysis and testing can be used hand-in-hand to iterate for a better design for manufacturing.

5. Which rubber material data is needed for nonlinear analysis (Uniaxial, Equibiaxial, Shear)?

For characterizing the time independent behavior of rubber, the following tests can be done:

i. Uniaxial tension or compression

ii. Equibiaxial tension

iii. Simple shear

iv. Planar shear

v. Volumetric

Calculation of the material coefficients for strain energy function requires simultaneous fitting to more than one deformation mode. Besides the uniaxial tension (or compression), another deformation mode should be selected depending on the application of the rubber component. For foam-like materials, a volumetric test is required.

To include strain-rate effects into the model (viscoelasticity), one requires either:

i. Stress-Relaxation test or

ii. Creep test

The stress-strain data must be obtained by applying ramp type loading if damage or stiffness degradation is to be considered in the elastomer.

Finally, during the fitting of the experimental data, care must be taken to insure the positive-definiteness of the material matrix as dictated by Drucker's Stability Postulate.

6. How realistically will the code simulate multiple deformation modes (for example, Tension, Compression, and Shear)?

Multiple deformation modes can be accurately predicted by fitting experimental data of these deformation modes simultaneously. The kinematics of deformation in Marc is general enough to accommodate any deformation mode.

7. How to incorporate stress relaxation and creep behavior of rubber in Finite Element Analysis?

Stress relaxation and creep phenomenon can be modeled by a finite strain viscoelasticity model in Marc. The viscous response is characterized by a linear rate equation leading to a convolution representation generalizing viscoelastic models. For extremely small or very large relaxation times, general finite elasticity is recovered.

8. What type of elements should be used for Finite Element Analysis of incompressible materials such as rubber?

Typically in elastomeric analysis, the nearly incompressible material behavior is modeled by using two- or three-field variational principle giving rise to the mixed elements. In Marc, either standard displacement based or Herrmann elements can be used for elastomer analysis since they treat the incompressibility constraint the same way. Compressible foam material can be modeled with standard displacement elements. The cord-rubber composites can be analyzed by using rebar elements. Analysis can be done using continuum, shell, or membrane elements depending on the kinematics of deformation. Computational efficiency can be obtained by reduced integration elements (requiring hourglass control for the lower-order elements). Thermal effects can be modeled using the heat transfer elements. Recently, special triangular and tetrahedral elements satisfying incompressibility conditions have been introduced to model elastomers.

9. What are the material models available in the program?

Marc offers a rich library of several material models, namely:

i. Generalized Mooney-Rivlin, Ogden, Boyce-Arruda, and Gent models for elastomers.

ii. Foam

iii. Finite strain viscoelasticity model appropriate for elastomers and Narayanswamy nonlinear viscoelasticity model for glass

iv. User subroutines allow the user to implement his/her own model (finite strain kinematics information is passed to the user) which may include temperature effects or internal variables in the model.

v. Discontinuous and Continuous Damage models to represent progressive stiffness loss, Mullins' effect, and fatigue behavior of the elastomer.

10. What are the major strategies for getting convergence for a rubber model?

Typically, full Newton-Raphson or secant methods are used to solve the nonlinear system of equations. When instabilities, buckling, snap-through phenomenon exist, then an arc length procedure needs to be used. Marc includes the full Newton-Raphson as well as arc length procedure for the analysis.

11. What are the convergence criteria?

Several convergence criterion exist in Marc, based on:

i. Displacement

ii. Rotation

iii. Residual force

iv. Residual moment

v. Strain energy

12. How to incorporate damage phenomena into Finite Element Analysis?

Damage effects can be incorporated in the analysis in two different ways. In a phenomenological model, the Kachanov factor for damage can be modified to accommodate the degradation of material properties with time through the Marc UELDAM user subroutine. Both, Mullin's model for discontinuous damage and Miehe's model for continuous damage are available in Marc.

13. How to consider fatigue in a rubber Finite Element Analysis?

Fatigue behavior due to cyclic loading and unloading of a rubber component can be simulated by Marc through the Continuous Damage Model due to C. Miehe. The model is available for all elastomeric strains energy functions in Marc. It allows modeling hysteresis and progressive loss of stiffness due to cyclic loading

14. How to model a dynamic rubber part with large deflection?

Small amplitude vibrations superposed on large static deflection can be analyzed by frequency domain dynamic analysis. Marc uses the phi-function approach to modal the vibrations in a sinusiodally excited, deformed viscoelastic solid.

15. How to incorporate a failure criteria into a Finite Element Analysis?

Simple fatigue, damage crack growth, and wear models can be used to analyze failure. Marc offers two different damage models: discontinuous damage model (to model Mullins' effect) and the continuous damage model (simulate fatigue behavior). Crack propagation is modeled using the energy release rate method using the quarter-point elements. The wear models can be constructed with the information regarding relative slip between contact bodies and the frictional forces given out in the program. Several subroutines exist in Marc to facilitate the user in developing his/her own failure models.

16. Do you have a quick summary of the deformation modes, deformation gradient, and principal stretch ratios?

Modes:	Uniaxial	Biaxial	Planar	Simple Shear	Univolumetric	Volumetric
Maping $\mathbf{X} = \begin{bmatrix} x_1 \\ x_2 \\ x_3 \end{bmatrix}$	$\begin{bmatrix} \lambda X_1 \\ \frac{X_2}{\sqrt{\lambda}} \\ \frac{X_3}{\sqrt{\lambda}} \end{bmatrix}$	$\begin{bmatrix} \lambda X_1 \\ \lambda X_2 \\ \frac{X_3}{\lambda^2} \end{bmatrix}$	$\begin{bmatrix} \lambda X_1 \\ \frac{X_2}{\lambda} \\ X_3 \end{bmatrix}$	$\begin{bmatrix} X_1 + \gamma X_2 \\ X_2 \\ X_3 \end{bmatrix}$	$\begin{bmatrix} X_1 \\ X_2 \\ \lambda X_3 \end{bmatrix}$	$\begin{bmatrix} \lambda X_1 \\ \lambda X_2 \\ \lambda X_3 \end{bmatrix}$
Deformation Gradient $\mathbf{F} =$	$\begin{bmatrix} \lambda & 0 & 0 \\ 0 & \frac{1}{\sqrt{\lambda}} & 0 \\ 0 & 0 & \frac{1}{\sqrt{\lambda}} \end{bmatrix}$	$\begin{bmatrix} \lambda & 0 & 0 \\ 0 & \lambda & 0 \\ 0 & 0 & \frac{1}{\lambda^2} \end{bmatrix}$	$\begin{bmatrix} \lambda & 0 & 0 \\ 0 & \frac{1}{\lambda} & 0 \\ 0 & 0 & 1 \end{bmatrix}$	$\begin{bmatrix} 1 & \gamma & 0 \\ 0 & 1 & 0 \\ 0 & 0 & 1 \end{bmatrix}$	$\begin{bmatrix} 1 & 0 & 0 \\ 0 & 1 & 0 \\ 0 & 0 & \lambda \end{bmatrix}$	$\begin{bmatrix} \lambda & 0 & 0 \\ 0 & \lambda & 0 \\ 0 & 0 & \lambda \end{bmatrix}$
Figer Tensor $\mathbf{b} = \mathbf{F}\,\mathbf{F}^T$	$\begin{bmatrix} \lambda^2 & 0 & 0 \\ 0 & \frac{1}{\lambda} & 0 \\ 0 & 0 & \frac{1}{\lambda} \end{bmatrix}$	$\begin{bmatrix} \lambda^2 & 0 & 0 \\ 0 & \lambda^2 & 0 \\ 0 & 0 & \frac{1}{\lambda^4} \end{bmatrix}$	$\begin{bmatrix} \lambda^2 & 0 & 0 \\ 0 & \frac{1}{\lambda^2} & 0 \\ 0 & 0 & 1 \end{bmatrix}$	$\begin{bmatrix} 1+\gamma^2 & \gamma & 0 \\ \gamma & 1 & 0 \\ 0 & 0 & 1 \end{bmatrix}$	$\begin{bmatrix} 1 & 0 & 0 \\ 0 & 1 & 0 \\ 0 & 0 & \lambda^2 \end{bmatrix}$	$\begin{bmatrix} \lambda^2 & 0 & 0 \\ 0 & \lambda^2 & 0 \\ 0 & 0 & \lambda^2 \end{bmatrix}$
Principal Stretch Ratios $\lambda_i, i = 1,2,3$ $\left\|\mathbf{b} - \lambda_i^2 \mathbf{I}\right\| = 0$	$\begin{bmatrix} \lambda \\ 1/\sqrt{\lambda} \\ 1/\sqrt{\lambda} \end{bmatrix}$	$\begin{bmatrix} \lambda \\ \lambda \\ 1/\lambda^2 \end{bmatrix}$	$\begin{bmatrix} \lambda \\ 1/\lambda \\ 1 \end{bmatrix}$	$\begin{bmatrix} \sqrt{1+\frac{\gamma^2}{2}+\gamma\sqrt{1+\frac{\gamma^2}{4}}} \\ \sqrt{1+\frac{\gamma^2}{2}-\gamma\sqrt{1+\frac{\gamma^2}{4}}} \\ 1 \end{bmatrix}$	$\begin{bmatrix} 1 \\ 1 \\ \lambda \end{bmatrix}$	$\begin{bmatrix} \lambda \\ \lambda \\ \lambda \end{bmatrix}$

SUGGESTIONS FOR FURTHER READING

Contact Problems, Static and Kinetic Friction

Chaudhary, A.B. and K.J. Bathe. "A Solution Method for Static and Dynamic Analysis of Contact Problems with Friction," *Computers and Structures*, V. 24, pp. 855-873, 1986.

Kikuchi, N. and J.T. Oden. *Contact Problems in Elasticity: A Study of Variational Inequalities and Finite Element Methods*, Society for Industrial and Applied Mathematics, Philadelphia, Pennsylvania, 1988.

Laursen, T.A. and J.C. Simo. "Algorithmic Symmetrization of Coulomb Frictional Problems Using Augmented Lagrangians," *Computer Methods in Applied Mechanics and Engineering*, V. 108, pp. 133-146, 1993.

Martins, J.A.C., J.T. Oden, and F.M.F. Simoes. "A Study of Static and Kinetic Friction," *Int. J. Engineering Sciences*, Vol. 28, No. 1, pp. 29-92, 1990.

Martins, J.A.C. and J.T. Oden. "Existence and Uniqueness Results for Dynamic Contact Problems with Nonlinear Normal and Friction Interface Laws," *Nonlinear Analysis, Theory, Methods and Applications*, Vol. 11, No. 3, pp. 407-428, 1987.

Oden, J.T. and J.A.C. Martins. "Models and Computational Methods for Dynamic Friction Phenomena," *Computer Methods in Applied Mechanics and Engineering*, Vol. 52, pp. 527-634, 1985.

Peric, D. and D.R.J. Owen. "Computational Model for 3-D Contact Problems with Friction Based on Penalty Method," *Int. J. of Numerical Methods in Eng.*, V. 35, pp. 1289-1309, 1992.

Simo, J.C., P. Wriggers, and R.L. Taylor. "A Perturbed Lagrangian Formulation for the Finite Element Solution of Contact Problems," *Computer Methods in Applied Mechanics and Engineering*, V. 50, pp. 163-180, 1985.

Wunderlich et al. (eds), "Formulation of Contact Problems by Assumed Stress Hybrid Model," *Nonlinear Finite Element Analysis in Structural Mechanics*, Springer, Berlin, 1981.

Finite Element Method

Bathe, K.J., *Finite Element Procedures*, Prentice-Hall, Englewood Cliffs, N.J., 1995.

Cook, R.D., D.S. Malkus, and M.E. Plesha. *Concepts and Applications of Finite Element Analysis* (3rd ed.), John Wiley and Sons, New York, N.Y., 1989.

Hughes, T.J.R. *The Finite Element Method—Linear Static and Dynamic Finite Element Analysis*, Prentice-Hall, Englewood Cliffs, N.J., 1987.

Oden, J.T. *Finite Elements of Nonlinear Continua*, McGraw-Hill, New York, N.Y., 1972.

Oden, J.T. (Ed.) *Research Directions in Computational Mechanics*, National Research Council, National Academy Press, Washington, D.C., 1991. ISBN 0-309-04648-3.

Zienkiewicz, O.C. and R.L. Taylor. *The Finite Element Method* (4th ed.) Vol. 1. Basic Formation and Linear Problems (1989), Vol. 2. Solid and Fluid Mechanics, Dynamics, and Nonlinearity, (1991), McGraw-Hill Book Co., London, U.K.

Nonlinear Elasticity

Ciarlet, P.G. *Mathematical Elasticity*, North-Holland Publishing Co., 1988.

Fung, Y.C. *Foundations of Solid Mechanics*, Prentice-Hall, Inc., Englewood Cliffs, N.J., 1965.

Fung, Y.C. *Biomechanics: Mechanical Properties of Living Tissues*, Springer-Verlag, New York, N.Y., 1981.

Green, A.E. and J.E. Adkins. *Large Elastic Deformations and Nonlinear Continuum Mechanics*, Clarendon Press, Oxford, U.K., 1960.

Ogden, R.W. "Large Deformation Isotropic Elasticity: On The Correlation of Theory and Experiment for Incompressible Rubberlike Solids," *Proceedings of Royal Society*, Vol. A (326), pp. 565-584,.1972.

Ogden, R.W. "Elastic Deformations in Rubberlike Solids," in *Mechanics of Solids* (Eds. H.G. Hopkins and M.J. Sewell), pp. 499-537, 1982.

Ogden, R.W. *Nonlinear Elastic Deformations*, Ellis Horwood Ltd., West Sussex, England, 1984.

Tschoegl, N.W. "Constitutive Equations for Elastomers," *J. Polymer Science*, AI, 1959-1970 (1971).

Yeoh, O.H. "Phenomenological Theory of Rubber Elasticity," *Comprehensive Polymer Science*, Ed.SL Aggarwal, 2nd Supplement, Pergamon Press, 1995.

Nonlinear FEA of Elastomers—Theoretical Developments

Argyris, J.H., P.C. Dunne, T. Angelpoulos, and B. Bichat. "Large Nature Strains and Some Special Difficulties Due to Nonlinearity and Incompressibility in Finite Elements," *Computer Methods in Applied Mechanics and Engineering*, Vol. 4, pp. 219-278, 1974.

Atluri, S.N. and E. Reissner. "On the Formulation of Variational Theorems Involving Volume Constraints," *J. Computational Mechanics*, Vol. 5, pp. 337-344, 1989.

Bercovier, M., E. Jankovich, F. Leblanc, and M.A. Durand. "A Finite Element Method for the Analysis of Rubber Parts. Experimental and Analytical Assessment," *Computers and Structures*, Vol. 14, pp. 384-391, 1981.

Brockman, R.A. "On the Use of the Blatz-Ko Constitutive Model for Nonlinear Finite Element Analysis," *Computers and Structures*, Vol. 24, pp. 607-611, 1986.

Cescotto, S. and G. Fonder. "A Finite Element Approach for Large Strains of Nearly Incompressible Rubber-like Materials," *Int. J. Solids and Structures*, Vol. 15, pp. 589-605, 1979.

Chang, T.Y.P., A.F. Saleeb, and G. Li. "Large Strain Analysis of Rubber-Like Materials Based on a Perturbed Lagrangian Variational Principle," *J. Computational Mechanics*, Vol. 8, pp. 221-233, 1991.

Gent, A.N., T.Y.P. Chang, and M.B. Leung. "Fracture and Fatigue of Bonded Rubber Blocks under Compression," *Engineering Fracture Mechanics*, V. 44, No. 6, pp. 843-855, 1993.

Nonlinear FEA of Elastomers—Theoretical Developments (cont.)

Herrmann, L.R. "Elasticity Equations for Nearly Incompressible Materials by a Variational Theorem," *J. AIAA*, Vol. 3, pp. 1896-1900, 1965.

Holownia, B.P. "Comparison Between Finite Element and Finite Difference Methods for Stress Analysis of Elastomers," *Plastics and Rubber Proc. and Appl.*, Vol. 5, pp. 379-380, 1985.

Key, S.W. "A Variational Principle for Incompressible and Nearly Incompressible Anisotropic Elasticity," *Int. J. Solids and Structures*, Vol. 5, pp. 951-964, 1969.

Liu, C.H., Choudhry, S., and Wertheimer, T. B. "Low-Order Triangular Elements with Volume Constraints," *Modeling and Simulation-based Engineering*, Vol. I, Eds. S.N. Atturi and P.E. O'Donoghue, pp. 272-277, 1998.

Liu, C.H., Choudhry, S., and Wertheimer, T. B. "Simulation of Embedded Reinforcements in Concrete," *Engineering Mechanics: A Force for the 21st Century*, Proc. of 12th Engineering Mechanics Conference, pp. 126-129, 1998.

Malkus, D.S. and T.J.R. Hughes. "Mixed Finite Element Methods—Reduced and Selective Integration Techniques: A Unification of Concepts," *Computer Methods in Applied Mechanics and Engineering*, Vol. 15, pp. 63-81, 1978.

Nagtegaal, J.C., D.M. Parks, and J.R. Rice. "On Numerically Accurate Finite Element Solutions in the Fully Plastic Range," *Computer Methods in Applied Mechanics and Engineering*, Vol. 4, pp. 153-178, 1974.

Needleman, A. "Inflation of Spherical Rubber Balloons," *Int. J. Solids and Structures*, Vol. 13, pp. 409-421, 1977.

Oden, J.T. and J.E. Key. "On the Effect of the Form of the Strain Energy Function of the Solution of a Boundary-Value Problem in Finite Elasticity," *Computers and Structures*, Vol. 2, pp. 585-592, 1972.

Padovan, J.F., M. Schrader, and J. Parris. "Buckling and Postbuckling of Elastomeric Components," *Rubber Chemistry and Technology*, Vol. 63, p. 135, 1990.

Padovan, J.F., F. Tabaddor, and A. Gent. "Surface Wrinkles and Local Bifurcations in Elastomeric Components: Seals and Gaskets. Part I. Theory," *Finite Elements in Analysis and Design*, Vol. 9, pp. 193-209, 1991. (Also: Padovan, J.F., K. Johnson, and A. Gent. "Part II. Applications," ibid., pp. 211-227.)

Peng, S.T.J., E.B. Becker, and T.M. Miller. "Computing Deformations of Rubbery Materials," *NASA Tech Briefs*, Vol. 14, No. 9, September 1990.

Scharnhorst, T. And T.H.H. Pian. "Finite Element Analysis of Rubber-Like Materials by a Mixed Model," *Int. J. Numerical Methods in Engineering*, Vol. 12, pp. 665-678, 1978.

Simo, J.C. and M.S. Rifai. "A Class of Mixed Assumed Strain Methods and the Method of Incompatible Modes," *Int. J. Numerical Methods in Engineering*, Vol. 29, pp. 1595-1638, 1990.

Simo, J.C. and R.L. Taylor. "Quasi-Incompressible Finite Elasticity in Principal Stretches, Continuum Basis and Numerical Algorithms," *Computer Methods in Applied Mechanics and Engineering*, Vol. 85, pp. 273-310, 1991.

Sussman, T. and K.J. Bathe. "A Finite Element Formulation for Nonlinear Incompressible Elastic and Inelastic Analysis," *J. Computers and Structures*, Vol. 26, pp. 357-409, 1987.

Taylor, R.L., K.S. Pister, and L.R. Herrmann. "On a Variational Theorem for Incompressible and Nearly Incompressible Elasticity," *Int. J. Solids and Structures*, Vol. 4, pp. 875-883, 1968.

Wriggers, P. and R.L. Taylor. "A Fully Non-Linear Axisymmetrical Membrane Element for Rubber-Like Materials," *Engineering Computations*, Vol. 7, pp. 303-310, December 1990.

Nonlinear FEA of Rubber Components—Engineering Applications

Billings, L.J. and R. Shepherd. "The Modeling of Layered Steel/Elastomer Seismic Base Isolation Bearings," *Proc. 1992 MARC Users Conference*, Monterey, California, September 3-4, 1992.

Bretl, J.L. "Implementation of the Elastomer Tearing Energy Approach in Finite Element Analysis," *Proc. 1988 MARC Users Conference*, Monterey, California, pp. 17-34, April 7-8, 1988.

Endo, H. and H. Sano. "Analysis of Rubber Parts for Automobiles," (in Japanese), *Proc. 10th Nippon MARC Users Meeting*, Tokyo, Japan, pp. 85-91, May 18, 1990.

Frankus, A. and S. Dhall. "Windshield Wiper Design/Analysis Using the New MARC Contact/Friction Capability," *Proc. 1988 MARC Users Conference*, Monterey, California., pp. 35-45, April 7-8, 1988.

Jyawook, S., R. LaPointe, and G. Le Compagnon. "Structural Analysis of a Typical Rubber Seal Section," *Proc. 131st Meeting of the Rubber Division of the American Chemical Society*, Montreal, Quebec, Canada, May 29, 1987.

Menderes, H. "Simulation of the Joining Processes for Structures Made of Elastomers," *Proc. 1988 MARC Users Conference*, Monterey, California., pp. 47-80, April 7-8, 1988.

Morman, K.N. and T.Y. Pan. "Applying FEA to Elastomer Design," *Machine Design*, Penton Publishing, Cleveland, Ohio, pp. 107-112., October 20, 1988

Ono, S. "Numerical Predictions of the Curing State of Bulky Rubber Goods Under Unsteady Curing Conditions," (in Japanese), *Proc. 11th Nippon MARC Users Meeting*, Tokyo, Japan, pp. 105-111, June 3, 1991.

Swanson, D.J. "Design and Analysis of an Elastomeric Constant Velocity Joint Seal," *Proc. 1990 MARC Users Conference*, Monterey, California, pp. 3-1 to 3-25, September 20-21, 1990.

Tada, H., M. Takayama, and T. Nishimura. "Finite Element Analysis of Laminated Rubber Bearing," (in Japanese), *Proc. 11th Nippon MARC Users Meeting*, Tokyo, Japan, pp. 85-92, June 3, 1991.

Numerical Methods

Daubisse, J., "Some Results About Approximation Functions of One or Two Variables by Sums of Exponentials," *Int. J. Numerical Methods in Engineering*, V. 23, pp. 1959, 1967, 1986.

Press, W.H., S.A. Tenkolsky, W.T. Vetterling, and B.P. Flannery. *Numerical Recipes in FORTRAN, The Art of Scientific Computing*, 2nd ed. Cambridge Univerisity Press, 1991.

Rubber Behavior and Characterization

Bauer, R.F. and A.H. Crossland. "The Resolution of Elastomer Blend Properties by Stress-Strain Modeling—An Extension of the Model to Carbon-Black-Loaded Elastomers," *Rubber Chemistry and Technology*, Vol. 63, No. 5, pp. 779-791, Nov-Dec. 1990.

Blatz, P.J. and W.L. Ko. "Application of Finite Elastic Theory to the Deformation of Rubbery Materials," *Trans. Soc. Rheology*, Vol. VI, pp. 223-251, 1968. (Paper describing the "Blatz-Ko model" for polymers.)

Finney, R.H. and A. Kumar. "Development of Material Constants for Nonlinear Finite Element Analysis," *Rubber Chemistry and Technology*, Vol. 61, pp. 879-891, Nov/Dec 1988.

Holownia, B.P. "Effect of Poisson's Ratio on Bonded Rubber Blocks," *J. Strain Analysis*, Vol. 7, pp. 236-242, 1972.

Lindley, P.B. "Effect of Poisson's Ratio on Compression Modulus," *J. Strain Analysis*, Vol. 3, pp. 142-145, 1968.

Mullins, L. "Softening of Rubber by Deformation," *Rubber Chemistry and Technology*, Vol. 42, pp. 339-362, 1969. (Paper describing the "Mullins' effect" in softening of rubber by deformation.)

Nau, B.S. "The State of Art of Rubber-Seal Technology," *Rubber Science and Technology*, Vol. 60, p. 381, 1987.

Treloar, L.R.C. *The Physics of Rubber Elasticity*, Clarendon Press, Oxford, U.K., 1975. (Classic text on rubber.)

Viscoelasticity, Hysteresis, Damage, and Failure

Beatty, M.F., "Instability of a Fiber-Reinforced Thick Slab Under Axial Loading," *Int. J. of Nonlinear Mechanics*, V. 25, N. 4, pp. 343-362, 1990.

Bernstein, B., E.A. Kearsley, and L.J. Zapas. *Trans. Soc. Rheology*, Vol. 7, pp. 391-410, 1963. (Paper describing the so-called "BKZ-shift" in analyzing polymers.)

Cheng, J.H. and E.B. Becker. "Finite Element Calculation of Energy Release Rate for 2-D Rubbery Material Problems with Non-Conservative Crack Surface Tractions," *Int. J. of Numerical Methods in Engineering*, V. 33, pp. 907-927, 1992.

Christensen, R.M. *Theory of Viscoelasticity—An Introduction* (2nd ed.), Academic Press, New York, N.Y., 1982.

Clark, S.K. "Mechanics of Pneumatic Tires," *U.S. Dept. of Transportation National Highway and Traffic Safety Administration*, Washington, 1981.

Ferry, J.D. *Viscoelastic Properties of Polymers* (2nd ed.), John Wiley & Sons, New York, N.Y., 1970.

Govindjee, S. and J.C. Simo. "A Micro-Mechanically Based Continuum Damage Model for Carbon Black-Filled Rubbers Incorporating Mullins' Effect," *J. Mechanics and Physics of Solids*, Vol. 39, No. 1, pp. 87-112, 1991.

Govindjee, S. and J.C. Simo. "Transition from Micro-Mechanics to Computationally Efficient Phenomenology: Carbon Black-Filled Rubber Incorporating Mullins' Effect," *J. Mechanics and Physics of Solids*, Vol. 40, No. 1, pp. 213-233, 1992.

Harper, C.A. *Handbook of Plastics, Elastomers and Composites*, 2nd ed. McGraw-Hill, Inc. 1992.

Konter, A., F. Peeters, and H. Menderes. "Analysis of Elastomeric and Viscoelastic Materials Using the Finite Element Method," *Proc. FEM'91 Congress*, Baden-Baden, Germany, November 18-19, 1991.

Mark, J.E., B. Erman, and F.R. Eirich. *Science and Technology of Rubber*, 2nd ed., Academic Press, 1994.

Morman, K.N., J.C. Nagtegaal, and B.G. Kao. "Finite Element Analysis of Viscoelastic Elastomeric Structures Vibrating About Nonlinear Statically Stressed Configurations," *Society of Automotive Engineers*, Paper 811309, 1981.

Morman, K.N. and J.C. Nagtegaal,. "Finite Element Analysis of Sinusoidal Small-Amplitude Vibrations in Deformed Viscoelastic Solids," *Int. J. Numerical Methods in Engineering*, Vol. 19, No. 7, pp. 1079-1103, 1983.

Narayanaswamy, O.S. "A Model of Structural Relaxation in Glass," *Proc. of Fall Meeting of Glass Division of the American Ceramic Society*, Bedford, PA, pp. 491-497, March 1971.

Pidaparti, R.M.V., H.T.Y. Yang, and W. Soedel, "Modeling and Fracture Prediction of Single Ply Cord-Rubber Composites," *J. of Composite Materials*, V. 26, N. 2, pp. 152-170, 1992.

Radok, J.R.M. and C.L. Tai, *J. Applied Polymer Science*, pp. 910, Vol. 48, 1962.

Rivlin, R.S., "Some Thoughts on Material Stability," *Proceedings of IUTAM Symposium on Finite Elasticity*, Lehigh Univ., Aug. 10-15, pp. 105-122, 1980.

Simo, J.C. "On A Fully Three-Dimensional Finite-Strain Viscoelastic Damage Model: Formulation and Computational Aspects," *Computer Methods in Applied Mechanics and Engineering*, Vol. 60, pp. 153-173, 1987.

Tabaddor, F. "Rubber Elasticity Models for Finite Element Analysis," *Computers and Structures*, V. 26, N. 1/2, pp. 33-40, 1987.

Walter, J.D. and H.P. Patel. "Approximate Expressions for the Elastic Constants of Cord-Rubber Laminates," *Rubber Chemistry and Technology*, Vol. 52, No. 4, pp. 710-724, 1979.

Williams, M.L., R. Landel, and J.D. Ferry. "The Temperature Dependence of Relaxation Mechanisms in Amorphous Polymers and Other Glass Forming Liquids," *J. American Chemical Society*, Vol. 77, pp. 3701-3707, 1955. (Paper discussing the so-called "WLF-shift" in analyzing polymers.)

Yeoh, O.H. "Characterization of Elastic Properties of Carbon-Black-Filled Rubber Vulcanizates," *Rubber Chemistry and Technology*, Vol. 63, No. 5, pp. 792-805, 1990. (Paper discussing the "Yeoh model".)

ABOUT MSC SOFTWARE

MSC Software is a global leader of multidiscipline simulation solutions that help companies improve quality, save time, and reduce costs associated with designing and testing manufactured products. MSC Software works with thousands of companies worldwide to develop better products faster with engineering simulation technology, software, and services. For additional information about MSC Software's products and services, please visit www.mscsoftware.com.

MSC Software's products and services are used by 900 of the top 1000 manufacturers in the world, across several industries including aerospace, defense, automotive, transportation, agricultural equipment, heavy machinery, medical devices, oil and gas, nuclear, consumer products, renewable energy, packaging, electronics, and shipbuilding.

Acknowledgments

Appreciation is also expressed to the many individuals for their interest and kind contributions to this White Paper by providing their research findings, references, analysis results, or valuable comments in reviewing a draft of this Paper: Professors J. Tinsley Oden (University of Texas at Austin), Y.C. Fung (University of California at San Diego), (Late) Juan C. Simo (Stanford University), Joe Padovan (University of Akron); Dr. Rudolf F. Bauer (Dunlop Tire Corporation) and the worldwide staff members of MSC Software Corporation. Use of these individuals' names does not necessarily imply their endorsement of Marc or the contents of this White Paper.

Corporate
MSC Software Corporation
4675 MacArthur Court
Suite 900
Newport Beach, CA 92660
Telephone 714.540.8900
www.mscsoftware.com

Europe, Middle East, Africa
MSC Software GmbH
Am Moosfeld 13
81829 Munich, Germany
Telephone 49.89.431.98.70

Japan
MSC Software LTD.
Shinjuku First West 8F
23-7 Nishi Shinjuku
1-Chome, Shinjuku-Ku
Tokyo, Japan 160-0023
Telephone 81.3.6911.1200

Asia-Pacific
MSC Software (S) Pte. Ltd.
100 Beach Road
#16-05 Shaw Towers
Singapore 189702
Telephone 65.6272.0082

The MSC Software corporate logo, MSC, and the names of the MSC Software products and services referenced herein are trademarks or registered trademarks of the MSC.Software Corporation in the United States and/or other countries. All other trademarks belong to their respective owners. © 2014 MSC.Software Corporation. All rights reserved.